DIGITALCOMMONS
@WAYNESTATE

Wayne State University

Wayne State University Dissertations

1-1-1997

Absolute tumor perfusion determined by nuclear magnetic resonance spectroscopy :

Nicholas Edward Simpson

Follow this and additional works at: http://digitalcommons.wayne.edu/oa_dissertations

Recommended Citation

Simpson, Nicholas Edward, "Absolute tumor perfusion determined by nuclear magnetic resonance spectroscopy :" (1997). *Wayne State University Dissertations.* Paper 1186.

This Open Access Dissertation is brought to you for free and open access by DigitalCommons@WayneState. It has been accepted for inclusion in Wayne State University Dissertations by an authorized administrator of DigitalCommons@WayneState.

ABSOLUTE TUMOR PERFUSION DETERMINED BY NUCLEAR MAGNETIC RESONANCE SPECTROSCOPY: OPTIMIZATION AND COMPARISON OF A DEUTERIUM UPTAKE METHOD

by

NICHOLAS EDWARD SIMPSON

DISSERTATION

Submitted to the Graduate School

of Wayne State University,

Detroit, Michigan

in partial fulfillment of the requirements

for the degree of

DOCTOR OF PHILOSOPHY

1997

MAJOR: CANCER BIOLOGY

Approved by:

5/15/97

Advisor **Date**

DEDICATION

I would like to dedicate this disser- tation to my lovely wife. Through her support, understanding and love, I am inspired to create at a level higher than ever before. It is said that behind every successful man is a great woman, and I owe much of my success in the pursuit of this degree to this great woman,

Chiab Panchapor Simpson.

♥

ACKNOWLEDGEMENTS

There is an unwritten rule which states that completing a work such as this requires the assistance and support of a great many people. With this work not being an exception to this rule, there is a large list of people whom I would like to acknowledge personally for their contributions to this manuscript; those who assisted directly in the research, and those who gave me the strength to enter and complete my graduate school training.

First, I would like to thank all of my family members for the love and support they each have bestowed upon me throughout my life, and particularly during my years pursuing this degree. There were some pivotal changes in my personal life during my graduate years, and without my family support, I doubt that I would have had the will to persevere through the tumultuous times to reach this milestone in my life. There are too many family members for a comprehensive list, but I would like to acknowledge in writing my immediate family. Those not listed are not to feel slighted, for there is only a limited amount of space here. They should realize that any support and love I have received is forever engrained in me, and will never be forgotten. I could not express how deeply I love and care for my family.

I wish to thank my father, Paul Simpson, for giving me an appreciation for science and the challenge of discovery early in my life. The stimulation he gave me during these early formitive years is undoubtedly responsible for any of the academic success I have had. He is an intelligent and loving man with a great diversity of interests (I share his enthusiasm for a broad spectrum of things cultural and scientific). I thank my mother,

Leone Burwell, for her guidance and assistance in molding me into the person which I have become. She is a model of parenting, and should be thanked for any positive traits I may exhibit. She also has given me a great appreciation of the arts; both the performance and fine arts. We have spent countless hours discussing wide ranges of subjects; times I will forever treasure. I thank my stepfather Norbert Burwell for the great job of parenting he did considering the difficult task of entering my life just prior to my teenage years. His steady demeanor and patience made easy my transition years from a boy to a man. His love of jazz music has influenced my own "semi-pro" career playing jazz trombone. My sisters Susan Johnson, Phyllis Williams and Laura Stewart have always shown me great support and love throughout my life, and I have a multitude of special memories of our childhoods. I hope to add to these treasured memories. My "much older" brother Robert Simpson has also shown me love and support. As we age, the differences in our ages becomes less a barrier, and we have grown much closer. I should also acknowledge my "even older" sister Kathy Lichnovsky, as well as my step-siblings Sally Lahte, and Ron and Sam Burwell. And I hope to have many special moments with my new family, my in-laws John and Sanab Knight (and family). I'd like to give a special thanks to my maternal grandmother Ida Lee for her kind love, wisdom and support throughout my life.

Directly regarding my research, I have many friends to thank. I appreciate their friendship and support foremost, but also wish to thank them for the tangible assistance they gave me with this research. First of all, Mr. Ludwig Fortan, for teaching me some new cell culturing techniques, assisting in general laboratory procedures, his strong friendship, and for teaching me the meaning of perseverance. Dr. Vishram Jalukar gave me insights into new surgical techniques which gave me a foundation of knowledge which

allowed for progression in the catheterization techniques I had to develop. Dr. Jyothi Raman assisted in some preliminary experiments, but more importantly was instrumental in keeping me on track during the roughest and darkest days of my graduate years. Her friendship will never be forgotten. My friend Dr. Cheryl McCoy gave me the confidence to undertake the step into graduate school, and is an inspiration for demonstrating what can be accomplished in the face of tremendous adversity. Dr. Jackie McDouall and Dr. James Mattiello were responsible for much of the early work performed using deuterated tracers in our lab, and I collaborated with them on many experiments while they were post-doctoral fellows in our laboratory.

Dr. Ming Zhao assisted in some of the early experimental work. Mr. Zhanquan He was invaluable with his expertise with computer programming and assistance in accessing files from various computer platforms. Dr. James Pipe helped me with his Mathematica® expertise and his general discussions on some of the research. Without these men's assistance in programming, the simulations performed in this work would have been much more difficult to accomplish. Mrs. Julia Moore helped with the cell cultures and animals, and helped with ordering materials necessary for the research, whereas the secretary for the research center, Ms. Terri Bing, assisted me in many day to day capacities. Also, I'd like to acknowledge Dr. Bonnie Sloane for allowing me to use her fluorescent spectrophotometer in the comparison experiments with the microspheres, as well as a thanks to Dr. Rosaria Haugland of Molecular Probes, for hand-manufacturing the fluorescent microspheres employed in this research.

I must not forget my friends who did not directly assist in this research, since their presence and friendships made laboratory life not only tolerable, but extremely enjoyable.

So a heartfelt thanks to my many friends at the M.R. Center: Ms. Amy Cunnings, Mrs. Paula Morton, Mrs. Mary Kalich, Mr. Archie Chu, Mr. Don Pata, Dr. Michael Crowley, Dr. Jiani Hu, many members of the clinical staff, and the late Dr. William Negendank for all the wonderful memories and friendships they have given me. I would also like to thank a couple of my Cancer Biology colleagues with whom I formed strong friendships: Dr. Marie Piechocki and Ms. Barb Frosch. We came in as classmates with dreams of science careers: we are now ready to embark on a new life journey.

I also want to thank my graduate committee: Dr. Joseph Ackerman, Dr. Ronald Hines, Dr. Gloria Heppner and Dr. Eric Wolman. These scientists were invaluable in giving me insights into my research, and directing me towards completing the research which is described in this dissertation.

Lastly, I would like to thank my advisor and mentor Dr. Jeffrey Evelhoch for his guidance. I have learned valuable lessons during my years in his lab; both as his technician and as one of his graduate students. These lessons should better prepare me for the "real world" of science. However, he has been not only a model for how one should approach scientific research, he is a great role model for how one should live life, by balancing a loving family life with a thriving scientific career. I would do well to achieve half as much as he has, and would be just as content.

TABLE OF CONTENTS

LIST OF TABLES

LIST OF FIGURES

LIST OF ABBREVIATIONS

A	AIF term: first pass area under the curve
AIF	arterial input function
AUC	area under the curve
B	AIF term: equilibrium concentration
C	AIF term
^{13}C	carbon thirteen
C.O.	cardiac output
C. V.	coefficient of variation
D_2O	deuterated water
DNA	deoxyribonucleic acid
dQt/dt	tissue uptake of an indicator
F	flow (in milliliters/minute)
f	perfusion (in milliliters/100 grams·min)
FID	free-induction decay
FIT	time-course fitting analytic approach
^{1}H	hydrogen ion (a.k.a. proton)
Hg	mercury
HOD	singly deuterated water
H_2O	water
$H_2{}^{15}O$	positron emitting water
Hz	Hertz (frequency)

INT	uptake integral analytic approach
^{85}Kr	Krypton
MHz	MegaHertz (frequency)
^{23}Na	non-radioactive sodium
^{24}Na	radioactive sodium
NaCl	sodium chloride (a.k.a. table salt)
NMR	nuclear magnetic resonance
$^{13}O \rightarrow {}^{20}O$	isotopes of oxygen
^{31}P	phosphorous
PDT	photodynamic therapy
PET	positron emission tomography
pH	hydrogen ion concentration
PS	permeability surface product
S/N	signal to noise ratio
t	time
$T_{½}$	radioactive halflife
t_p	time to peak (tracer concentration)
V/V	volume per volume
W	weight or mass of tissue
^{133}Xe	Xenon gas
λ	tissue to blood partition coefficient
τ	dispersion time constant

CHAPTER I. BACKGROUND AND LITERATURE REVIEW

A. Introduction to the problem

All tissues need a supply of well-oxygenated blood to survive. However, the perfusion of blood through tissues is more than just a mechanism which brings in nutrients necessary for cell survival and cleanses out waste products; it is also a means through which the physiologic status of the tissue may be appraised, and is an important player in the response of tissues to therapies. Consequently, there is a need for methods which can estimate tissue perfusion, especially in the experimental laboratory setting. In the field of cancer research, there is a great demand for such methods, since the measure of solid tumor perfusion may be instrumental in both monitoring and designing therapeutic approaches to the treatment of this disease.

An ideal perfusion measuring method would have the following characteristics: it would be non-destructive to the tissue being monitored; it would allow for repeated measures over time; it would allow either regional or whole-volume perfusion measurement; and it would yield absolute (*i.e.* accurate and precise) measures. At present, no commonly used methods performed in the laboratory to measure tissue perfusion fulfill all these requirements. Most are invasive, and require the killing of the animal to extract information from the tissue under study.

A few years ago, our laboratory introduced a novel approach to monitoring tissue perfusion. This method (termed the uptake approach) uses Nuclear Magnetic Resonance (NMR) to detect a remotely injected indicator (isotopic water), and fulfills three of the above requirements for an ideal method: it is non-invasive, repeatable, and can yield whole-volume or regional perfusion measurement through spectroscopic or imaging

detection, respectively. However, the uptake approach has limitations. Most critical is that in order to extract absolute perfusion measures using this approach, the arterial concentration of the indicator must be known over time (this is commonly referred to as the arterial input function, or AIF). This function is easily measured in man and larger animals, but is difficult if not impossible to determine in the rodent models currently used in most laboratory research. Without knowledge of this function, absolute perfusion measurement may be unattainable with the uptake approach.

Essentially, the goals of this dissertation work were twofold. The first goal was to optimize and modify the NMR approach by developing an NMR technique with which to extract an AIF from an individual rat, performing computer simulations to determine optimum data analysis approaches, and determining the consequences of using a common (rather than individual) AIF in perfusion estimations. The second goal was to test the ability of the modified NMR uptake approach *versus* that of a commonly used absolute perfusion measure (which does not require knowledge of the AIF) to determine absolute perfusion in a rat tumor.

This initial chapter will further explore the rationale for determining perfusion in tissues, with an emphasis on its importance regarding perfusion measurements in solid tumors. It also contains a section which will introduce the reader to the development of tissue flow and perfusion measurement techniques commonly implemented in experimental laboratories and in medical settings. This section does not analyze every perfusion method ever developed, but discusses the indicator techniques from which the NMR perfusion method evolved, as well as the commonly used microsphere technique against which most perfusion methods (including the NMR methods) have been

compared. It also explores the preliminary work which was performed in our laboratory using the novel NMR uptake approach, discusses the strengths and shortcomings which this early approach displayed, and outlines the objectives of the research presented in the remainder of this dissertation.

B. Measurement of perfusion in tissues

There has been research interest focused on designing methods to measure the presence and tissue concentrations of cellular nutrients such as glucose, oxygen, hormones and growth factors, since it is the presence and abundance of these factors which is critical to the growth and metabolic state of the tissue under study. More generally, knowledge of the characteristics of blood delivery to tissues can elucidate the physiology and metabolic status of a tissue, particularly since it is the blood through which these nutrients, as well as waste products, drugs and even heat are delivered to, or removed from, the tissue. As a consequence, many diverse methods have been used over the past century to obtain some measure of tissue vascularity and function which may yield useful information relevant to the tissue physiological status. Among these methods are measures of tissue vascularization [1], capillary permeability [2], total volume blood flow [3], vascular volume [4,5], and capillary perfusion.

Arguably the most relevant measure is of the *perfusion* (*i.e.* the blood flux through the tissue, commonly expressed in ml/(100 g·min)). Most of the tissue perfusion occurs at the capillary level, precisely where the majority of molecular exchange takes place between the tissue and the blood. Furthermore, it is the delivery of the nutrients and drugs at this capillary level which can influence energy status, metabolism, proliferative

potential and the tissue response to therapeutic intervention. Though the literature often treats the terms flow and perfusion as equivalents, to avoid any confusion between the two terms, this dissertation will define flow to be the volume of blood entering and leaving a tissue over a period of time (*i.e.* a *rate* in ml/min), and define perfusion to be this rate per volume of tissue as described above.

C. Influence of perfusion on therapy

1. Rationale

The knowledge of volume-average perfusion through tissues may be of essential value when describing the tissue's metabolic status, predicting its growth potential, and perhaps most importantly, when trying to improve and measure response to a therapeutic intervention. Data regarding the regional variations of perfusion may yield additional information helpful in diagnostics and treatment. Generally, the normal tissues are well- and homogeneously perfused. However, the presence of conditions such as embolisms, aneurysms and vascular disease may significantly disrupt perfusion in normal tissues and create areas of low or no perfusion. Methods to quantitate and localize areas with compromised perfusion characteristics would be indispensable in diagnosing problematic conditions, planning therapeutic interventions, and monitoring the response of the tissue over time. Solid tumors, on the other hand, have long been known to exhibit perfusional heterogeneity [6-11], a characteristic which may complicate therapies. Examples of how perfusion through tissue can influence the response to common therapy modalities are discussed below. The ability to quantitate whole-volume or regional perfusion in any tissue is of relevance, but in this dissertation, an emphasis will be placed on the

importance of measuring the perfusion in solid tumors.

2. Drug delivery

The relationship between the effectiveness of drug therapy and perfusion is straightforward. For efficacious tissue response to a drug, one needs to be certain that the agent is delivered to the tissue in sufficient concentration, and/or maintained over a sufficient period of time. Tissue cells which experience a low perfusion will necessarily have less drug delivered than cells experiencing a higher perfusion, limiting the efficacy of the therapy. The success of solid tumor chemotherapy can also be greatly affected by perfusion. Cells residing in regions with low perfusion will experience a lower concentration of drug, and chance of survival of the cells in these regions will be enhanced. Furthermore, intracellular metabolism of some agents is necessary to create an active compound from the delivered pro-drug, so cells which are quiescent and energy starved due to poor perfusion may not spend the metabolic energy to activate sufficient amounts of a pro-drug to the active form. Additionally, the cytotoxicity of some chemotherapeutic agents depends on the environmental acidity [12]. Since the pH of the tissue is regulated by the perfusion, the inherent efficacy of an agent may be predicated by the perfusion, regardless of the amount of drug delivered. Each of these factors may need to be considered, along with the tissue perfusion characteristics, when planning and predicting a chemotherapeutic approach and outcome.

3. Radiotherapy

Radiotherapy is a common modality for treating solid tumors. Importantly, this form of therapy can also be impacted by the perfusion through the tissue for the following reason. It has been long known [13] that radiation is not as effective in causing cellular

damage and death when oxygen is present in very low concentrations (below 0.5%, or 3 mm Hg). This is because the most significant radiation damage occurs through the production of oxygen radicals caused by the transfer of energy from the ionizing radiation to oxygen molecules. These oxygen radicals can cause extensive damage to most cellular materials, and often exert their lethal effect by causing DNA strand breakage. Low tissue perfusion means lower delivery of oxygen-carrying red blood cells. Therefore, less oxygen will be available within the tissue to be converted into a radical state and cause damage. Cells residing in low perfusion regions are therefore less radiosensitive than those cells experiencing a normal oxygen tension, and will need more ionizing radiation to achieve an equivalent amount of radiation induced damage.

4. Alternative modalities

There are also other therapeutic approaches currently being tested against solid tumors whose effectiveness may benefit from knowledge of the tumor perfusion. Therapy through the temperature modulation of a tissue by the addition or subtraction of heat (termed hyper- and hypo-thermia, respectively) may be enhanced by low perfusion through a tissue, since the maintenance of the tissue temperature is critical to success with these therapies, and low perfusion will reduce the dissipation or arrival of the heat from the solid tumor. Moreover, hyperthermia has been found to be more effective under low pH conditions [14]. Since tissues with low perfusions often have a buildup of acidic metabolic waste products in the extracellular space, and therefore exhibit a reduced pH, such tissues would be more amenable to this form of therapy. As a consequence of Chu's finding [14], therapeutic approaches have been developed to enhance hyperthermic therapy by perfusion modulations through the use of vasoactive agents. By reducing the

tumor perfusion in this fashion, resultant hyperthermic therapy was found to have an enhanced cell kill [15]. There also has been interest in so-called bioreductive agents; bifunctional alkylating agents which have preferential cytotoxicity under hypoxic conditions [16]. Therefore, these compounds may have applications in tumors which demonstrate low perfusion, or have the perfusion lowered (ideally after delivery of the bioreductive agent) through the use of vasoactive agents [17-19]. Knowledge of tissue perfusion would aid in adapting an appropriate therapeutic approach.

D. Tumor vasculature

1. Characteristics

It should be clear from the above discussion that the sensitivity of normal and cancer tissues to a variety of therapies can be profoundly influenced by the perfusion. Efficacious therapy against a solid tumor is further complicated by the fact that solid tumors often have vascular characteristics which are not observed in normal tissues - characteristics which impact the delivery of blood to the tissue. For example, the blood vessels that supply the solid tumor are often built rapidly as an angiogenic response to rapid tumor growth. To keep up nutrient supply with the metabolic demands of a rapidly growing tissue, angiogenic factors are produced from the nutrient deprived tissue, and new vasculature is constructed towards it from the normal vasculature. However, these rapidly built vessels are often poorly constructed, and do not always follow branching patterns found in normal tissues (*e.g.* artery, arteriole, capillary, venule, vein), but often contain shunts between artery and vein which bypass traditional capillary beds [20]. These shunts therefore reduce the surface area of nutritive exchange within the tumor.

There are many other unusual characteristics that tumor vasculature exhibits. Generally, the vasculature that develops in tumors often lacks smooth muscle and nerve termini [21]. This prevents these blood vessels from directly responding to vasodilators, though tumor perfusion modulation may be achieved by systemically modulating normal vessels in the host. Another characteristic of tumor vasculature is that the blood vessels themselves are often tortuous, with irregular vascular diameters and aborted blind ends [22]. The vascular vessels, in particular capillary vessels, have generally larger diameters [22,23] than the blood vessels found in normal tissue [24], thus reducing the exchange area per volume of blood present in the capillary. The vessels may also be constructed with incomplete basement membrane and cell lining [25,26], causing the vessels to contain fenestrations (holes) and leak, and so have a significant exchange in areas other than capillary vessels. The rapidly constructed vessels at the leading edge of tumors have been demonstrated to contain a significant number of these endothelial fenestrations [27].

Another characteristic of solid tumors which may alter perfusion is that the complementary lymphatic system (which allows drainage of excess extracellular fluids in tissues) is not developed adequately [28]. This can lead to an inability of the tissue to regulate the interstitial pressures which arise. If the interstitial pressure exceeds that of the blood pressure within any of the blood vessels within the tissue, these functional blood vessels can collapse, resulting in alterations in perfusion.

Also, a rapidly developing tumor may grow faster than a sufficient vascular supply can be constructed, resulting in sparsely perfused regions within the tumor, especially towards the central core [6,29]. Lastly, blood has been observed actually reversing direction through the vasculature in tumors grown under a window chamber

[30]. When such reversals occur, the nutrient poor (and waste product high) venous blood, rather than the nutrient rich arterial blood, is sent through the capillaries. These blood flow directional reversals may be a consequence of shunting, poor definition of vessels, or an elevation of interstitial pressure [31].

2. Implications

The vascular abnormalities described in the preceding section are not necessarily distributed homogeneously in solid tumors, but are often found to occur heterogeneously, especially in larger tumors, resulting in perfusional heterogeneity [7-11]. This regional tumor perfusion heterogeneity may have its greatest impact in the treatment of cancer through its effect on therapeutic response. Resistance to therapy need not be due to inherent factors in the tissue, but may be a reflection of the tumor vascularization. Consequently, to gain a better understanding of the physiological status of the tissue, to gain insight into how efficacious an anti-tumor therapy has been, and to tailor a form of therapy which may be most appropriate for a given tumor given its vascular status, methods to measure perfusion through solid tumor tissues are needed. Importantly, methods which can measure whole-volume perfusion, as well as obtain spatial information concerning the possible perfusional heterogeneity through the tissue of interest, are needed to better aid the researcher and physician in attaining these goals.

E. Measurement techniques

1. Background

Since manipulating tumor vasculature and perfusion has become a recent focus in anticancer research [32], accurate measurements of tissue perfusion, as well as following

perfusional change in response to therapy, are of interest. The development of tracer techniques which perform quantitative measurements of blood flow (tissue perfusion measurements among these) has been in progress for well over a hundred years [33]. Most of these techniques can be placed into two well-studied categories, each of which was first developed through different assumptions: the particulate methods, in which small particles embolize in the arterial vasculature (microspheres are the classic example); and the indicator methods, in which there is an exchange of the tracer between the tissue and blood. All of these methods are well established for measuring perfusion in a variety of living tissues, yet none can be said to be an ideal perfusion measurement method as defined in the introduction to this chapter. As both particulate and indicator methods are employed in this dissertation, the general history and mathematical description of these two widely used methods is included.

2. Particulate methods

a. Initial attempts

The first use of small blood-borne particles to study circulation was described over 100 years ago [34]. The rationale for this approach was that small particles carried in the blood stream would embolize in the small vasculature in direct proportion to the blood flow to the tissue. Earlier this century, small particle studies to determine the path of blood through the heart were reported by Pohlman [35], who injected cornstarch granules into the umbilical vein of fetal pigs, then counted the granules in the blood of different chambers of the heart. To perform repeated measurements on the same animal, he used granules stained with iodine in a second injection to distinguish them from the initial injection granules. Though this procedure could yield important information

regarding the path which blood followed through tissues, the impermanence of the particles becomes a major limitation for longer term studies. It was nearly forty years later when the use of what can be described as true microspheres was first introduced into the literature, when Prinzmetal used glass microspheres (10 - 400 μm diameter) to study the coronary circulation of the human heart [36]. Though this technique was successfully implemented, the microspheres had to be counted and laboriously separated from the tissue by hand under a light microscope.

b. Development of radioactive microspheres

A significant improvement in the detection of the deposited microspheres occurred in 1958, when a pair of researchers at the Oak Ridge National Laboratory created the first radioactive glass microspheres by placing them in a nuclear reactor [37,38]. In the reactor, neutron bombardment resulted in the conversion of some of the stable ^{23}Na in the glass into radioactive ^{24}Na. Consequently, using these microspheres, one could simply detect and quantitate with a gamma counter any microspheres which were trapped in a tissue sample. Homogeneous radiolabelling of the spheres was possible if the microsphere size and incubation times in the reactor were uniform. Then, if similarly sized and labeled microspheres were used, the radioactivity in a tissue sample was directly proportional to the number of trapped spheres. By injecting uniform ^{24}Na labeled microspheres into dogs, these researchers performed the first radioactive microsphere circulation studies [37,38].

The short radioactive half-life ($T_{½}$ = 15 h) of the ^{24}Na labeled microspheres made experimentation with them inconvenient (though others did work with them [39,40]), and spurred development of alternative microsphere materials, as well as use of longer-lived

radioactive labels. What was to become the industry standard was an insoluble carbonized plastic microsphere developed by the 3M Company. This material could be created in a variety of sizes, and be labeled with a selection of much longer-lived radioactive materials. These plastic microspheres gained in popularity, and spurred much research on the circulation in organs and animals. In 1967, methods were developed to derive the cardiac output and tissue perfusion through radiolabeled microspheres [41]. By using different radiolabels with differing radiation emissions, multiple experiments may be performed on a single animal before extracting the tissue for observation.

c. Development of non-radioactive microspheres

There are a number of concerns raised whenever radioactive materials are present in the laboratory. Any use of radioactivity in the laboratory, especially when administered to animals, is becoming increasingly difficult to maintain. From a safety concern, there is an interest in reducing the direct exposure of workers to radiation. Accidental contamination of lab areas or co-workers is also a potential problem whenever radioactive materials are present. This concern for safety results in necessary, yet restrictive legislation and control. And there are economic concerns as well, since radioactives are often expensive in terms of purchase, storage and disposal. There are further costs in properly training workers to handle radioactives, as well as the cost of the machinery to detect and analyze the radiation. These factors have driven the recent progress towards alternative methods to label and detect microspheres.

The first documented method of an easily quantifiable non-radioactive microsphere was published in 1988 [42]. This method used colored microspheres, and quantified the microspheres through direct counting. The tissues under study were

removed, weighed, and digested (releasing the microspheres), then the microspheres were collected and hand-counted with a haemocytometer under a light microscope. A similar method using fluorescent microspheres was introduced five years later [43], with the benefit that the microspheres could be machine counted using a fluorescent activated cell sorter. Each of these non-radioactive methods was validated against standard radioactive microspheres by simultaneous injection of the two types of microspheres [42,43].

An alternative method which did not require the counting of individual microspheres was introduced by Kowallik *et al.* [44] who used uniformly labeled colored microspheres. In this method, rather than trying to count the microspheres individually with a microscope, the microspheres are separated from the tissue, then dissolved. This releases the dye from within the microspheres into a solvent. Quantification of the number of microspheres which were trapped within a given tissue sample is straightforward with spectrometry. To take advantage of the higher sensitivity and specificity of fluorescent dyes over visible dyes, methods using fluorescently labeled microspheres were then developed and validated *versus* radioactive microspheres [45,46]. As is true for distinctly labeled radioactive microspheres, by using different colors and dyes, multiple experiments with these non-radioactive microspheres could be performed on an individual animal. The fluorescently-labeled microsphere technique as described by Glenny [45] was the approach utilized in this dissertation research.

d. Reference organ technique

The theoretical principles on which tissue perfusion measurements with microspheres are based are straightforward. A bolus of the small particles is injected into the left atrium or left ventricle (the arterial side), where they are mixed into the

bloodstream, and allowed to circulate freely through the arterial vasculature. If the microspheres are well-mixed, of a reasonable diameter, and not aggregated, the individual microspheres are free to distribute through the vascular system. The fraction of the microspheres which arrive at a given vascular region is directly proportional to the fraction of the cardiac output to that region. When a microsphere enters a blood vessel which is smaller in diameter than itself, it will become trapped. By choosing a microsphere diameter somewhat larger than the average capillary size found in a tissue. the microspheres will embolize at the capillary level, and give information concerning the perfusion through the capillary bed. When the microsphere technique is optimally performed, the collection of a number of arterial-borne particles embolizing in the capillary bed of any given tissue will be proportional to the arterial blood perfusing the tissue. Therefore, one can derive the true perfusion by determining the number of particles trapped, and comparing this number to a known standard, by application of the following general equations.

One assumption which must be taken is that the blood flow (in ml/min) is the only factor which affects the distribution and deposition of the microspheres. If true, then the number of microspheres in any organ or tissue sample will be directly proportional to the flow to that tissue, as described in **Equation I.1**.

[Eq I.1]

$$\frac{\text{blood flow to organ A}}{\text{microspheres in organ A}} = \frac{\text{blood flow to organ B}}{\text{microspheres in organ B}} = \textit{etc.}$$

Furthermore, the total body flow is defined as the cardiac output, which is a measurable physiological characteristic (for many large animals). If there is conservation of matter

(the microspheres neither increase nor decrease in number after injection), then the following equation is true.

[Eq I.2] $$\frac{\text{total body blood flow}}{\text{total body microspheres}} = \frac{\text{cardiac output}}{\text{total microspheres injected}}.$$

Therefore, by considering the total body blood flow to be a general case of organ blood flow, one can substitute **[Eq. I.2]** into **[Eq. I.1]** to obtain **[Eq. I.3]**.

[Eq. I.3] $$\frac{\text{blood flow to organ A}}{\text{microspheres in organ A}} = \frac{\text{cardiac output}}{\text{total microspheres injected}}.$$

This relationship means that if both the cardiac output and the total number of microspheres injected are known, the flow to any given tissue or organ can be determined by counting the number of deposited microspheres in that tissue or organ. As an example, if 10,000 microspheres are injected into an animal which has a cardiac output of 1 liter/minute (l/min), an organ with 1000 deposited microspheres had a flow of 0.1 l/min, or 100 ml/min during the experiment. Likewise, if 5,000 microspheres were injected into an animal with the same cardiac output (1 l/min), an organ with 1000 deposited microspheres would have a flow of 200 ml/min. By weighing the tissue of interest, a perfusion for that tissue in terms of ml/(min·gram of tissue) can be calculated.

In smaller animals commonly used in experimental research, the cardiac output is difficult (rat) if not presently impossible (mouse) to measure with accuracy. However, since the knowledge of the flow to any one organ allows determination of flows to any other **[Eq. I.1]**, an alternative approach using an artificial reference organ was developed [47,48], and later validated for use in the laboratory rat [49]. In this now commonly used

approach, an artery (generally the femoral artery) is catheterized, and a reference sample of arterial blood is drawn into a syringe (the reference organ) from the animal at a known flow rate (ml/min) throughout the microsphere injection period. Then, because the flow rate of the reference sample is known, by counting the microspheres trapped in the reference organ, one can determine what the flow was to any tissue or organ by counting the microspheres trapped in the tissue of interest. The cardiac output of the animal can be back-calculated if desired by application of **[Eq I.3]**, if the total number of microspheres injected is known. It is an adaptation [50] of this reference method [48,51] using fluorescent methods [45,46] that was employed in the comparison experiments of this dissertation. The methods are discussed in full in Chapter III.

e. Sources of error

There are several potential sources of error when using the microsphere technique to measure tissue perfusion. Some of these are unavoidable, being a consequence of the particles themselves. Others are methodological errors, with good technique being a way to reduce the influence these potential errors may have on the perfusion measurement. Many of the errors common to the most widely used microsphere quantification techniques (radioactive detection; microsphere counting; fluorescent dye detection) are delineated along with their solutions in **Table I.1**, which is adapted from Prinzen and Glenny [52].

Table I.1

Sources of error in blood flow measurements with microspheres

Potential error	*Method*			*Solution*
Stochastic errors	**RA**	**CM**	**FL**	
sphere distribution	✸	✸	✸	use more spheres
decay distribution	✸			use more, or more active spheres
gamma counting error	✸			increase counting time or activity
Methodological errors				
non-uniform mixing	✸	✸	✸	use mixing chamber
aggregation	✸	✸	✸	use sonication, use detergent
reference sample	✸	✸	✸	√ withdrawal speed, sampling site
circulatory impairment	✸	✸	✸	use smaller or fewer spheres
flow biasing	✸	✸	✸	use smaller spheres
non-entrapment	✸	✸	✸	use larger spheres
diameter variability	✸	✸	✸	quantify
signal quenching			✸	dilute sample with solvent
loss of spheres when isolating		✸	✸	use single tube processing
inaccurate solvent volumes		✸	✸	use accurate pipettes
dye stability			✸	check stability in solvent
background signal			✸	choose appropriate colors

RA = radioactive spheres; CM = counting of spheres; FL = dye extraction of fluorescent spheres

Stochastic errors (alternatively termed random errors) occur as a result of statistical variations, and may become a pronounced problem when a sample size is small. Theoretical studies were performed to determine how a microsphere measurement's precision (defined as the coefficient of variation) changes as the number of microspheres trapped within a sample changes [53]. This work indicated that the coefficient of variation is less than 5% if more than 400 microspheres are in the measured tissue sample. The coefficient of variation approaches 9% if only 100 spheres are

trapped, but increases rapidly as fewer microspheres are trapped. These simulated results were later independently verified in an animal model [54]. These results indicate that to maintain precision in the perfusion measurement, there must be a sufficient number of microspheres in the sample to represent the perfusion adequately [53]. A consequence of this type of potential error is that it becomes less a factor with higher flowing tissues, as more microspheres are delivered to the tissue, but remains a concern when measuring lower flowing tissues or smaller volumes. Since there is a limit to the number of microspheres which can be safely administered to an animal before severe hemodynamic effects due to the microsphere embolization occur, there are limits to the possible resolution obtained through this method.

There are also methodological errors that need to be minimized. Aggregation of the microspheres before injection can be a problem since the microspheres will not distribute proportionally in the vasculature. This will lead to an overestimation of perfusion in areas where the aggregates become trapped (since the signal or dye concentration will be much elevated over what should have been deposited in the region). This subsequently causes other regions to have an under-representation of microspheres, and results in an underestimation of perfusion for these regions. The potential for microsphere aggregation can be eliminated by sonication of the microspheres prior to injection, addition of a mild detergent to the microsphere carrier liquid, and by manually agitating the microsphere solution (by tapping the catheter containing the microspheres) immediately before intra-arterial delivery. Also, because a common enhancer of aggregation is bacterial growth on the outside of the microspheres, reduction of aggregation potential can be accomplished through sterile technique.

When using the reference sample technique, all tissue perfusion measurements are dependent on accurate sampling. The reference sampling should begin just prior to the systemic introduction of the microspheres, and should continue until sufficient time has elapsed to ensure no microspheres are flowing in the vasculature. The rate of withdrawal must be constant, in order to derive flow rates to other tissues. Also, care should be taken to ensure that the reference organ sample is not withdrawn too rapidly. If too rapid, the catheterized artery may collapse from the pull, resulting in little blood or microspheres actually withdrawn. A further concern is that if too much blood is withdrawn from a small laboratory animal such as a rat, gross hemodynamic changes can occur which alter the tissue perfusion throughout the animal by altering the cardiac output. A method to reduce any hemodynamic changes associated with reference organ sampling is to replace simultaneously the blood taken with an equal volume of blood from a matched donor (generally through a venous catheter).

There are also problems to consider regarding the size of microspheres used in the study. If the microspheres are too large, embolisms may occur at the artery (rather than arteriole or capillary) level. Sufficient embolization in critical organs or tissue sites can alter the cardiac output or organ physiology of the animal and result in death. Also, large microspheres are prone to a physical process called axial streaming, in which large spheres preferentially stream in the center of a high speed artery and do not distribute proportionally at branching junctions in the arterial system [55,56]. However, microspheres which are smaller than the capillary bed of the tissues of interest will not trap, but will pass through and underestimate the perfusion through that tissue. Further, if too many microspheres are used for perfusion studies, the cardiac output and organ

functions are susceptible to alteration. One must balance the need for increased precision (by getting more microspheres into the sample) with what can safely be administered to the animal. Consideration of both the volume of the tissues being sampled and the range of perfusions generally found in such tissues are necessary in designing proper experimental protocols using microspheres.

3. Indicator methods

a. Introduction

Over the past century and a quarter, there has been a tremendous development of indicator approaches to measure blood flow and tissue perfusion. What follows is a brief history of the development of the indicator techniques, from the first method proposed by Fick [57] to the methods proposed by Mattiello and Evelhoch [58], with an emphasis on the equations which describe these methods.

b. Fick

The development of the indicator technique to estimate circulatory characteristics was initiated in 1870 by Fick [57]. The relationship he derived, the Fick Principle, is an application of the Law of Conservation of Matter, and proposes that in a system in which the arterial flow equals the venous flow (a steady-state system), the tissue uptake (dQ_t/dt) of an indicator equals the difference between the amount of indicator entering (C_{in}) and leaving (C_{out}) the tissue at a flow F (commonly expressed in units of ml/min), as described in **[Eq.I.4]**.

[Eq. I.4]
$$F \cdot C_{in} - F \cdot C_{out} = dQ_t/dt$$

Note that this relationship has conservation of flow, such that the flow into the tissue

equals the flow out of the tissue. This can therefore be simplified to **[Eq. I.5]**.

[Eq. I.5] $$F \cdot (C_{in} - C_{out}) = dQ_t/dt$$

Fick rearranged this equation to form **[Eq. I.6]**, and then used this relationship to estimate cardiac output by considering the cardiac output (C.O.) to be defined as the total F into (and out of) the body tissues; the total body oxygen uptake (VO_2) to be dQ_i/dt; and the oxygen concentrations of the arterial (C_aO_2) and venous (C_vO_2) blood to be equivalent to C_{in} and C_{out}, respectively **[Eq. I.7]**.

[Eq. I.6] $$F = dQ_t/dt \cdot (C_{in} - C_{out})$$

[Eq. I.7] $$C.O. = VO_2/(C_aO_2 - C_vO_2)$$

Then, by measuring the blood oxygen levels in the artery and vein (C_aO_2 & C_vO_2), and determining the amount of oxygen "taken-up" by the body (VO_2), he obtained the first estimate of the C.O. through an indicator technique.

c. Steady-state measures

In 1897, the first practical application using an indicator for determining flow measurements in a biological system was introduced by Stewart [59]. His approach used a constant infusion (at the rate F_i ml/sec) of an indicator (at concentration C_i) upstream of a tissue until that indicator had reached a steady-state concentration downstream of the tissue (C_{out}). The influx into the tissue under study can be described as $F_i \cdot C_i$. Once at the steady-state condition, the outflux of indicator is equal to the concentration (C_{out}) times the total flow (the tissue through-flow F plus the infusate flow F_i). Stewart

reasoned that once a steady-state has been achieved, by definition the influx of an indicator into a tissue will equal the outflux of the indicator from the tissue, yielding the following relationship.

[Eq.1.8.] $$F_i \cdot C_i = C_{out} \cdot (F + F_i)$$

However, if the infusion rate is much smaller than the tissue through-flow, then the equation can be written as follows.

[Eq.1.9] $$F \cong F_i \cdot (C_i / C_{out})$$

Stewart used an infusion of NaCl as an indicator, and by measuring the conductivity of the fluids entering and exiting the tissue, he could determine the indicator concentrations both upstream and downstream of the tissue of interest. Since the infusion flow rate was known, by applying **[Eq.I.9]** with this information, he calculated the blood flow to tissues. Volume average perfusion rates could be extracted if the mass of the tissue is known. This constant infusion, steady-state approach has been used successfully with numerous varieties of indicators and detection techniques.

d. Bolus-injection measures

The first published account of measuring flow or perfusion by bolus injection of an indicator was introduced by Henriques [60]. The principles this method is based on were so thoroughly studied by Hamilton [61,62], that it has been termed the Henriques-Hamilton Principle. In this model, a known amount (m_0) of an indicator is injected into a system with one or more inlets and a single well-mixed outlet from which one samples. Over very short periods of time (dt), the amount of indicator leaving the system (dm_{out}) is equal to the volume of blood leaving ($F \cdot dt$) times the concentration of the indicator

(c(t)). If the indicator is sampled until it has completely cleared the tissue, the following mass-balance equation results.

[Eq.I.10] $$m_0 = F \cdot \int_0^\infty c(t)\, dt$$

The equation can be easily rearranged to solve for the tissue flow. Like many researchers before him, Hamilton used the equation to calculate the cardiac output in man.

e. Kety

The successful application of diffusible indicators in obtaining flow and perfusion measurements is largely due to work performed in the 1940's by S. S. Kety [63-65]. He derived his equations from an equation of Fick **[Eq.I.5]**, which stated that the amount of metabolically inert indicator taken up by a tissue is equal to the amount brought to the tissue by arterial blood minus the amount taken away by the venous blood. He reasoned that if the mass of the tissue is known, the concentration of the indicator in the tissue (C_t) is given by the equations

[Eq.I.11] $$\frac{dCt}{dt} = \frac{dQt}{dt} \cdot 1/W = F \cdot (C_a - C_v)/W$$

[Eq.I.12] $$C_t = \lambda \cdot C_v,$$

where λ is defined as the partition coefficient which expresses the ratio of the solubility of an inert indicator between the tissue and blood, and W is the mass of the tissue. Kety also derived the following to account for the extent diffusional equilibrium is attained between the blood and the tissue at the capillary level,

[Eq.I.13] $$m = 1 - \exp(-\frac{PS}{f})$$

where m is the extraction fraction (the fraction of the tracer which can extract from the

blood to the tissue), PS is the permeability-surface area product for the tissue volume being measured, and f is defined as the perfusion. In tissues with low enough perfusion or sufficiently high PS, $m \cong 1$. In this case, the indicator is termed a freely-diffusible, or flow-limited tracer (*i.e.* the exchange is determined by the rate of perfusion). By realizing that perfusion (f) is the flow (F) per mass (W), then combining **[Eq.I.11]** with **[Eq.I.12]**, one obtains the following.

[Eq.I.14]
$$\frac{dCt}{dt} = (mf/\lambda) \cdot (\lambda \cdot C_a - C_t)$$

Then, by substituting $k = mf/\lambda$, the equation simplifies to

[Eq.I.15]
$$\frac{dCt}{dt} = k \cdot (\lambda \cdot C_a - C_t).$$

This resultant relationship **[Eq.I.15]** is a linear differential equation which has the following three solutions for the instantaneous indicator concentration in a tissue at any time T ($C_{t(T)}$).

(Solution 1) If the arterial concentration of the indicator varies with time (*i.e.* as occurs with a bolus injection), there is the general solution

[Eq.I.16]
$$C_{t(T)} = \lambda \cdot k \cdot e^{-kT} \int_0^T C_{a(t)} \cdot e^{kt}\, dt \quad .$$

The term $C_{a(t)}$ describes the indicator concentration in the artery as a function of time (t), and is commonly referred to as the arterial input function (AIF). Generally $C_{a(t)} = 0$ at time zero. However, if the indicator concentration is not zero, but is in equilibrium with the tissue at time zero (perhaps as a residual from a previous measurement), the equilibrium indicator concentration should be subtracted from both $C_{a(t)}$ and $C_{t(T)}$ when

applying this equation.

(Solution 2) If the indicator is given as a constant infusion, then C_a is a constant, then Equation I.15 simplifies to

[Eq.I.17] $$C_{t(T)} = \lambda \cdot C_a \cdot (1 - e^{-kT}).$$

(Solution 3) Finally, if the indicator is already present within the tissue (at an initial tissue concentration of C_0), the tissue may be allowed to desaturate (*i.e.* the $C_a = 0$). This is the special case in which the indicator is directly injected into the tissue of interest, and allowed to clear from the tissue.

[Eq.I.18] $$C_{t(T)} = C_0 \cdot e^{-kT}$$

The Kety method was initially used by Kety [63,64] with nitrous oxide, though he later extended the technique with radioactive sodium [65]. Subsequently, the method became more widely implemented with radioactive inert gases such as ^{85}Kr and ^{133}Xe as indicators. Each of these indicators has some inherent limitations though. Among these limitations are: (a) different solubilities in lipids and water; (b) partition coefficients which are difficult to evaluate with certainty; and (c) low-energy radiation with ^{133}Xe, limiting tissue perfusion measurements with this tracer to tissues near the surface.

F. Water as an indicator

1. Introduction

The aforementioned indicator limitations led workers to search for superior tracers. A logical choice was water. Its characteristics offer these advantages over inert gases: (a) it is an ideal indicator for observing the water compartment of tissues; (b) it is

easy to measure the partition coefficient by calculating the relative amounts of water in the tissue of interest and the blood; and (c) the solubility of the tracer water into the tissue water and blood water is infinite compared to the limited solubility of inert gases [66].

Exogeneously administered water can be distinguished from the natural abundance blood and body tissue water (and thereby used as an indicator) by replacing either the hydrogen or the oxygen atoms with an isotopic equivalent. Hydrogen isotopes which are of extremely low natural abundance are deuterium (a non-radioactive isotope which contains a proton and neutron in its nucleus) and tritium (a radioactive isotope which contains a proton and two neutrons in its nucleus; $T_{½}$= 12.26 yr). Oxygen has eight isotopes, ranging from ^{13}O to ^{20}O, of which only ^{16}O, ^{17}O and ^{18}O are stable. A radioactive oxygen isotope which is commonly substituted in water and used for isotopic water studies is ^{15}O ($T_{½}$ = 124 s).

Detection of water containing substitutions for either the normal oxygen or hydrogen is possible with various techniques. An early study with an isotopic water demonstrated that the delivery of deuterated water (D_2O) into tissues is dictated by the tissue perfusion [67]. However, this dissertation will concern itself with two modes of indicator detection: positron emission tomography and nuclear magnetic resonance.

2. PET

The invention of the positron emission tomograph (PET) scanner [68] led to the development of new methods with which to estimate tissue perfusion using this alternative tool [69-72]. An advantage of the PET scanner is that an indicator can be non-invasively and spatially localized within a tissue, leading to studies of potentially important regional differences in perfusion. Raichle and Herscovitch [73] developed

techniques which used an isotopic form of water ($H_2{}^{15}O$) as the indicator. As with all isotopic waters, $H_2{}^{15}O$ freely exchanges with the water in the body, and is a freely-diffusible tracer under most conditions. However, like most positron-emitting radioisotopes used as indicators, it is quite radioactive, and must be administered in extremely small concentrations for safety concerns. As a consequence, it is not possible to receive sufficient instantaneous indicator concentration in a tissue to apply **[Eq.I.16]** with confidence and extract perfusion information using this isotopic water. Herscovitch *et al.* recognized that when performing PET experiments, because the data are collected over a period of time, rather than instantaneously, the collected PET data (I) contain an integration of the instantaneous indicator concentration between the time limits of the scan (t_1 to t_2).

[Eq.I.19]
$$I_{(t1,t2)} = \int_{t1}^{t2} C_{t(t)}\, dt$$

With knowledge of the AIF (attainable in large animals), they could relate this uptake integral ($I_{(t1,t2)}$) to perfusion through a second-order polynomial **[Eq.I.20]**, where a and b are coefficients determined through non-linear least-squares fitting of the perfusion:uptake integral pairs, such that

[Eq.I.20]
$$f = a \cdot (I_{(t1,t2)})^2 + b \cdot I_{(t1,t2)}$$

They applied these principles to studies using the radioactive water and were able to validate their PET technique in adult baboon brain perfusion measurements [74]. Perfusion measurements with this PET method in man followed shortly [75].

3. NMR-direct injection

a. Background

Calculation of perfusion with any of the equations discussed above only requires the application of an indicator, and a method with which to detect and quantitate the indicator in a tissue of interest. In the late 1980's, Ackerman recognized that since quantitative measures are routinely performed using nuclear magnetic resonance (NMR), a suitable indicator could be used for perfusion measurements [76,77]. Since isotopic water was being successfully used in PET approaches, there was no reason that an appropriate NMR detectable isotope of water distinguishable from normal water could not be utilized. The isotopic water Ackerman introduced as an NMR detectable perfusion indicator was deuterated water (D_2O), which was described above.

The direct-injection method which was introduced uses deuterium NMR spectroscopy to observe the clearance of deuterated water that has been injected into the tissue of interest. To derive absolute perfusion from an injected tissue, one must obtain a time-course of the tissue indicator concentration with sufficient time resolution. Then, the exponential decay of the observed signal over time can be related to the perfusion through application of a Kety equation **[Eq.I.18]** which was described earlier. Alternative multi-compartmental analytic approaches were also suggested to account for non-negligible recirculation of the indicator [78] in the small animals commonly used in experimental research. This direct-injection approach was successfully implemented in a murine tumor model [78, 79], and later validated as a method which measures absolute tissue perfusions through comparisons *versus* microsphere measurements in normal rat muscle [80].

b. Strengths

There are many strengths associated with the tracer clearance approach. First, the method is easy to implement in principle since it requires only that a bolus volume of tracer is injected directly into the tissue. The clearance of this tracer (or wash-out) can be monitored by NMR detection, and related to absolute quantitative perfusion by a relatively simple mathematical analysis (as described above). Through either spectroscopic or imaging detection, quantitative whole-volume or local perfusion values can be obtained in this manner. Since the D_2O tracer is also non-radioactive, none of the precautions and hazards associated with radioactives need to be considered. Also, since D_2O is in essence water, the tissue-blood partition coefficient is easy to determine [81]. Further, since the tracer is directly injected, the concentration can be made high enough so that clinical use is possible in today's existing clinical magnets despite its relative insensitivity (deuterium being < 1% as sensitive to detection as protons [82]). Perhaps most importantly, by concurrent NMR detection of other nuclides (*e.g.* ^{31}P, ^{1}H, ^{13}C), information regarding the relationship between the tissue physiology and the tissue perfusion can be discerned.

c. Weaknesses

The weaknesses of the direct injection technique, though, are not insignificant. First of all, the direct injection, though it does measure absolute perfusion in the area labeled, only labels a small area (a 10 μm D_2O injection labels about 50 mm^3 [83]). For normal tissues, this should not be of concern, since most normal tissues are homogeneously perfused. However, tumors have been shown to develop inhomogeneous perfusion patterns as they increase in size [7-9]; therefore a single sampling can be

misleading if it does not represent the entire tumor. As an example, an injection into the center of a large tumor may label the necrotic core, where the perfusion is negligible. Therefore, if patterns of heterogeneic perfusion are suspected, and need to be measured, multiple tracer injections are required to obtain a fair sampling of the tissue.

Second, the tracer injection itself may affect the perfusion of the tissue being measured. An injection can directly disrupt tissue vasculature, and cause internal bleeding. It may also affect the tissue's interstitial pressure either by causing vessels to be pinched down if the injection increases the pressure, or by opening vessels if the needle puncture relieves the pressure. In either case, the insertion of the needle and injection of the bolus of tracer can alter the perfusion precisely at the site at which the measurement is being made. In tumors, the interstitial pressure is often high [84], and perturbations of this pressure by insertion of a needle into the tumor tissue can alter the perfusion. This disruption of perfusion in a tissue may be more significant in subsequent measures of the same tissue, as would be the case in a long term study of perfusional changes as a consequence of some form of therapy. This makes these long-term studies difficult to perform, and the data difficult to interpret.

Third, accurate injection of deep tissues is difficult, if not impossible, due to the problem of delivering tracer to any given area. Lastly, intra-tissue injection of tracer requires the removal of the subject from the magnet. The difficulty in reproducibly repositioning a subject within the magnet will invariably result in a shift from the original placement. This changes the magnetic field strength over the tissue under observation, and will affect both the shimming and the voxel location (if imaging), confounding interpretation of long-term, multiple measurement studies. The misplacement of the

subject may not pose a significant hurdle in obtaining adequate signal from the tracer, but can easily cause difficulties acquiring and interpreting interleaved, multi-nuclei data.

4. NMR Uptake-approach

a. Background

Shortly after deuterium was first used as an indicator in NMR perfusion studies, Evelhoch and Mattiello introduced methods which allow for detection of the indicator after remote injection (*i.e.* not directly into the tissue, but into the subject's blood stream) [58]. This method (called the uptake-approach) is based upon the work of Herscovitch [73] which was described earlier. In essence, a bolus indicator is injected remotely into the blood stream, and NMR is used to detect the presence and concentration of the indicator in a tissue of interest. Analysis can be performed in either of two ways. One may fit the time-course to the Kety model, or, as with the PET approach discussed above. one may effectively sum the instantaneous concentrations over a window of time (the area under the curve, termed the uptake integral). Perfusion measurements from this uptake integral can be estimated through application of **[Eq.1.19]**. With either analytic approach taken, the AIF is needed for absolute tissue perfusion extraction from the data.

b. Strengths

The strengths of the NMR uptake-approach are substantial. First of all, the tissue being measured is not directly affected by the procedure. In other words, there is no puncture of the tissue to perturb the interstitial pressure or to damage the vasculature. Therefore, the perfusion being measured is not directly altered by the delivery of tracer. Second, this approach measures the perfusion throughout the tissue. This means that both whole-volume average perfusion measurements (through spectroscopic analysis of

the whole tissue volume) or regional perfusion measurements (through imaging the tissue) can be obtained. And if imaging of the tissue is performed, perfusional heterogeneities can be discerned. Finally, since the subject does not have to be repositioned, but remains stationary throughout the study, the uptake-approach is ideal for interleaved multi-nuclei experiments.

c. Preliminary studies

Using this NMR uptake approach, our laboratory performed some preliminary studies to test the power of this approach in perfusion studies of murine tumors. Since the AIF of the deuterated tracer was not known, an estimate of the AIF was assumed, using the shape of an AIF from man, with a modification to account for non-negligible recirculation. The indicator was delivered into the tail vein as a bolus volume (50 μl/injection). By performing the NMR uptake experiment in an imaging mode like the PET technique, our group related the intensity of the image pixels (the **pic**ture **el**ements) to the concentration of the indicator within these pixels. First, a proton image was obtained to measure the tissue's size and to select an appropriate slice through which a perfusion image could be taken. Then, a deuterium image was taken through this slice. Isotonic (0.9% NaCl) deuterated water was injected as a remote bolus through an inserted tail-vein catheter, and images were acquired at appropriate times post-injection. The following examples of regional information which can be obtained through this NMR uptake approach are described briefly.

i. Mapping perfusion

Figure 1.1 shows the early data sets of deuterium images (in plane resolution of 1.1 mm x 1.1 mm) taken through a 4.8 mm slice at the post-injection times indicated.

Pixels of high, medium, and low or no intensity are easily observed in each image, indicating a heterogeneity of tracer delivery to the tissue, or a perfusional heterogeneity. Although absolute regional perfusions were not determined here (since the AIF and the parameters which are important in reducing errors of perfusion estimation were not known at this point), a relative regional perfusion was estimated in those pixels with a sufficient HOD delivery (and thus sufficient intensity). A critical threshold intensity (minimum detectable intensity) for each experiment was determined from the images by calculating the mean and variance of random pixels clearly outside the tumor slice in the image (representing noise), and defining the critical intensity (I_c) of the image to be $I_c = N + 3.82 \cdot (\sigma n)$. By this approach, it becomes highly unlikely (< 0.01%) that any signal above this threshold level within the image is due to random spatially uncorrelated noise.

To determine the level of perfusion necessary to create a detectable pixel intensity in a given image, a limit of detection study was performed. This was accomplished by assuming that the mean pixel intensity in an uptake image acquired 30 minutes post-injection was equal to the volume-average uptake integral determined spectroscopically at approximately the same time. After determining the I_c for the image as described above, the integral limit of detection could be estimated. Since the relationship between the uptake-integral and perfusion had been determined, an estimation of the perfusion yielding the critical uptake integral was possible, and determined to be approximately 7 ml/(100 g·min). Pixels which appear in the first image therefore have perfusions above this estimated level. Moreover, due to the near linearity of the relationship between perfusion and the uptake integral (at least over the lower range of perfusions), pixels with more than twice this threshold intensity have perfusions > 14 ml/(100 g·min): those with

more than three times the threshold intensity have perfusions > 21 ml/(100 g·min); *etc.*

Those pixels which are deemed unmeasurable in the first image set therefore have perfusions estimated at less than 7 ml/(100 g·min). However, it may be important to distinguish between low and no perfusion. Therefore, images of longer duration or at a later time post-injection must be obtained to distinguish between these two important groups. When this is done, areas with low blood perfusion may have sufficient delivery of the tracer necessary for detection. Uptake image acquisitions between 510-600 seconds and 510-870 seconds post-tracer injection were used to detect minimum regional perfusions estimated at 3 and 1 ml/(100 g·min), respectively (by the methods described above). By creating perfusion categories (< 1 ml/(100 g·min), designated no perfusion; 1-3 ml/(100 g·min), very low perfusion; 3-7 ml/(100 g·min), low perfusion; 7-14, medium; 14-21, medium high; 21-28, high; > 28, very high perfusion), a relative tissue perfusion map can be constructed which allows for easy recognition of the regional perfusion variations. Figure 1.2 is an example of what type of information can be extracted through perfusion mapping. The low perfusions seen in this example are not atypical for solid tumors, which generally have much lower perfusions than do most normal, uncompromised tissues.

ii. Observing regional therapeutic response

To demonstrate how the novel NMR technique can be a valuable tool in observing the response of regional tumor perfusion to a therapy, the following experiment was done. Regional perfusion changes can be created by selective therapy of a portion of a tumor using photodynamic therapy (PDT). Here, the photosensitizing drug Photophrin II was administered. This drug, upon photoillumination, becomes activated and destroys nearby

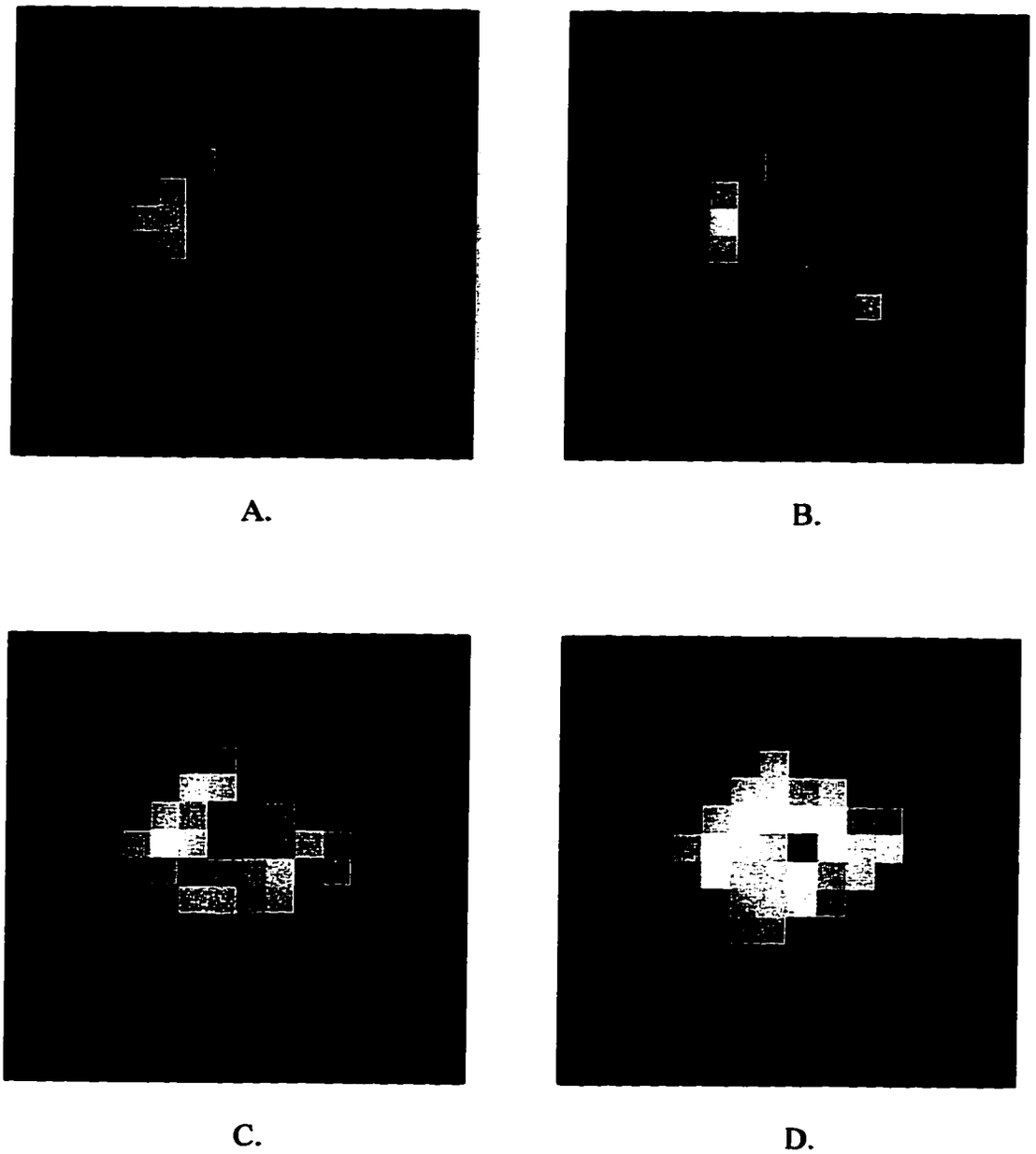

Fig. 1.1 (A- D). Deuterium NMR uptake images acquired from a 461 mm^3 RIF-1 tumor transplanted on the flank of a C_3H/HeJ female mouse. The images were obtained over the following time periods: 0 - 47 sec; 48 - 94 sec; 282 - 329 sec; and 611 - 658 sec (Fig. 1.1 A, B, C, and D respectively) after remote tail vein injection of 100 µl isotonic D_2O. Note that certain pixels are brighter much earlier than others, and others lighten slowly over time.

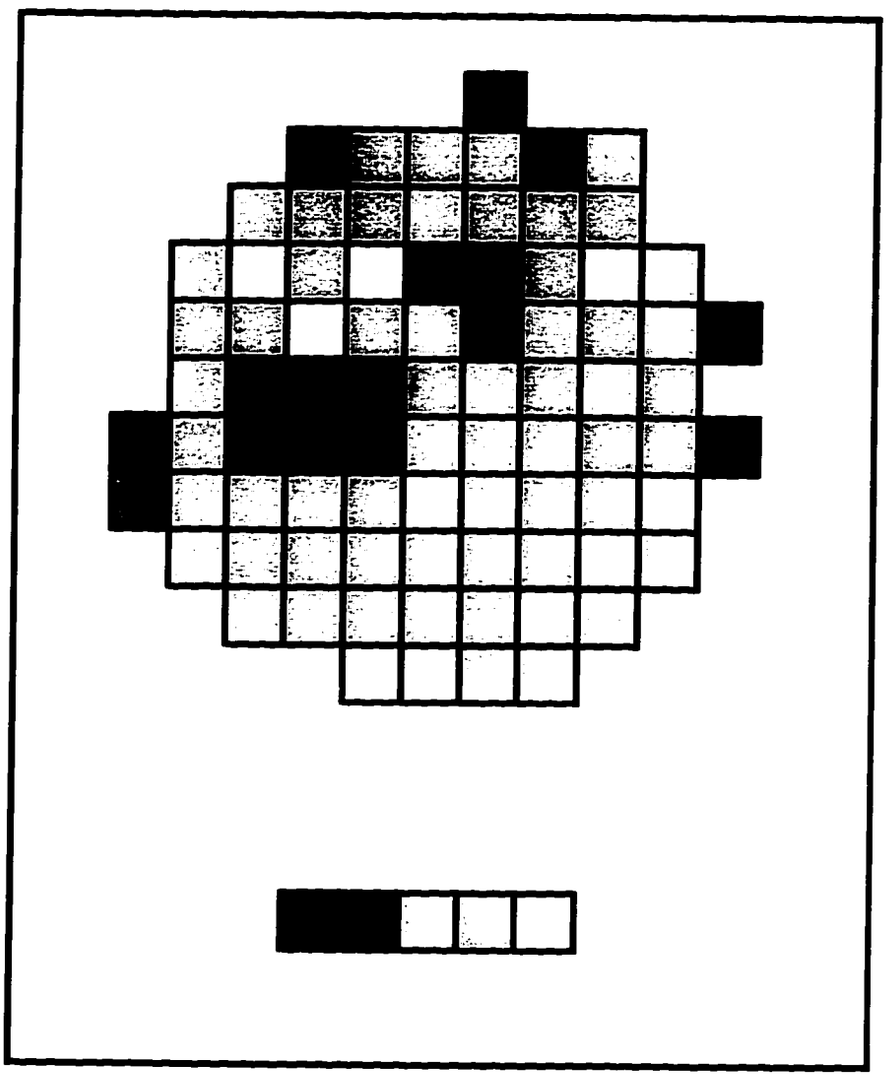

Fig. 1.2 This is an example of a typical composite regional tissue perfusion map constructed from uptake images taken from a tumor. The perfusion categories were estimated as described in the text. The pattern key for the perfusions ranges from very low perfusion (far left) to high perfusion (far right). The lack of higher perfusions is a common characteristic of solid tumors.

vascular tissue, and thereby compromises perfusion through the tissue. First, a mouse bearing a RIF-1 flank tumor (688 mm^3) was given an intravenous injection of Photophrin II 24 hours prior to the photo-illumination experiment. The following day, pre-PDT treatment proton (Fig. 1.3 A) and deuterium uptake (Fig. 1.3 B and C) images were acquired from this tumor after bolus injection of 100 μl isotonic D_2O to determine relative tumor perfusion. A 90 sec deuterium image acquired 30 seconds after injection of the indicator (Fig. 1.3 B) clearly shows a well-lit periphery about a lower lit core, suggesting that the tumor is well perfused in the outer region, but exhibits heterogeneous perfusion. The inner core has some pixels with little or no signal, indicating that perfusion is not as strong here. The later image acquired 10 minutes post-tracer injection (Fig. 1.3 C) shows many of these central pixels lighter, indicating that lower perfusion was present, and sufficient to deliver the indicator.

To create a spatial difference in response to the PDT treatment, the top left half of the tumor was covered with aluminum foil to attenuate the light, and thus prevent the activation of the Photophrin II accumulated in the cells in this region of the tumor tissue. Fifteen minutes after light was applied to the tumor (at a light and drug dose sufficient to cause an estimated 86% perfusion reduction in RIF-1, as estimated by D_2O clearance measurements [85]), a post-treatment proton (Fig. 1.4 A) and two deuterium images were acquired (Fig. 1.4 B and C). It can be seen in the early deuterium image acquired 90 sec post-injection of the indicator (Fig. 1.4 B) that the uncovered portion (light treated) of the tumor displays a vast reduction in perfusion. Even in the deuterium image acquired 10 minutes post-indicator injection (Fig. 1.4 C) there is little evidence of perfusion in the treated area, though there is some accumulation of the tracer in the tumor. The covered

region (untreated) still exhibits perfusion, although this perfusion appears to be attenuated. This could be a consequence of insufficient light shielding, or more likely, vascular coupling between the regions. Nonetheless, this PDT experiment clearly demonstrates the power of this NMR perfusion monitoring technique, both in its repeatability, and in its ability to monitor therapy-induced regional changes in perfusion in tissues. A caveat to consider, because only relative perfusion is measured, the magnitude of these changes may not be accurately reflected by the NMR measurements.

iii. Observing perfusion pattern

The following study [9] was performed to provide the first evidence that the NMR uptake approach could provide information concerning the distributional patterns of tumor perfusion. For this study, nineteen female C_3H/HeJ mice bearing RIF-1 flank tumors were binned into four groups distinguished by tumor volume. Group 1 consisted of tumors between 225 - 325 mm^3 (n = 5). Group 2 were between 340 -465 mm^3 (n = 5); Group 3 between 565 - 700 mm^3 (n = 4); and Group 4 between 890 - 1625 mm^3 (n = 5). The tissue perfusion maps were obtained for each tumor using the method described above, and from each map the distributions of the relative regional tumor perfusion were calculated. Then, multivariate analysis of variance was performed to test for a difference in distributions in perfusion as the tumor groups increased in mean volume. Analyses were performed on tumors as a whole, and with tumors divided into two portions: a central core, and a peripheral ring (defined as the ring of the outermost pixels after elimination of those pixels considered to be only partially tumor). Figure 1.5 shown the histograms of the regional perfusion from each of the four binned groups after separation into the two portions. The perfusions are divided into five categories: very low

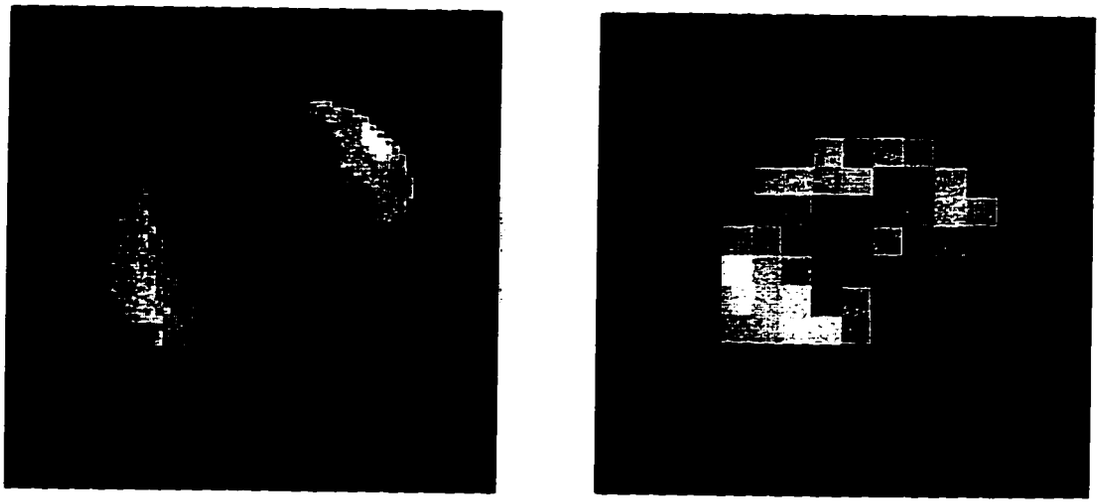

A. B.

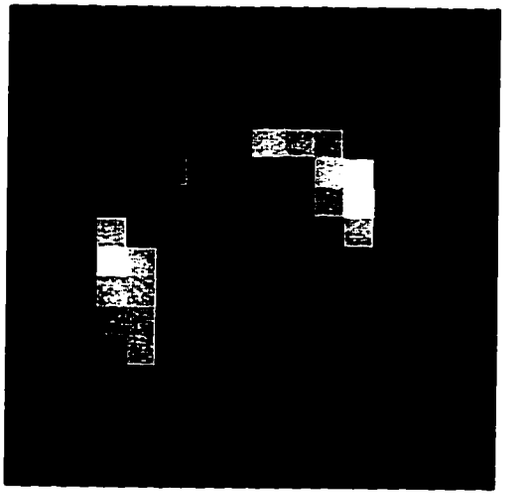

C.

Fig. 1.3 (A - C). Images of a 668 mm^3 RIF-1 tumor taken just prior to commencement of a PDT treatment. The proton image (A) was acquired initially, then two 90 sec deuterium images were acquired: one at 30 sec (B), and one at 10 min (C) post remote tail vein injection of isotonic D_2O.

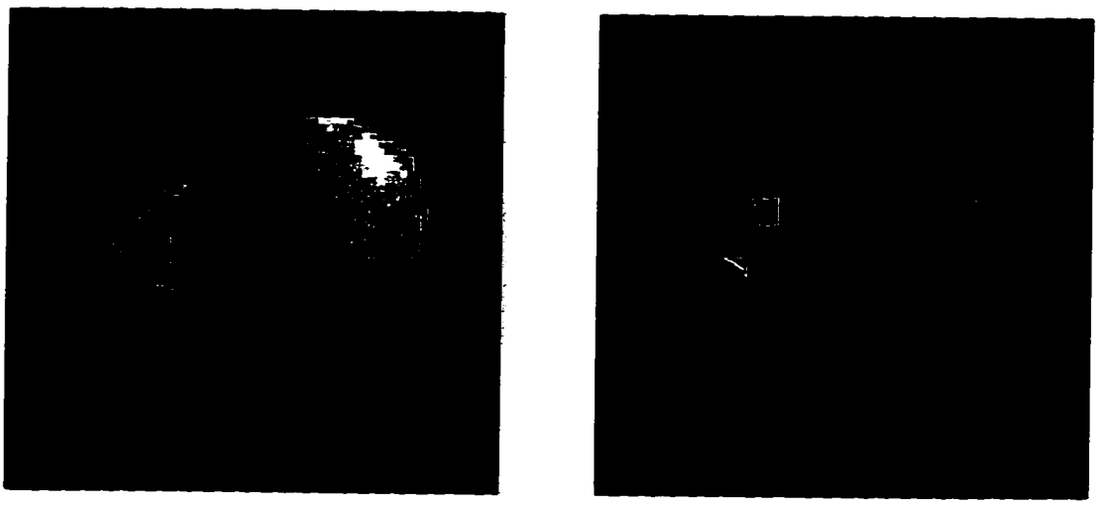

A. B.

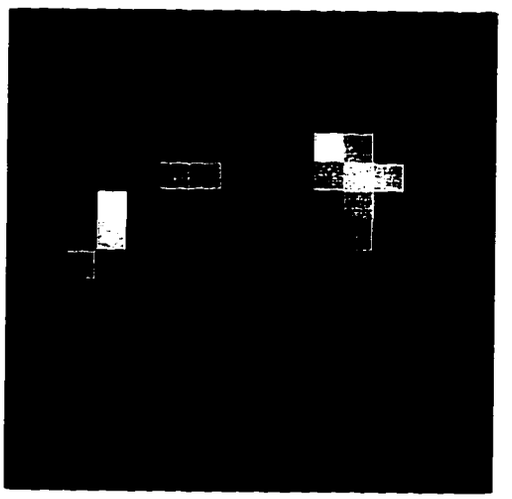

C.

Fig. 1.4 (A - C). Images of the same 668 mm^3 RIF-1 tumor shown above, but taken 15 minutes after the conclusion of the PDT treatment. The proton image (A) was acquired initially, then two 90 sec deuterium images were acquired: one at 30 sec (B), and one at 10 min (C) post remote tail vein injection of isotonic D_2O.

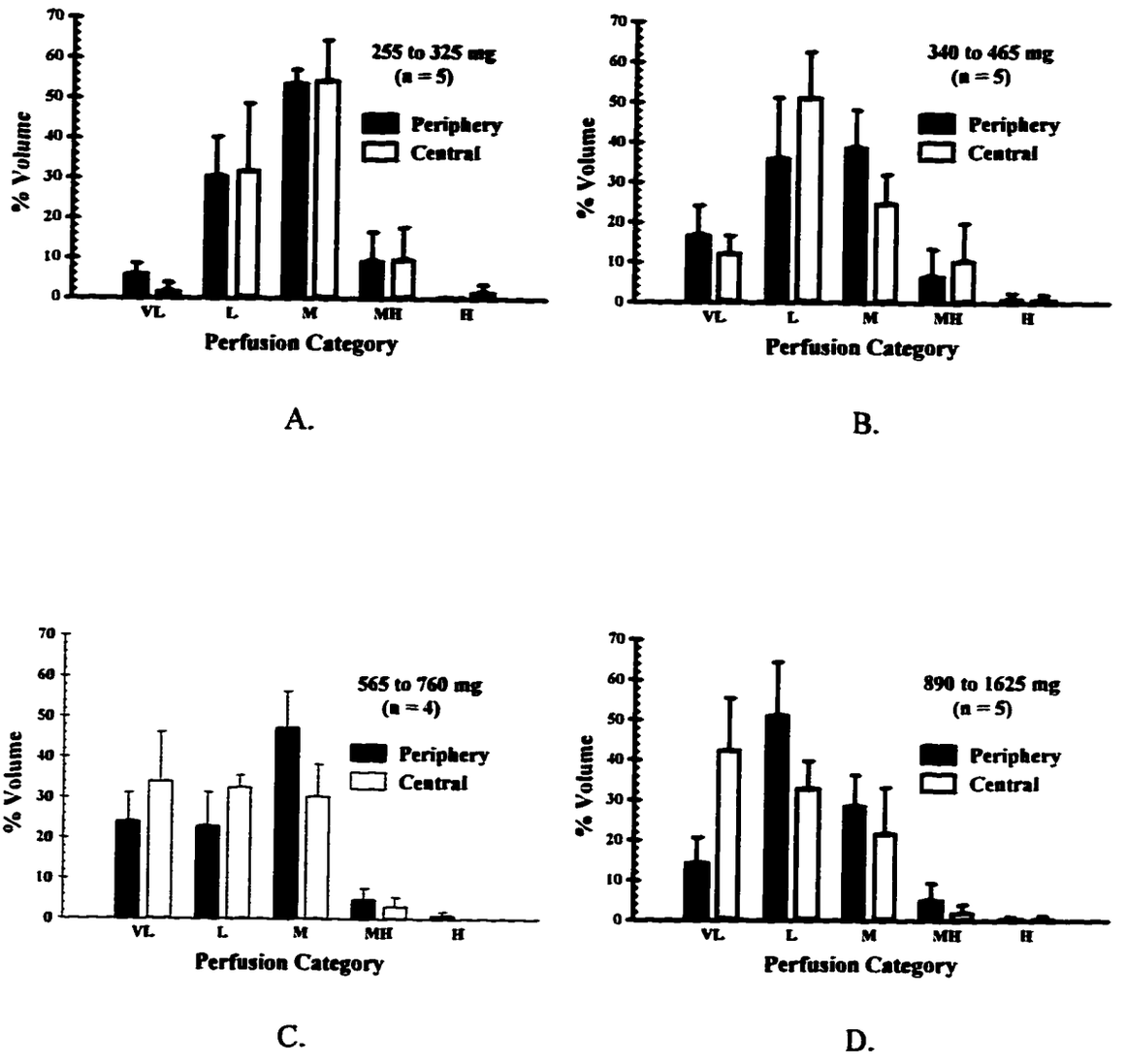

Fig. 1.5 (A - D). Relative regional tumor perfusion distributions of the periphery and central regions. The perfusions were categorized into the following: very low (**VL**); low (**L**); medium (**M**); medium high (**MH**) and high (**H**) perfusions. The animals were binned into four groups, based on their tumor volume, with the distributional patterns of Group 1 through Group 4 represented by Fig.s 1.4 A through D., respectively. The range of tumor volumes, as well as the number of mice in each binned group, are displayed for each of the above four Figures.

(or no); low; medium; medium high; and high perfusions.

The results were as follows for the tumor groups considered as a whole. The regional perfusional distribution is dependent on size ($p = 0.016$), with the percentage of very low perfusion pixels {< 1 ml/(100 g-min)} significantly reduced in the small tumors (Groups 1 and 2) compared to that found in larger tumors (Groups 3 and 4) ($p < 0.01$). Also, the percentage of medium perfusion pixels was greater in the smallest tumors (Group 1) compared to the largest tumors (Group 4) ($p = 0.028$). There was no difference between any of the groups in the percentages of pixels in the low, medium high or high perfusion categories ($p = 0.35$; $p = 0.9$; $p = 0.72$, respectively).

Analysis of all tumors after division into peripheral and central portions shows that for all tumors considered together, the regional perfusional distribution differs between the center and the periphery ($p = 0.0037$). This is primarily due to a difference in the distribution of the percentage of pixels in the very low, low, and medium perfusion categories. Tumor size influences the regional distributions only for the central core ($p = 0.0017$), and not for the periphery ($p = 0.13$). This is due mostly to the increase in the very low fraction in the core as the tumor group size increases ($p = 0.022$ between the core of the smaller tumor groups and the core of the largest tumor group). These results corroborate other evidence (extracted *via* invasive means) which suggests that the pattern of regional perfusion distribution has a size dependence [7,8].

d. Limitations

Though the NMR uptake method fulfills most requirements of an ideal perfusion measuring method, and exhibits the advantages and obvious utility in observing perfusional changes and perfusional heterogeneity as described above, there are certain

limitations with the method which need to be addressed. The most significant limitation is that in order for this method to become widely accepted in the experimental research community as an alternative (and superior in certain aspects) method for perfusion determination to those commonly used presently, the NMR uptake approach must fulfill another requirement of an ideal perfusion method - that it yields an absolute (*i.e.* accurate and precise) measurement. However, for solution of a quantitative absolute value of perfusion after data acquisition through application of the uptake approach, the AIF of the indicator must be known and applied in the Kety equations. In humans and large animals, determining a usable estimate of the AIF for an indicator does not pose a great problem, other than somewhat complicating the perfusion measurement experiment. However, in many small laboratory animals commonly used in research facilities (such as rat and mouse models), determination of the AIF is difficult (rat) if not impossible (mouse). There is an often-used method for determining the AIF from a rat, but it is a carotid puncture approach which obtains the information by bleeding the animal, and then measuring the indicator concentration in the arterial blood. Though this method can obtain a measure of the tracer concentration in the artery immediately after injection, it obtains these results by bleeding the animal to death in under a minute. This procedure alters the AIF as it attempts to measure it, and this approach is therefore of questionable utility in obtaining a usable AIF measure for future perfusion measurements from this same animal. Not surprisingly, the uncertainty concerning the knowledge of the true AIF in a given animal has made the NMR animal research community reluctant to embrace the uptake technique.

A second limitation involves the uncertainty of the most appropriate means to analyze the data. There are presently two common methods used to analyze the acquired tissue perfusion data obtained with the uptake approach. One may either fit the time-course data to the Kety model, or one may analyze the area-under-the-curve between some time limits as described in section I.F.2. Two potential situations which may affect accurate measurement are perfusional heterogeneity (the implications of which are discussed in section I.D.2), and the indicator signal-to-noise ratio (S/N) in the measurement. The impact that perfusional heterogeneity and S/N have on the ability of the uptake approach to extract absolute perfusion information with the two methods of data analysis has not before been rigorously studied.

Another limitation is that the NMR uptake approach is not likely to be performed routinely in many laboratories since it requires fairly expensive machinery. But as more research facilities gain access to such machinery (the number of NMR research centers is increasing steadily), research relevant to the design and follow-up of therapeutic protocols will be initiated. Also, at present, clinical implementation of the NMR uptake technique using deuterated water as the indicator is not possible due to the amount of tracer requires in such human measurements. This dissertation research does not specifically address either of these limitations.

Lastly, though the perfusion measurement is non-invasive to the tissue under measurement, the approach is not non-invasive to the subject under study, since the procedure requires the intravenous injection of the indicator through a catheter. In large subjects (including humans), this would not be a significant problem. However, in the commonly used rodent models (rat and mouse) used in many laboratory experiments, the

insertion of a catheter may be difficult, and can require surgical procedures. Furthermore, if the individual AIF must be measured in each animal, more invasive actions must be included in the study, further complicating the uptake approach procedure.

G. Dissertation overview & objectives

The ultimate goal of this dissertation is to describe the optimization and implementation of an NMR indicator uptake technique which can non-invasively and repeatedly measure absolute tissue perfusion. Chapter II concerns itself with the method optimization of the NMR approach to measuring tissue perfusion. Since the prime goal of the dissertation research is to obtain absolute measurements, and the AIF is required for this, Chapter II discusses the development of the apparatus and NMR method with which one can extract an apparent AIF from individual rats without necessarily killing the animals. As a further extension of this goal, research was performed to determine the feasibility of eliminating the need for individual AIF measurement by construction and application of a common AIF from a small set of animals, and then using this derived common AIF for all subsequent animals within a study. Chapter II also describes results of computer simulations performed to assess the impact that tissue perfusional heterogeneity, indicator S/N within the tissue sample, and variations in the AIF have on determining absolute perfusion with the two methods of data analysis used with the NMR uptake approach.

In Chapter III, a modified uptake approach is introduced (developed as a consequence of the results reported in Chapter II). This modified approach uses a common AIF; delivery of the indicator is done as a bolus dose (based on animal mass); and the data are analyzed optimally. The modified approach is tested *versus* a commonly

used method (which does not need an AIF to measure perfusion quantitatively). The comparison was performed by designing the necessary apparatus, and developing techniques which allowed the simultaneous performance of whole-volume average perfusion measurements of an *in vivo* rat tumor model with both the modified NMR uptake approach and the commonly used microsphere method. Finally, Chapter IV summarizes the dissertation experiments, and briefly comments on future studies and concerns as a consequence of this dissertation research.

CHAPTER II OPTIMIZATION OF METHODS FOR DEUTERIUM NMR TISSUE PERFUSION MEASUREMENT USING THE TRACER UPTAKE APPROACH

A. Introduction

1. Background

As discussed in Chapter I (section E.3), the concept of measuring tissue perfusion through external detection of inert diffusible tracers within a tissue of interest was introduced and formalized by Kety nearly 50 years ago [65,86]. To restate this method, the Kety approach takes advantage of the exchange of diffusible tracers between the tissue and blood. This exchange occurs primarily at the capillary level, and therefore is a measurement of the nutritive tissue perfusion (also commonly termed blood flow). Quantitation of this exchange is arguably the most pertinent measure of tissue vascularity, as discussed in Chapter I C. The equations and theoretical framework which Kety introduced to make this form of perfusion measurement possible have been well studied and developed for a variety of tracers and detection techniques. Among these are γ-counter detection [87], positron emission tomography [73,88], near-infrared spectroscopic detection [89], and NMR [58,76].

2. NMR perfusion measures

In recent years, both tracer clearance [76] and tracer uptake [58] NMR methods applying the Kety approach using freely-diffusible deuterium-labeled water as the tracer have been proposed as methods which quantitatively measure tissue perfusion. These were introduced in Chapter I F.3 & F.4. Advantages of these methods over other

perfusion measurements are that they are easily repeatable and do not require killing the subject under study (as is the case with commonly used perfusion measurement methods using iodo-antipyrine, rubidium or microspheres). However, the tracer clearance approach, while simpler in both design and analysis, has distinct limitations. First, it measures perfusion only in the small local labeled area of tracer injection (10 μl D_2O injected directly into a tumor labels about 50 cm^3) [83]. Therefore, in tissues with perfusional heterogeneity, particularly tumors [7-11], multiple injections are required to better sample the tissue [83]. Moreover, the injections themselves are invasive to the tissue under study. Direct injection of a tracer can alter the interstitial pressure of the tissue, and could alter the perfusion by causing vessels to be pinched down if the injection increases the interstitial pressure, or could cause an opening of previously closed vessels by relieving this interstitial pressure. This may be a greater factor with tumor perfusion measurement, since the interstitial pressures of tumors can be elevated over that found in normal tissues [84]. The NMR indicator uptake approach avoids these problems through remote injection of the tracer, and has the added benefit of being able to measure either whole-volume average perfusion with spectroscopy, or determine regional perfusion throughout a tissue with imaging [90].

3. Limitations

Although the NMR uptake approach has many attractive features, it is not without drawbacks. Though non-invasive to the tissue under study, the tracer must be injected through an implanted intravenous catheter. Further, though the Kety approach relates the instantaneous concentration of any flow-limited inert diffusible tracer to the tissue perfusion, it requires knowledge of the changing arterial tracer concentration over time

(the so-called arterial input function, AIF) for perfusion calculations, evident in Eq. I.16. Unfortunately, determination of individual AIFs is difficult (in rats) if not impossible (in mice) in many commonly used experimental animal models. Ideally, for the uptake method to yield absolute values, yet remain easily applicable in a laboratory setting, one would desire the ability to apply a common AIF (rather than measure each animal's AIF) to members of the animal model studied when deriving absolute perfusion with the NMR uptake method. The impact of deriving and subsequently using such a common AIF for perfusion measurements has not been previously examined.

NMR perfusion data must also be properly analyzed to extract useful perfusion information. Data collected by external tissue tracer detection methods (deuterium NMR spectroscopy or imaging among these) are commonly analyzed in one of two ways. Either the instantaneous tracer concentration time-course is fitted according to the Kety model to extract the perfusion (hereafter referred to as the fitting approach: FIT), or an integration of the instantaneous concentrations between two time-limits can be related to perfusion through a second-order polynomial (the uptake-integral approach: INT; [58,88]). Although both methods can be used to estimate perfusion, the limitations of these two methods have not been rigorously studied. Since the NMR method can be used as either an imaging (small regional volumes) or spectroscopic (whole-volume) measure, it is important to test the analytic approaches to the problems which may arise as a consequence to the type of experiment performed. The two problems considered here to be most prominent in the NMR perfusion experiment are perfusional heterogeneity and the signal-to-noise ratio (S/N) of the indicator time-concentration data.

The S/N is mainly a concern when performing an imaging experiment, since the volumes of observation are greatly reduced (thus decreasing the potential signal from a tissue, while the random noise inherent in the sampling remains constant). Also, regions with lower perfusion will have less of the tracer available for detection, even early after tracer injection, and therefore have less signal. Since lower perfusion is a characteristic of solid tumors, there will be a reduced S/N. However, the S/N in a whole-volume spectroscopic data acquisition should be less of a concern as the volume of observation increases. Whole-volume spectroscopic measurement of tissues (even in tumors, with their generally lower perfusion) will have sufficient S/N to mitigate this concern. The S/N issue is further worsened by the intrinsic insensitivity of the nuclide (deuterium being < 1 % as sensitive to NMR detection as protons). If the indicator was much more sensitive to detection by NMR, the S/N would increase per unit volume, and smaller imaging volumes could be obtained. However, regardless of the absolute size of the volume being observed, it is important to determine the impact of S/N to discern how best to analyze imaging data sets.

Likewise, accurate analysis of spectroscopic whole-volume data obtained from a diseased tissue or solid tumor may be affected by the perfusional heterogeneity in the tissue. A whole-volume measure will usually experience much more of this heterogeneity than will the imaging data obtained from a small (generally homogeneous) volume. Therefore, to determine the proper analysis of spectroscopic data, the effect of heterogeneity on the two analytic approaches should be studied.

4. Aim of study

The aims of this Chapter's work are to determine the following for the NMR tracer uptake method: (1) assess the limitations of the two methods of data analysis in terms of random noise and perfusional heterogeneity through computer modeling; (2) derive a method to measure an individual AIF in a rat; (3) determine the impact which inter-animal AIF variability has on accurately measuring true tissue perfusion; (4) discern how changes in the AIF influence perfusion measurements, and how these changes may occur *in vivo*; and (5) test whether a common AIF can be used in perfusion assessment by external detection techniques. With this information, the appropriate approach to apply when measuring perfusion of most tissues can be theoretically determined, and tested in future *in vivo* studies.

B. Materials and methods

1. Arterial input function

a. Design of observation chamber

An observation chamber sufficient for NMR spectroscopic determination of the indicator concentration in the blood was designed and hand-crafted. The observation chamber with the attached catheter lines (not to scale) is illustrated in Fig. 2.1. The cylindrical observation chamber (300 μl observation volume) was constructed from a section of a 1 ml syringe tube [Becton-Dickinson, Oxnard, CA]. The chamber ends were plugged with rubber (each containing a small hole for catheter lines), and 15 & 21 mm long polyethylene input and output lines [PE-50 tubing; Clay Adams, Parsippany, NJ] were inserted into each end. The catheter ends were constructed with knobs near the end

so that a tight ligation to the carotid could be accomplished, reducing the risk of the catheter pulling out and the animal bleeding to death.

b. *In vitro* testing

The observation chamber was tested in an *in vitro* system to test the NMR observation of the indicator, and to derive a simulated AIF to study how the shape of the simulated AIF changes as the flow rate of a carrier fluid (grossly simulating the arterial blood) is altered. The simulation was performed by use of a Harvard Apparatus infusion pump [Harvard Apparatus, Millus, MA] which simulated the blood flow through a vessel of an animal. Water was placed into a 50 cc syringe [Becton-Dickinson, Oxnard, CA], onto which a long catheter created from PE-50 tubing [PE-50 tubing; Clay Adams, Parsippany, NJ] was attached. The end of this tubing was connected to the observation chamber, allowing infusion of the carrier water through the chamber at any set flow rate. Three flow rates were used and determined to be 0.52 ml/min, 0.37 ml/min and 0.27 ml/min (quantified by weighing the amount of water which was pushed through the system over a time period of two minutes). The tracer-concentration time-course within the chamber was acquired spectroscopically using NMR in an eight-turn, 10 mm i.d. deuterium solenoid coil (30.77 MHz). These studies were performed in a horizontal 4.7 T, 31 cm clear-bore Oxford magnet [Oxford Inst., Oxford, UK] (with a 20.5 cm gradient insert) equipped with a Bruker Biospec II console [Bruker Instruments, Billerica, MA]. Static magnetic field homogeneity was optimized by maximizing the free-induction decay (FID) lifetime of the proton signal from within the chamber [91]. Deuterated water [Cambridge Isotopes, Woburn, MA] was injected into the flowing water as a small bolus volume (10 μl) through a Tee connection. Immediately after bolus injection of the tracer,

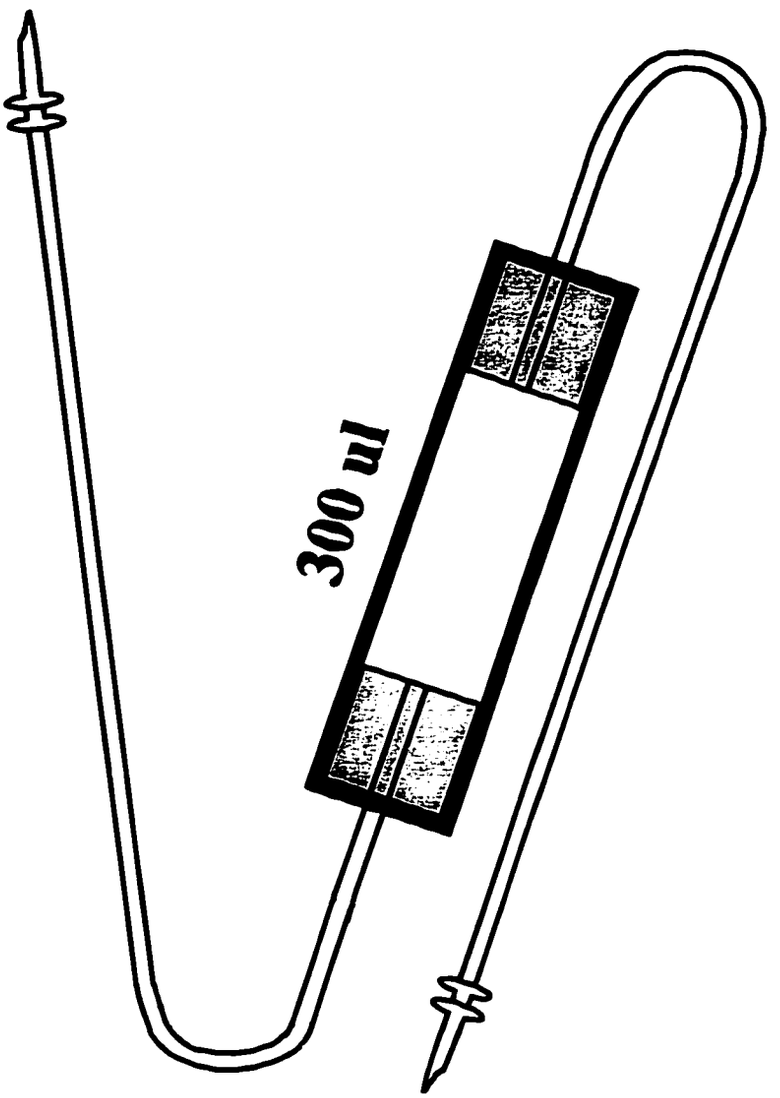

Fig. 2.1 Illustration of the observation chamber which was used to determine indicator concentrations from the blood of rats. By placing this chamber within a receiver coil, NMR spectroscopy could determine the concentration time-course after injection of a suitable NMR observable indicator. The catheter ends were given knobs so that tight ligation to a blood vessel could be accomplished. The lengths of the catheters (15 and 21 mm) are not to scale, but are longer relative to the chamber than those depicted here.

NMR spectroscopic observation of the chamber determined tracer concentration [$C_c(t)$] of the arterial blood as a function of time by reference to a previously constructed calibration curve (signal amplitude *vs.* D_2O content).

c. Determination of the AIF in rats

Sixteen male Fisher-344 rats [Harlan Sprague-Dawley, Indianapolis, IN] weighing between 180 and 305 g were used to determine individual rat AIFs. These animals were divided into two experimental groups, with ten rats receiving a constant tracer volume (500 μl), and six rats receiving a constant tracer dose (2 μl/g). Animals were supplied with food and water *ad libitum*, and were housed and cared for in accordance with institutional guidelines. During surgery and spectroscopic examination, animal core body temperature was monitored rectally and regulated by placing the animal on a pad heated with warmed circulating water. Pre-surgical anesthesia was induced with isoflurane (Aerrane: 2.5% V/V in O_2) [Ohmeda, Madison, WI] and maintained at 2% V/V in O_2 throughout the study. Total time under anesthesia for the animals was approximately 75 minutes. An apparent individual AIF for each rat was extracted and estimated by the following method. The observation chamber was placed within an eight-turn, 10 mm i.d. deuterium solenoid coil (30.77 MHz). This chamber was then placed in-line with a rat carotid by surgical catheterization of the lines into a carotid artery (in these studies the left carotid was used, though each carotid should be equivalent): first the 21 mm line was inserted distally into the carotid, then secured by ligation around the knob to the carotid. Then, the 15 mm line was advanced proximally towards the left ventricle, and ligated in the same manner. Figure 2.2 is an illustration depicting the placement of these implanted catheters in a rat. As is also illustrated in Fig. 2.2, the

deuterium tracer input line was catheterized and tied into the right femoral vein with PE-10 tubing connected to a syringe containing the deuterated tracer {D_2O [Cambridge Isotopes, Woburn, MA] made isotonic (0.9% NaCl [Sigma Chemicals, St. Louis, MO]}. Patency of all catheters was determined by visual inspection.

Immediately after the surgical operation and catheterizations, the animal was transferred into the Bruker Biospec II spectrometer [Bruker Instruments, Billerica, MA]. As described above, the magnetic field homogeneity was optimized by maximizing the FID lifetime of the proton signal from within the chamber [91]. Immediately following the bolus injection of the tracer (delivered in approximately three seconds), NMR spectroscopic observation of the chamber determined tracer concentration [$C_c(t)$] of the arterial blood as a function of time by reference to a previously constructed calibration curve. Acquisition parameters for deuterium NMR were as follows: flip angle of 67°; spectral width of 2000 Hz; repetition time of 0.25 s; eight transients per spectrum (one spectrum every 2 s); and 480 spectra acquired (total experiment time 16 min).

The tracer concentration measurement from the observation chamber [$C_c(t)$] is not the true AIF due to dispersion (mixing) within the chamber. However, using an approach introduced by Iida *et al.* [92], one can extract the apparent AIF which enters the chamber by considering the observed concentration [$C_c(t)$] to be the true AIF [$C_a(t)$] convolved with a dispersion function [d(t)], such that $C_c(t) = C_a(t) * d(t)$. The following AIF waveform used by the PET community [73,92] (with a modification to account for non-negligible HOD recirculation which occurs in the rat), and the dispersion function as defined by Iida [92] were employed.

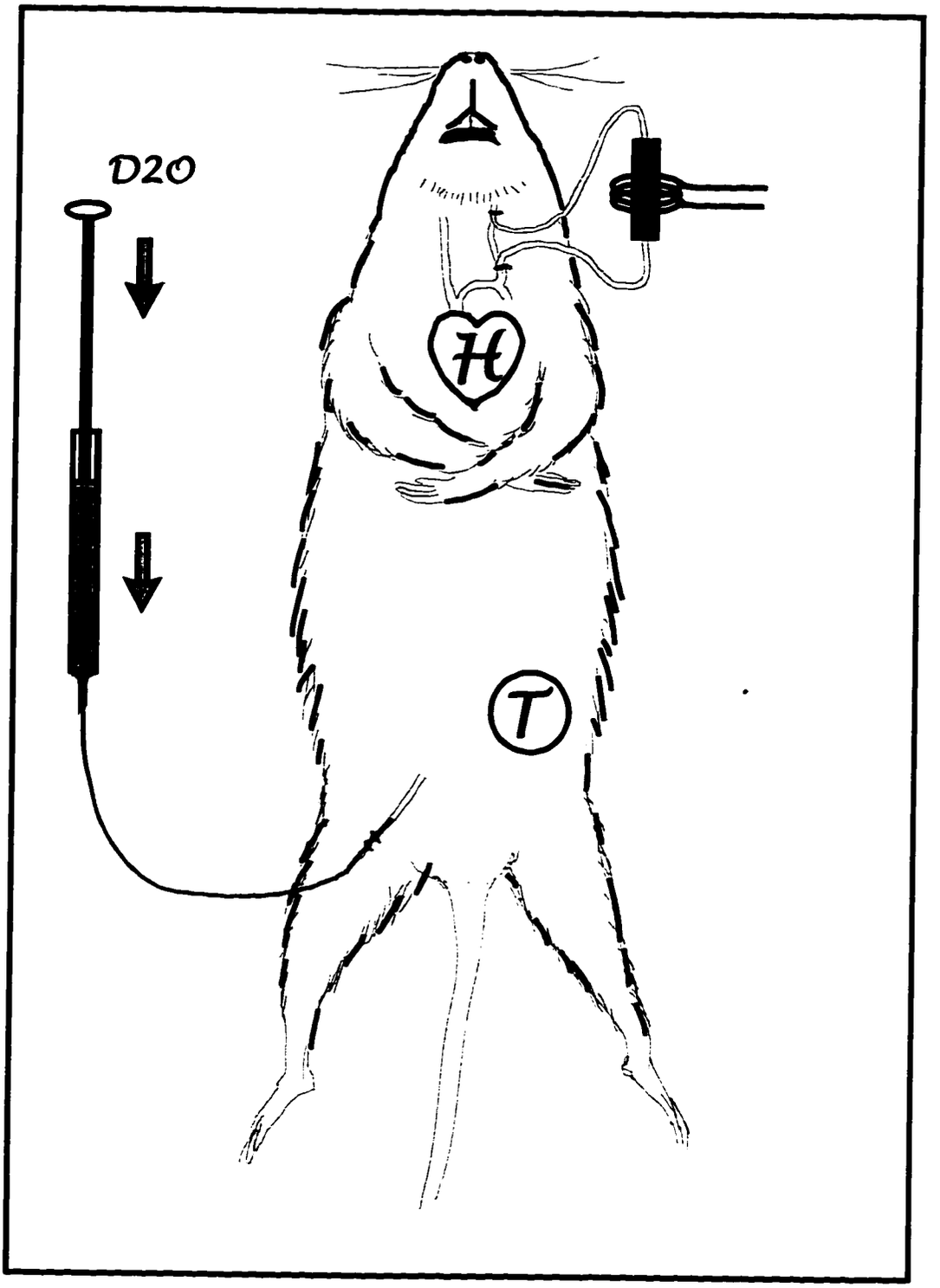

Fig. 2.2 Illustration of a rat with the implanted catheters used in the AIF *in vivo* determination studies. Pictured here are the deuterated tracer (D_2O) input catheter, and the carotid observation chamber placed within a solenoidal NMR coil. The implanted tumor is indicated by a **T** in the illustration, and the heart is indicated by the **H**.

[Eq. II.1] $C_a(t) = (A/t_p^2) \cdot t \cdot e^{(-t/t_p)} + B \cdot [1 - e^{(-C \cdot t/t_p)}]$ and

[Eq. II.2] $d(t) = (1/\tau) \cdot e^{(-t/\tau)}$

In the AIF model, A is the Molar·second area under the curve (AUC) contributed by the first term. It is related to the amount of tracer injected, the rate of tracer injection, and the flow rate in the injection site vessel (the carrier fluid). This A value is a constant after the first pass of tracer, and should not be confused with the total AUC observed, which also contains contributions from the second term (this term approaches equilibrium at large times and therefore the total AUC never reaches a constant value). The t_p is the time to the peak concentration of the AIF; B is the equilibrium concentration value; and C is a constant term related to the recirculation of the tracer. The dispersion function contains a parameter τ which is defined as the dispersion time. This τ value is influenced by both the tracer injection rate and the carrier fluid flow rate.

Mathematica® [Wolfram Research, Champaign, IL] convolved these two equations into another **[Eq. II.3]** so that the convolved data could be fit by non-linear least squares regression [Simplex/Quasi-Newton algorithm; *CSS:Statistica/w*® (Statsoft, Tulsa, OK)].

[Eq.II.3] $$C_c(t) = B - B \cdot e^{(-t/\tau)} + A \cdot \tau / [e^{(t/\tau)} \cdot (\tau - t_p)^2] - B \cdot t_p / [e^{(t/\tau)} \cdot (C \cdot \tau - t_p)] + B \cdot t_p / [e^{(C \cdot t)/t_p} \cdot (C \cdot \tau - t_p)] + A \cdot [-(\tau \cdot t_p) - \tau \cdot t + t_p \cdot t] / [e^{t/t_p} \cdot (\tau - t_p)^2 \cdot t_p]$$

Apparent individual AIFs were extracted from the rats placed into two groups; one group receiving a constant tracer volume (n = 10), and another group receiving a constant tracer dose (n = 6). A common AIF for each group was constructed by using the mean of each individually extracted AIF parameter {A, B, C, t_p} as a common AIF

parameter. A mean AIF curve was also constructed by averaging the individual time data points of the AIFs. For the 10 rats given the constant volume of 500 μl, a Pearson (product-moment) correlation between body weight and the value derived for the equilibrium concentration of the AIF was performed.

d. Computer simulation of error using common AIF

The Kety flow equation **[Eq.I.16]** was used to simulate noiseless "true" tracer concentration *vs.* time curves at 1, 5, 10, 20, 40 & 60 ml/(100 g·min) for each animal using that animal's extracted individual AIF. The extremes in error introduced by assuming a common AIF were examined by analyzing the curves from animals with the highest (High) or lowest (Low) equilibrium concentrations (the extreme cases of the group). Perfusions from these curves were determined with the FIT and INT approaches (FIT: fitting the time-course to the Kety model; or INT: relating the initial area under the curve to the perfusion) using the common AIF, and were compared with the "known" simulated perfusion value.

e. Computer simulation of the influence of changes to the AIF

Simulations to determine the influence of changes in the AIF parameters on accurately measuring the true perfusion by either the INT or FIT approaches were performed over a range of physiologically relevant perfusion values (1 - 60 ml/(100 g·min)). The percentage error in perfusion estimation when using the original AIF was determined for each AIF parameter after alteration by up to ± 75% the original AIF parameter value. Terms of the AIF were altered independently of the others to discern the effect each term has on measuring the true perfusion of the tissue under observation. For the FIT approach, perfusion curves were constructed using the Kety equation and the

altered AIF, then analyzed with the Kety equation using the original AIF. For the INT approach, Molar·second *vs.* perfusion curves were constructed using a *Mathematica*® routine applying the Kety equation and the altered AIF, with the resultant Molar·second value compared to a look-up table (constructed with the original AIF) to determine the perfusion which would have been calculated with the original AIF. The % error by using the common AIF to analyze the data could then be determined.

2. Modeling flow heterogeneity

The percentage error in calculating the true perfusion from either the INT or FIT approach as a function of perfusional heterogeneity was determined through computer simulations. Perfusional heterogeneity was modeled by considering the tissue to consist of a distribution of twenty homogeneous perfusion elements. The extent of heterogeneity was altered by changing the variance of the perfusion distribution of these elements (10 - 70 % C.V.), and/or through considering the perfusion as being comprised of two separate mixed dual compartments (with each compartment comprising 50 % of the modeled tissue; both compartments containing 20 elements), each with a separate variance (10 - 50 % C.V.). True perfusion is defined as the weighted average of the perfusions from all volume elements. The uptake-integral (INT) perfusion is determined by summing the 90-second uptake-integrals (between the time-limits 30 and 120 seconds) from the volume elements, and calculating the perfusion of the summed uptake-integral by comparison to a previously constructed lookup table; the time-course (FIT) perfusion is derived by fitting the weighted sum of the mean-tracer concentration (calculated from the Kety equation) in 10 s blocks for each volume element. The perfusions simulated were 5, 10, 20, 40, and

60 ml/(100 g·min); the mixed dual compartments were 5:10, 5:20, and 5:30 ml/(100 g·min). The simulation included twenty points to fit over a 10 minute study (simulating what would be necessary for sufficient S/N in an imaging experiment).

3. Modeling random noise

The effect of random noise on the precision of perfusion measurements with either analytic approach was also studied through computer "Monte Carlo" simulations. First, noiseless tracer concentration curves for perfusions of 1, 5, 10, 20, 40 and 60 ml/(100 g·min) were created with a 30-second time resolution using the Kety flow equation and the constant-tracer-dose-derived common AIF. Random Gaussian noise of a given standard deviation (50-500 mMolar) was added to these curves. Each curve was analyzed with either the INT or FIT approach, with the resultant derived perfusion calculated and compared to the known perfusion. This process was repeated 100 times for each perfusion value, with the precision (described as the coefficient of variation) and accuracy for each approach determined.

C. Results

1. AIF

a. Extraction of the AIF

A typical *in vivo* (or carefully executed *in vitro*) tracer time-course measured by NMR spectroscopic observation through the carotid observation chamber is depicted in Fig. 2.3. The inset in Fig. 2.3 shows the mathematically extracted AIF from this time-course data, as well as the shape of the dispersion function ($\tau = 50$ sec).

Figure 2.4 shows the extracted AIFs from the three *in vitro* studies. As the flow

rate of the carrier liquid (normal water) is altered (0.53, 0.37, and 0.27 ml/min), the shape of the extracted AIF curves changes, with the parameters which describe the AIF changing in the following manner. Since there was no recirculation with the *in vitro* studies, the B value (the equilibrium concentration) goes to zero in all cases, as expected. The time to peak (t_p) increases (5.2 to 6.1 sec) as the flow rate decreases from 0.53 to 0.27 ml/min, while the A parameter increases (576 to 1290 Mol·sec) as the flow rate decreases. Also, the dispersion constant (τ) increases (47 to 91 sec) as the carrier flow rate decreases.

The two extracted AIFs from the *in vivo* studies with the highest (High) and lowest (Low) derived equilibrium concentrations (the extreme cases), as well as the common AIF calculated from the mean values of fitted parameters of the constant tracer volume group AIFs (n = 10) are shown in Fig. 2.5. There is no difference between this common AIF and the mean AIF created by averaging the concentrations at each time-point. Therefore, the common AIF as defined above (and not the mean AIF) was used in the computer studies to determine if accurate perfusion measurements can be obtained without explicit knowledge of the true individual AIF. The inset of Fig. 2.5 is an enlargement of the later time-points of these AIFs, and better depicts the variation of the equilibrium values of the extreme cases from the common AIF.

b. Effect of using common AIF (bolus tracer volume)

The commonly used approach of administering a tracer has been to deliver the tracer as a constant bolus volume [10,76,83,88]. The effect of using a common AIF derived from animals receiving a constant volume of bolus tracer, rather than the animal's extracted true AIF, on accurately measuring a known perfusion (for both the INT and FIT

analytic approaches) is demonstrated for the High and Low tracer equilibrium concentration cases (defined previously) [Fig. 2.6]. This figure illustrates that the High case has the predicted perfusions overestimated when application of the common AIF is used to determine perfusion, rather than the High AIF. Likewise, the Low case has its perfusions underestimated relative to the true perfusion regardless of the analytic method.

c. Effect of altering AIF parameters

The errors observed and illustrated in Fig. 2.6 are far too great to give confidence in subsequent perfusion measurements, and will not allow for qualitative, much less quantitative measurement using a common AIF to analyze the NMR data, regardless of the analytic approach taken. However, it would be much easier to use a common AIF for calculations rather than measure each animal's individual AIF. Therefore, since the common AIF will undoubtedly differ from that of any given animal, it was important to study to what extent the various modeled parameters of the AIF influence the perfusion measurements, because the sensitizing parameters may be identified and dealt with accordingly. Figures 2.7 through Fig. 2.10 show computer simulations of the parameters (A, B, C, and t_p, respectively) of the AIF model and their effect on perfusion estimation when altered from their original values (analyzing with both the INT and FIT approaches, over the tissue perfusions shown). For the parameter A [Fig. 2.7], the % error increases linearly as the parameter changes when the data are analyzed by the FIT approach (with an error of about 25% with a change of 20% in the parameter). These % errors remain steady over the range of perfusions studied. However, when analyzing with the INT approach, the % error worsens with increasing perfusion, especially when the "true" A is greater than that used in the common AIF. The % error in perfusion estimation also

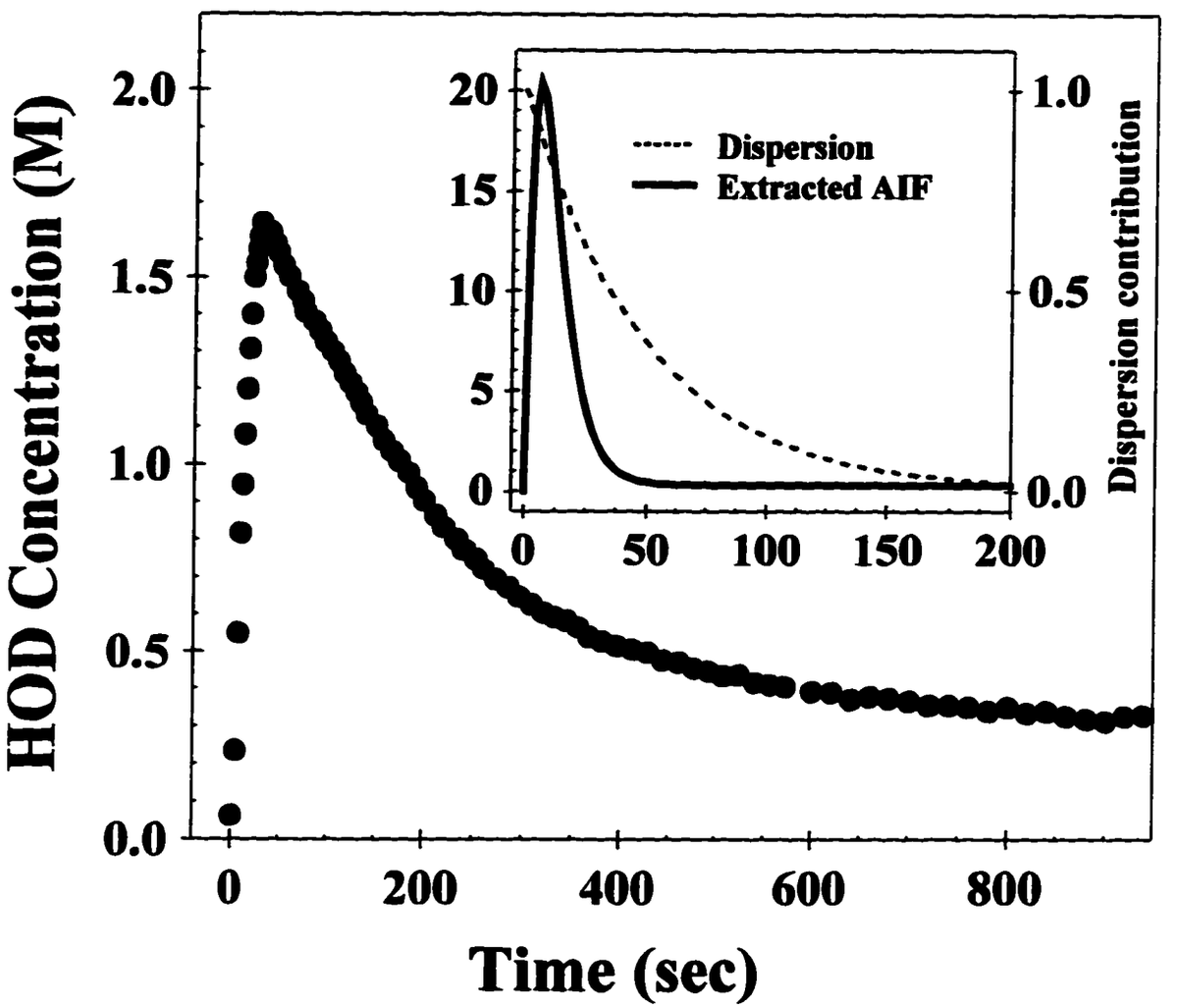

Figure 2.3 Typical timecourse of [HOD] within a carotid observation chamber implanted in a F344 male rat after *i.v.* injection of 500 μl D_2O (0.9% NaCl). The inset shows the derived AIF extracted from the observed data, as well as a representation of the dispersion function (exp $-t/\tau$). The observed timecourse is assumed to be a convolution of the AIF and the dispersion function. The indicator deuterium rapidly exchanges with the body water to form HOD, which is what is measured.

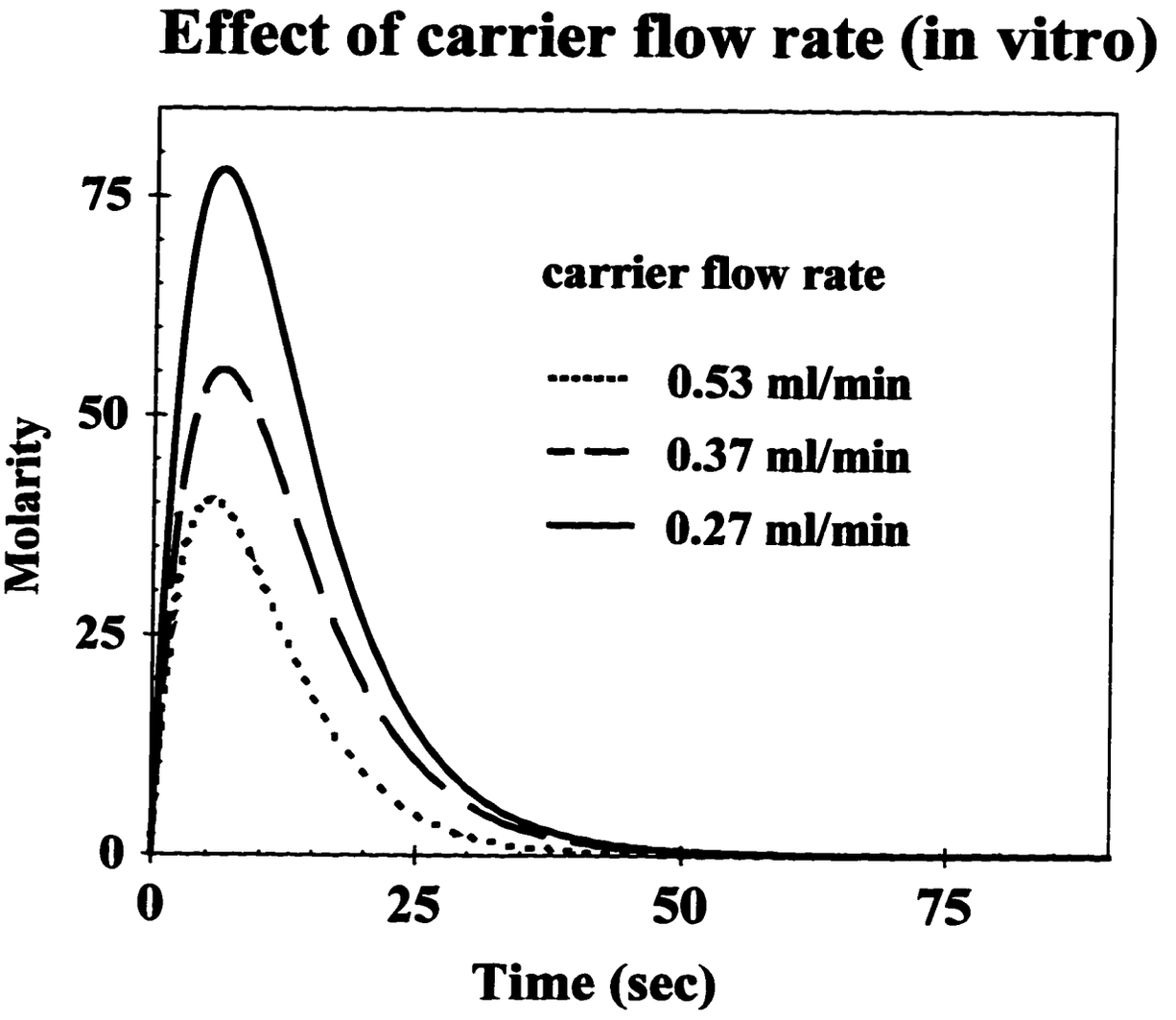

Fig. 2.4 The AIFs extracted from the NMR observation chamber time-course data following an *in vitro* procedure. Here, the carrier liquid was normo-isotopic water which was pumped into the chamber at three flow rates: 0.53, 0.37, and 0.27 ml/min. The AIFs were extracted from the data as described in the text.

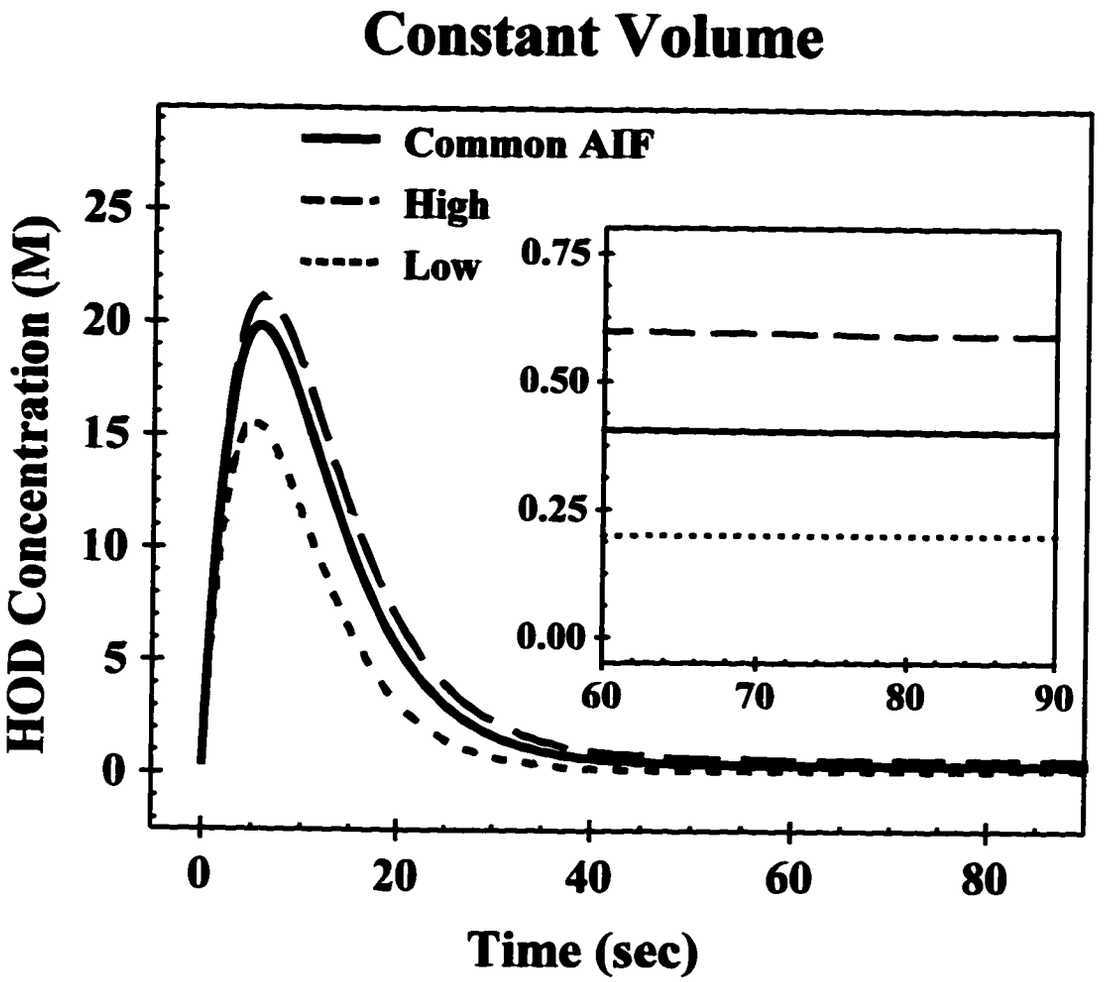

Figure 2.5 Extracted arterial input functions (AIF) from the group of animals receiving a bolus constant tracer volume (500 μl D_2O). Shown are the extreme cases (High and Low equilibrium values) as well as the common AIF. The common AIF was constructed from the mean of all parameters which describe the AIF from the rats observed (n = 10). The inset is an enlargement of the last 30 seconds of the graph to better illustrate the differences between the equilibrium values of the three cases shown.

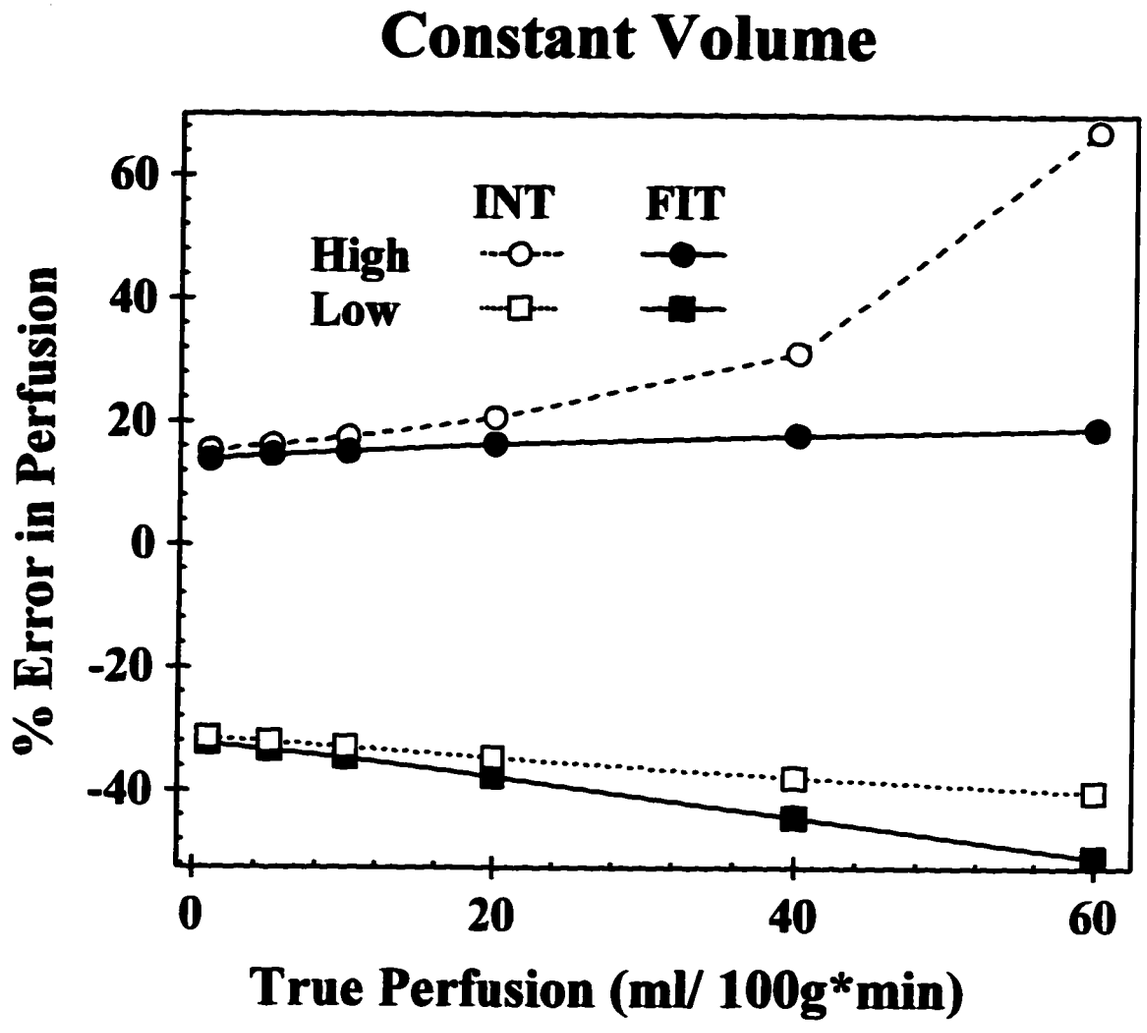

Figure 2.6 Effect of interanimal AIF variation on estimating true perfusion using a common AIF when delivering a bolus constant tracer volume (500 µl D_2O) into a rat. The errors in perfusion estimation when using the common AIF rather than the animals' actual AIF are shown for the extreme cases (High and Low equilibrium values), and are calculated for various perfusions {1, 5, 10, 20, 40 & 60 ml/(100 g·min)} by both the FIT and INT analytic approaches.

increases linearly with increased variation in the equilibrium concentration (B) [Fig. 2.8] for both analytic approaches, but to a lesser extent than with variations in A. Again, the INT approach is more sensitive to changes in the parameter for any simulated perfusion. The other two parameters used to describe the AIF (t_p [Fig. 2.9] and C [Fig. 2.10]) could undergo large variations (± 75%) without greatly altering perfusion estimations (± 5 & 3% respectively). The scale of the % error is the same for all four of these graphs, to illustrate which parameter has the greatest effect on perfusion estimation when altered. However, the variations which each modeled parameter experienced differ.

d. Effect of using common AIF (bolus tracer dose)

A Pearson (product-moment) correlation test between the animal body mass and fitted tracer equilibrium concentration was performed for all the animals within the constant tracer volume group, and showed a highly significant correlation ($p = 0.00002$). The relationship between these two is shown in Figure 2.11. This correlation suggests that by adjusting the tracer injection volume to the animal body weight (*i.e.* by giving the animals a constant tracer *dose* rather than a constant volume), a fixed tracer equilibrium concentration can theoretically be achieved, thereby reducing the variability of one parameter (B) defining the modeled AIF, and reducing the potential errors associated with this parameter. Furthermore, since A is related to the AUC resulting from the first term of the AIF, by adjusting the tracer volume, changes in the AUC (and therefore A) should be reduced, further helping reduce perfusion errors when applying a common AIF.

To test the theory that the equilibrium concentrations of the extracted AIFs will not correlate with the B parameter, and thereby reduce perfusion errors, AIFs from a set of animals ($n = 6$) were extracted after injection of a constant tracer *dose* by the methods

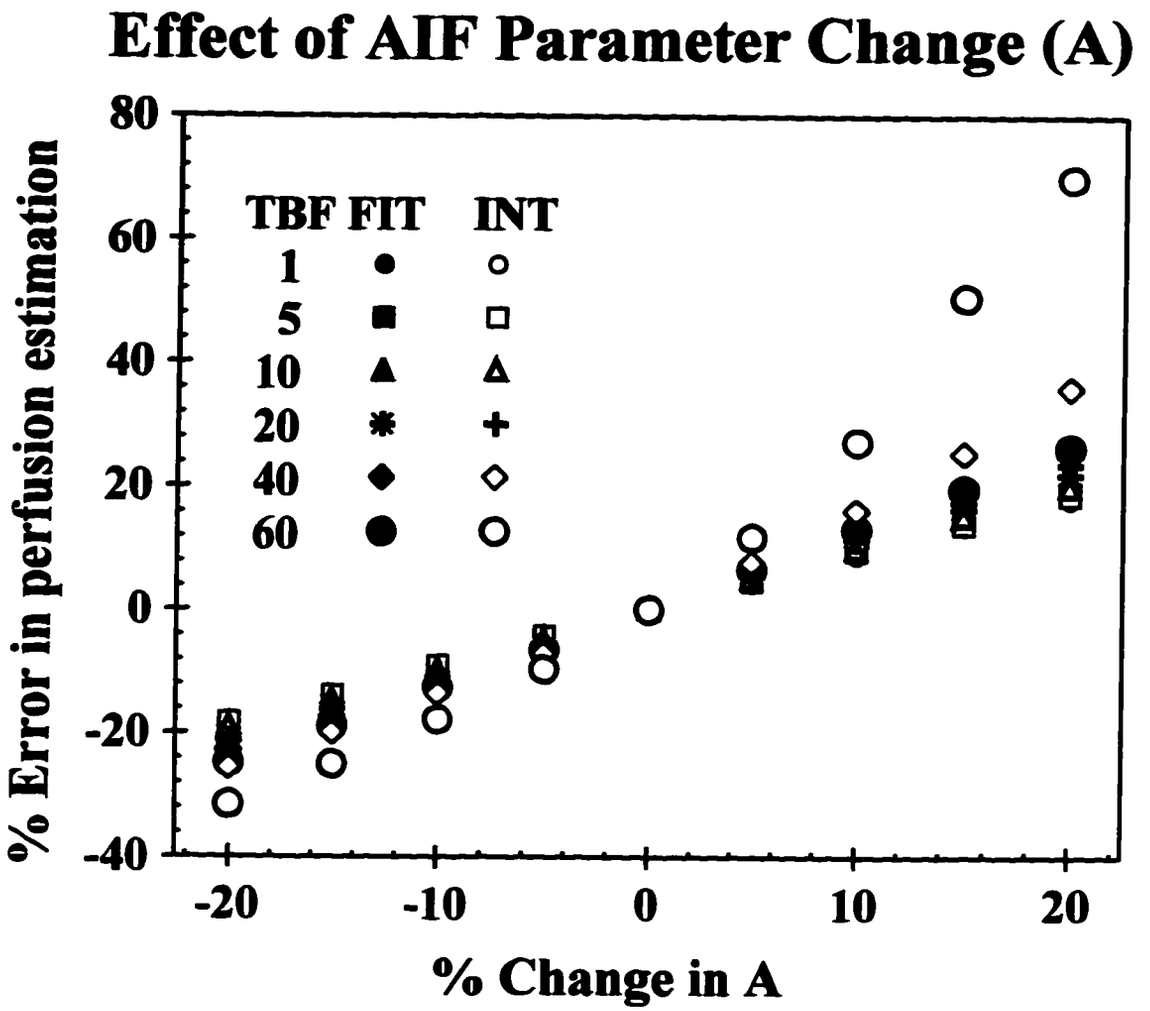

Fig. 2.7 Graph showing the effect of varying an individual AIF on the ability to accurately measure perfusion (here abbreviated as TBF) with the INT and FIT approaches using the original AIF (shown as % error) over a range of tissue perfusions {1, 5, 10, 20, 40 & 60 ml/(100 g·min)}. For all cases, the original AIF is described by parameters holding these values: A = 208 M·sec; B = 0.38 M; C = 0.5; t_p = 3.9 sec. All AIF parameters were held constant except the one undergoing a percentage change; in this case, A.

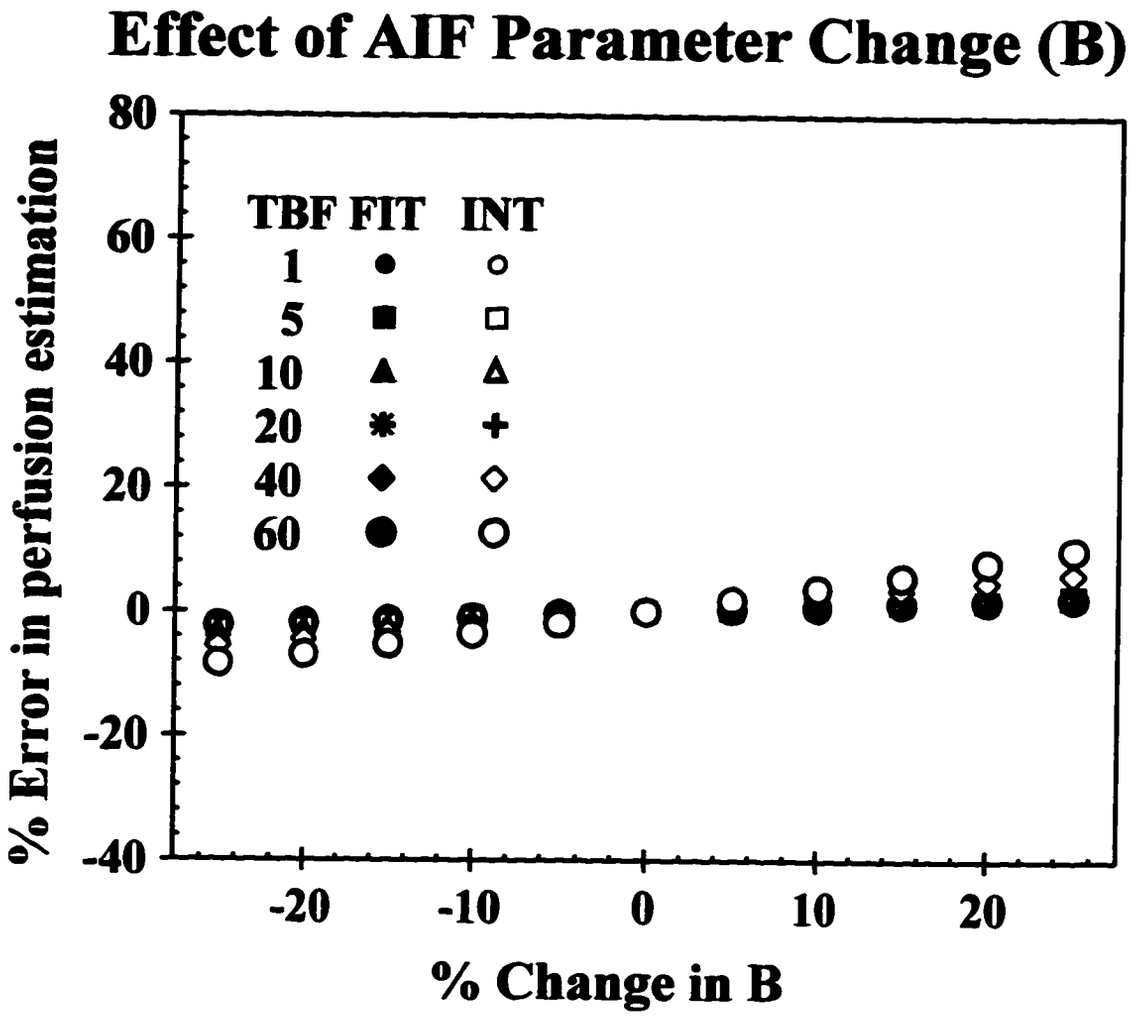

Fig. 2.8 Graph showing the effect of varying an individual AIF on the ability to accurately measure perfusion (TBF) with the INT and FIT approaches using the original AIF (shown as % error) over a range of tissue perfusions {1, 5, 10, 20, 40 & 60 ml/(100 g·min)}. For all cases, the original AIF is described by parameters holding these values: A = 208 M·sec; B = 0.38 M; C = 0.5; t_p = 3.9 sec. All AIF parameters were held constant except the one undergoing a percentage change; in this case, B. The % error scale (y-axis) is the same as for Fig. 2.7, though the % change-scale has a slightly larger range.

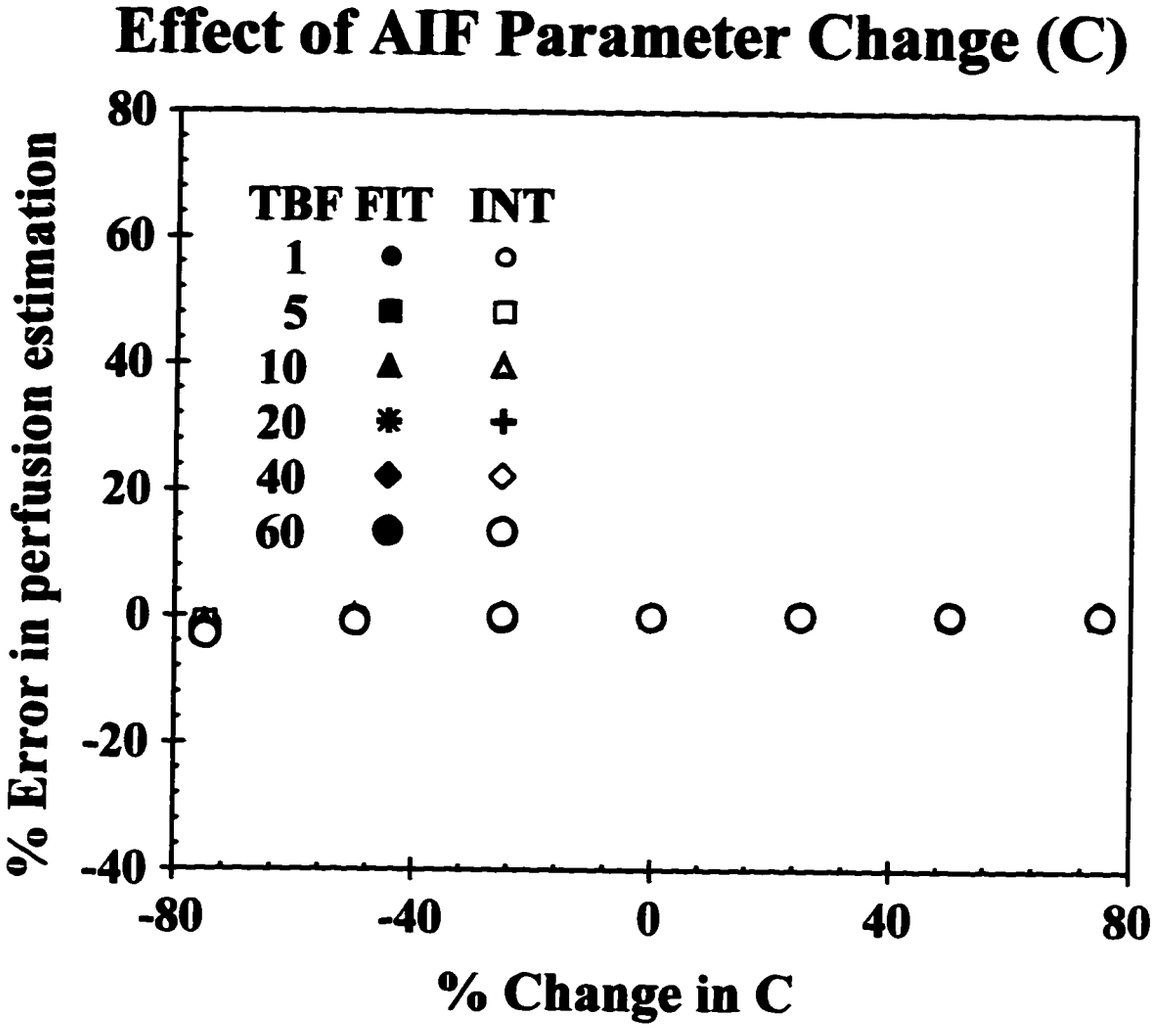

Fig. 2.9 Graph showing the effect of varying an individual AIF on the ability to accurately measure perfusion (TBF) with the INT and FIT approaches using the original AIF (shown as % error) over a range of tissue perfusions {1, 5, 10, 20, 40 & 60 ml/(100 g·min)}. For all cases, the original AIF is described by parameters holding these values: A = 208 M·sec; B = 0.38 M; C = 0.5; t_p = 3.9 sec. All AIF parameters were held constant except the one undergoing a percentage change; in this case, C. The % error scale (y-axis) is the same as for Fig. 2.7, though the % change represented is grossly larger.

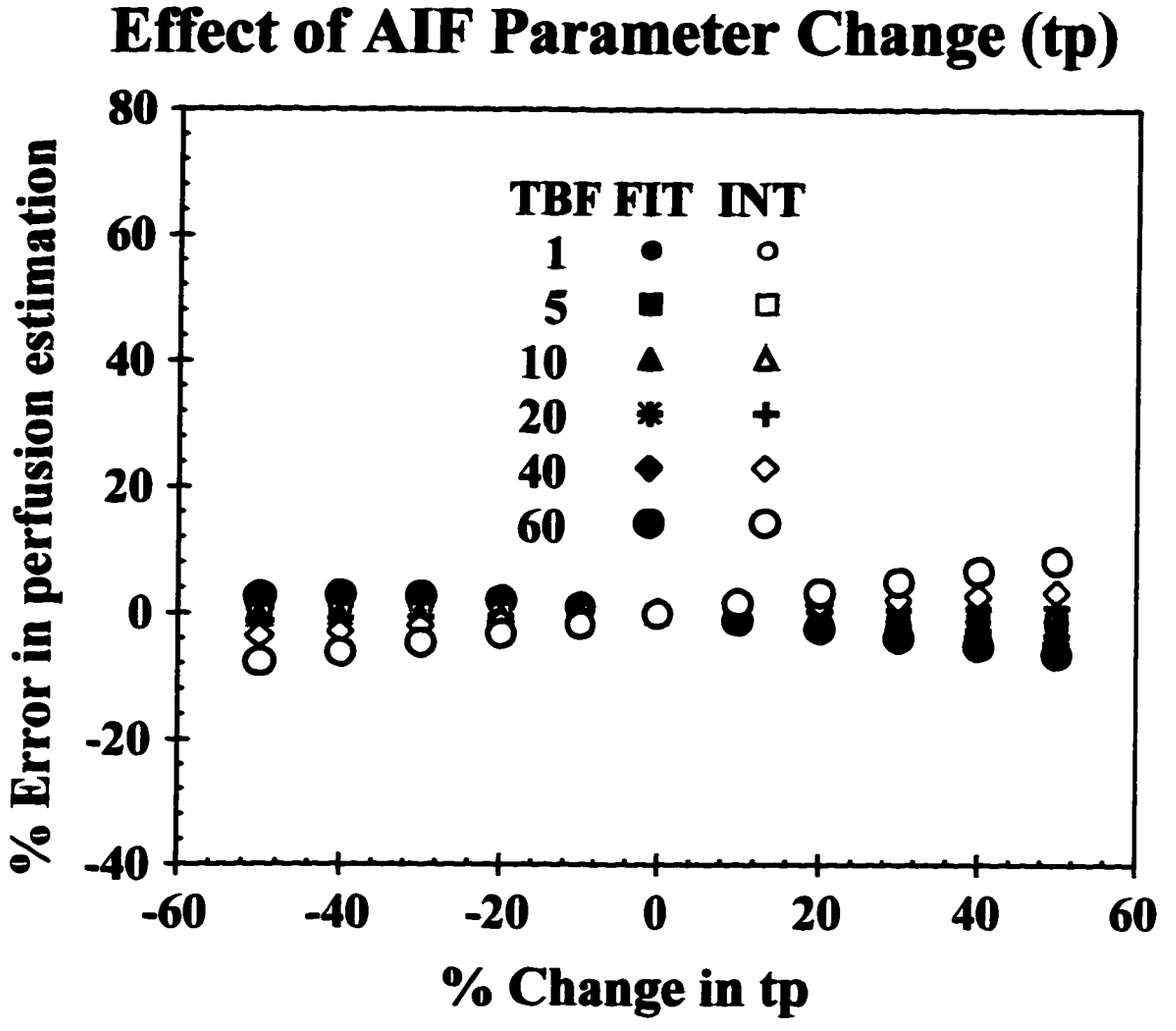

Fig. 2.10 Graph showing the effect of varying an individual AIF on the ability to accurately measure perfusion (TBF) with the INT and FIT approaches using the original AIF (shown as % error) over a range of tissue perfusions {1, 5, 10, 20, 40 & 60 ml/(100 g·min)}. For all cases, the original AIF is described by parameters holding these values: A = 208 M·sec; B = 0.38 M; C = 0.5; t_p = 3.9 sec. All AIF parameters were held constant except the one undergoing a percentage change; in this case, t_p. The % error scale (y-axis) is the same as for Fig. 2.7, though the % change shown is much greater.

described above. Figure 2.12 (and in particular, the enlarged inset) demonstrates that by this tracer delivery approach, the equilibrium concentrations of the common AIF and the extreme cases (High & Low) are much more consistent (range reduced twofold) than that which was observed with the constant tracer bolus injection [Fig. 2.5]. Importantly, there is no longer a correlation ($p = 0.55$) between the animal mass and B [Fig. 2.13] when administering the tracer as a bolus dose. Furthermore, the A values are much more similar (range reduced threefold), and the peaks exhibit a more consistent shape than is seen in Fig. 2.5.

The effect of using a common AIF derived from the constant *dose* group on accurately measuring perfusion with either the INT or FIT analytic approaches is shown in Figure 2.14. By adjusting the tracer volume by the animal's weight (effectively dosing the indicator), the errors in perfusions for both the High tracer equilibrium concentration case and the Low case fall within 10% of the defined true perfusion for either analytic approach over the range of perfusions simulated {1, 5, 10, 20, 40 & 60 ml/(100 g·min)}. The scale is maintained between Figs. 2.14 & 2.6 for ease of comparison.

2. Effect of perfusional heterogeneity

Perfusional heterogeneity is a potential problem when estimating perfusion from a tissue. Tumors are known to often exhibit such heterogeneity [7-11]: however, even in normally "homogeneously" perfused tissues there is likely a distribution of tissue perfusions if the tissue has been compromised (*e.g.* embolism; severe bruising; diseased state). Figure 2.15 shows the effect that changes in perfusional heterogeneity have on accurately deriving true perfusion over a range of perfusions with either analytic approach. As the heterogeneity increases (simulated by increasing the coefficient of variation of the

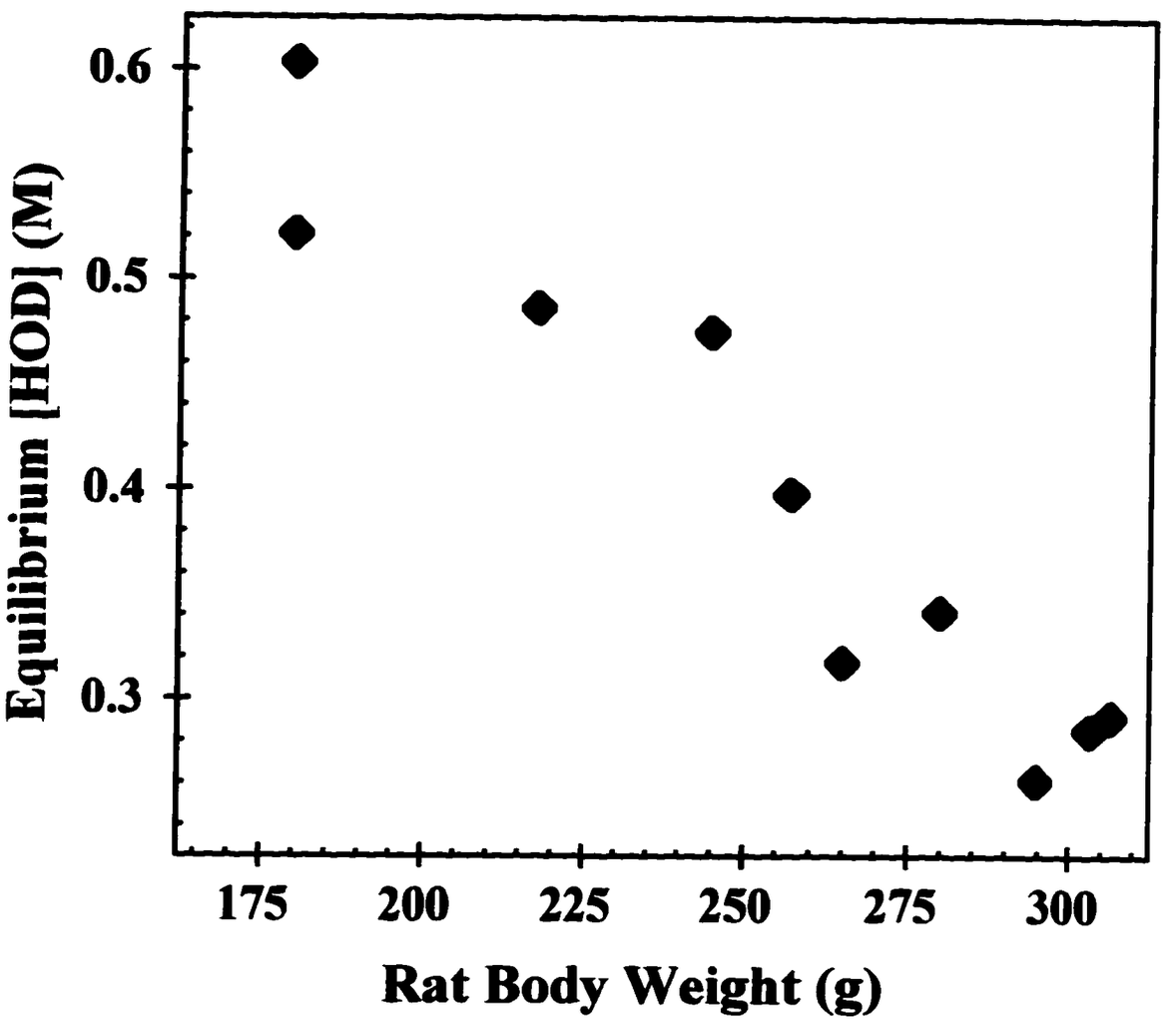

Figure 2.11 Plot relating the rat body mass to the fitted end-equilibrium tracer concentration (the AIF parameter B) for animals receiving a constant tracer volume (n = 10; 500 µl D_2O). The two parameters correlate highly (Pearson correlation, P = 0.00002).

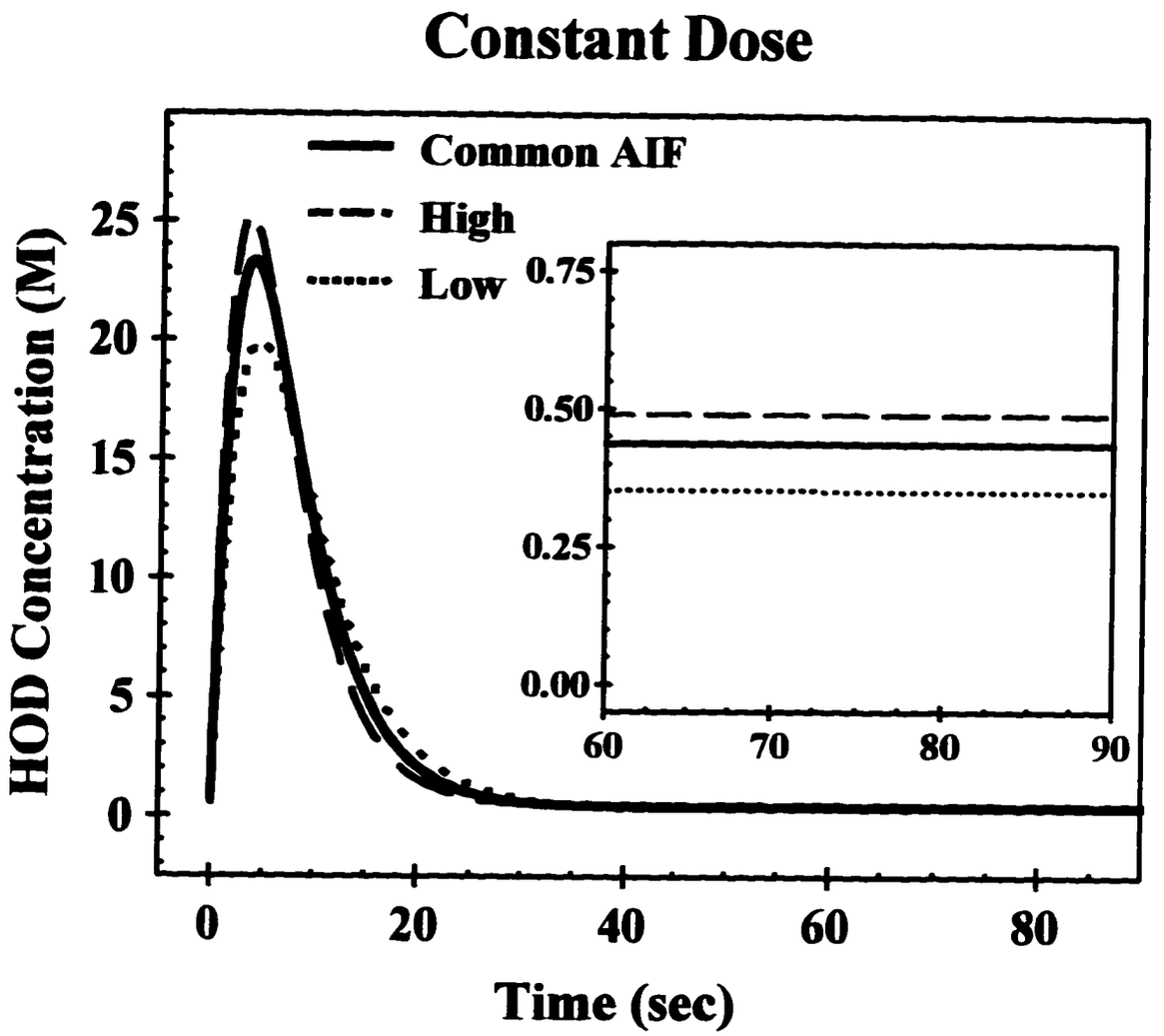

Figure 2.12 Extracted AIFs from animals receiving a constant tracer dose (D_2O given at 2 μl/g rat mass). Shown are the extreme cases (High and Low equilibrium values) as well as the common AIF. The common AIF was constructed from the mean of all parameters which describe the AIF from the rats observed (n = 6).

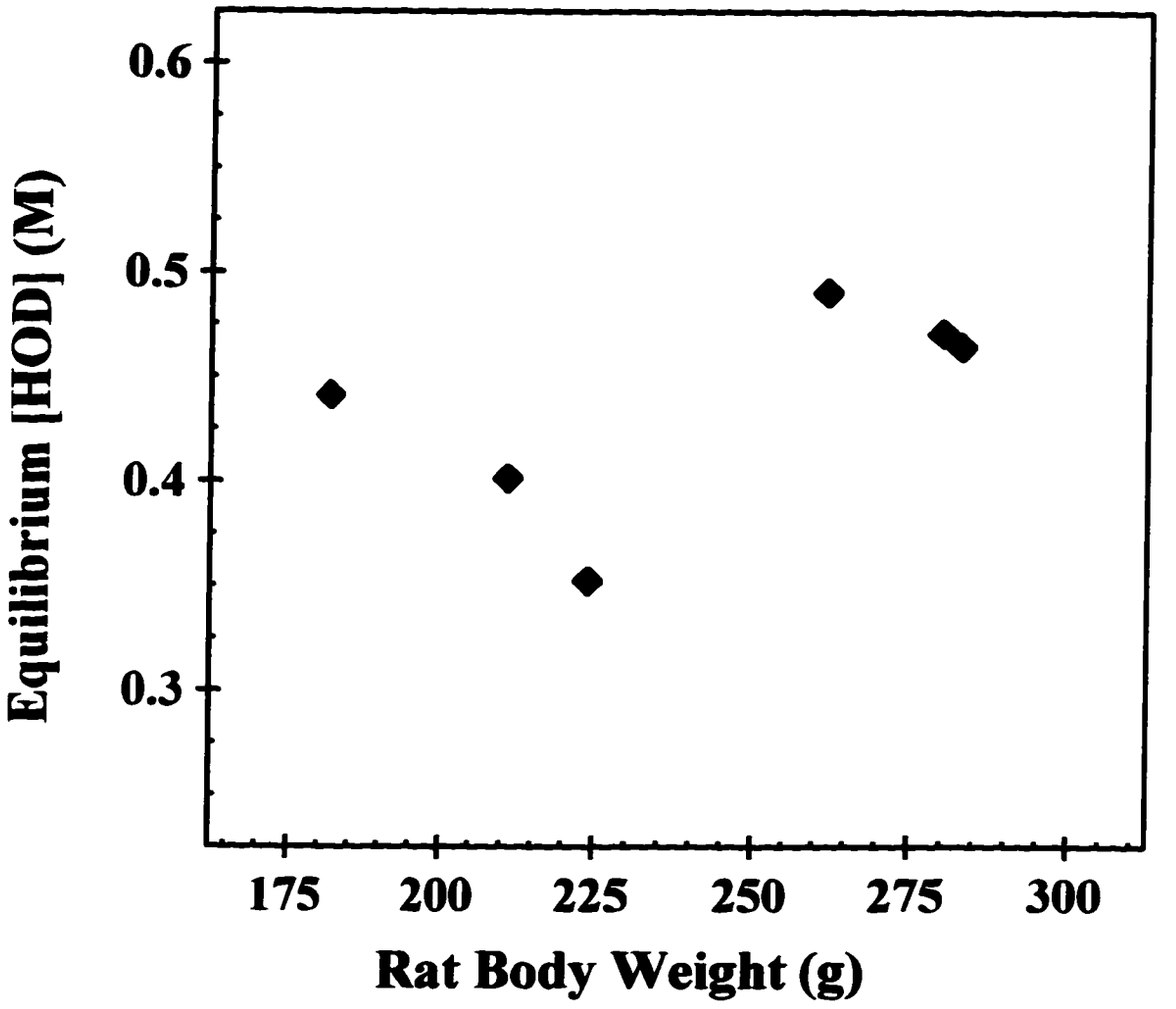

Figure 2.13 Plot relating the rat body mass to the fitted end-equilibrium tracer concentration (the AIF parameter B) for animals receiving a constant tracer volume (n = 6). The dose given was 2 μl D_2O per gram animal mass. The two parameters do not correlate (Pearson correlation, P = 0.55).

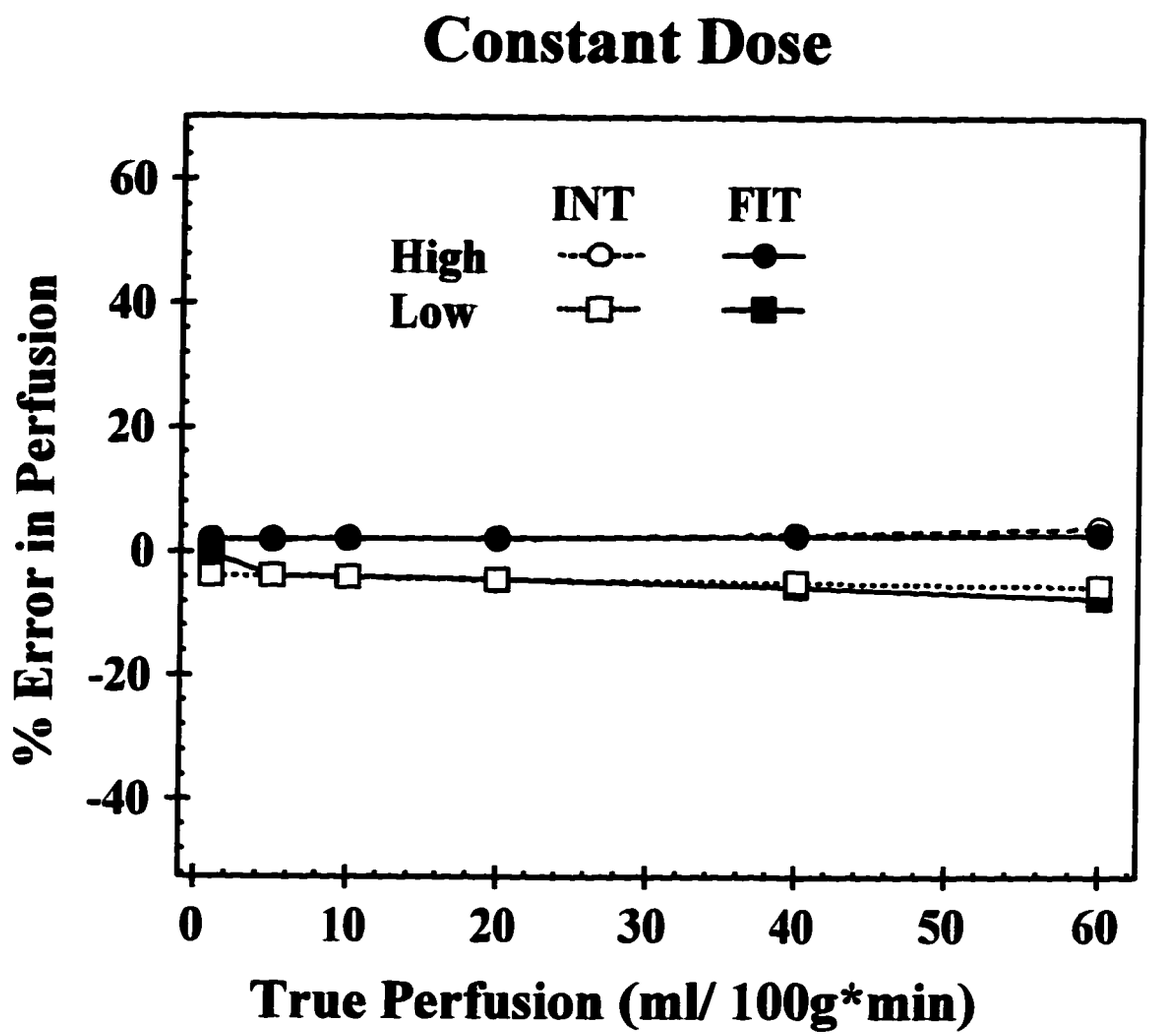

Fig. 2.14 Effect of AIF variation on estimating true perfusion using a common AIF and delivering a constant tracer dose (D_2O given at 2 μl/g rat mass). Errors in perfusion estimation when using the common AIF rather than the animals' actual AIF are shown for the extreme cases (High and Low equilibrium values), and are calculated for various perfusions {1, 5, 10, 20, 40 & 60 ml/(100 g·min)} by both the FIT and INT analytic approaches. Errors are within 10 % for all cases.

perfusion), the % error in perfusion estimation increases. This effect is much more pronounced in data analyzed by the FIT analytic approach than by the INT approach, when the data are fit as one would fit imaging data (*i.e.* pixel values from images acquired in 30-second blocks), particularly in low perfusions common to tumors (below 40 ml/(100 g·min)). Simulations of heterogeneity in which perfusion is split into distinct compartments, each with a heterogeneity (such as what might occur intrinsically in tumor, or in a normal tissue which has undergone a regional change) shows that the INT analytic approach is less sensitive than the FIT approach to this heterogeneity. This sensitivity of the FIT approach increases as the difference between the dual perfusions increases.

3. Effect of random noise

Noise in NMR measurements is often a problem, especially when observing relatively insensitive nuclei such as those of deuterium. This will be compounded in imaging experiments, where the pixel volume under observation will be much smaller. Figure 2.16 shows the impact that random (uncorrelated) noise in the data has on precisely measuring perfusion by either the INT or FIT methods, over a range of perfusions {1, 5, 10, 20, 40 & 60 ml/(100 g·min)}. The computer simulations demonstrate that random noise affects the precision of the derived perfusion for either the INT or FIT approaches, with the precision described as the % coefficient of variation. This effect on precision is greater for perfusions derived with the INT approach for any perfusion tested, with this effect markedly worse (*i.e.* higher % C.V.) at the lower perfusion rates {*e.g.* 1 or 5 ml/(100 g·min)}. At perfusions greater than 20 ml/(100 g·min) and noise less than 300 mM, the error is less than 10% for either analytic approach. The amount of noise routinely observed in imaging experiments is on the order of 150 - 300 mM: spectroscopic

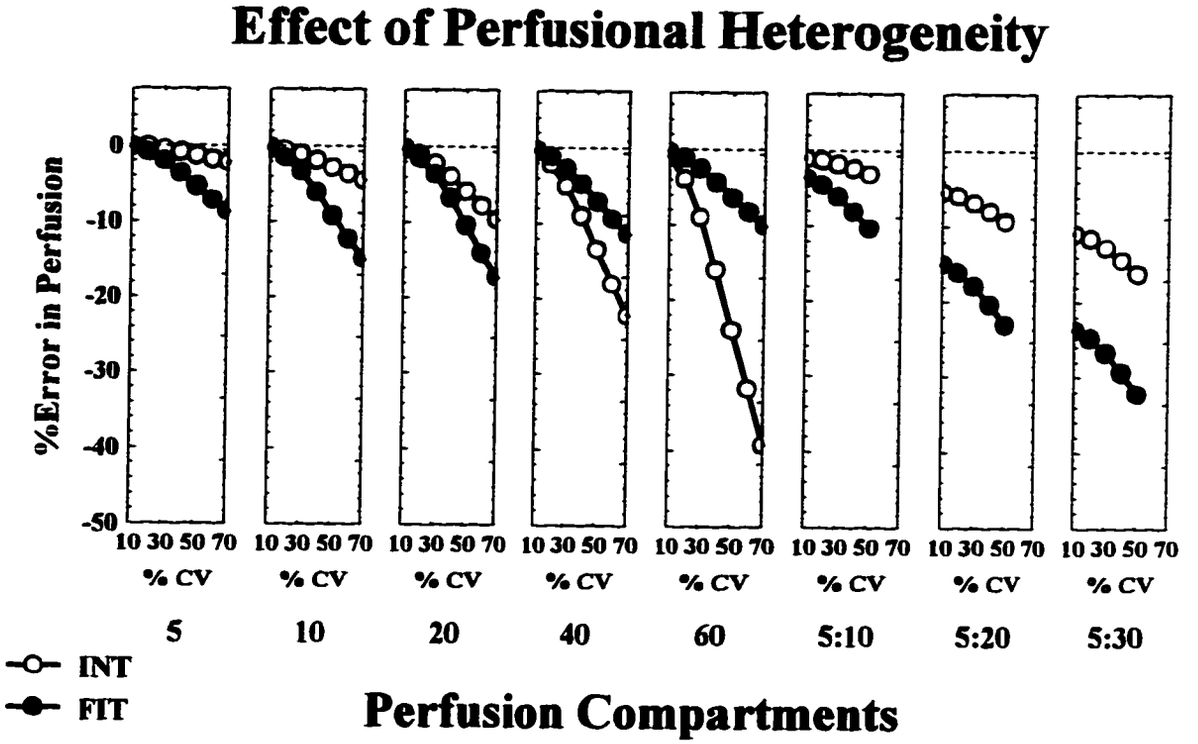

Fig. 2.15 Relationship between perfusional heterogeneity and accuracy of deriving true tissue perfusion with either the INT or FIT analytic approaches to the data. Perfusional heterogeneity is modulated by considering single perfusion {5, 10, 20, 40 or 60 ml/(100 g·min)} to have a coefficient of variation (with the variation ranging from 10 - 70%), or by simulating a mixed dual compartment {50% 5 ml/(100 g·min), and 50% 10, 20 or 30 ml/(100 g·min)}, each perfusion with a coefficient of variation.

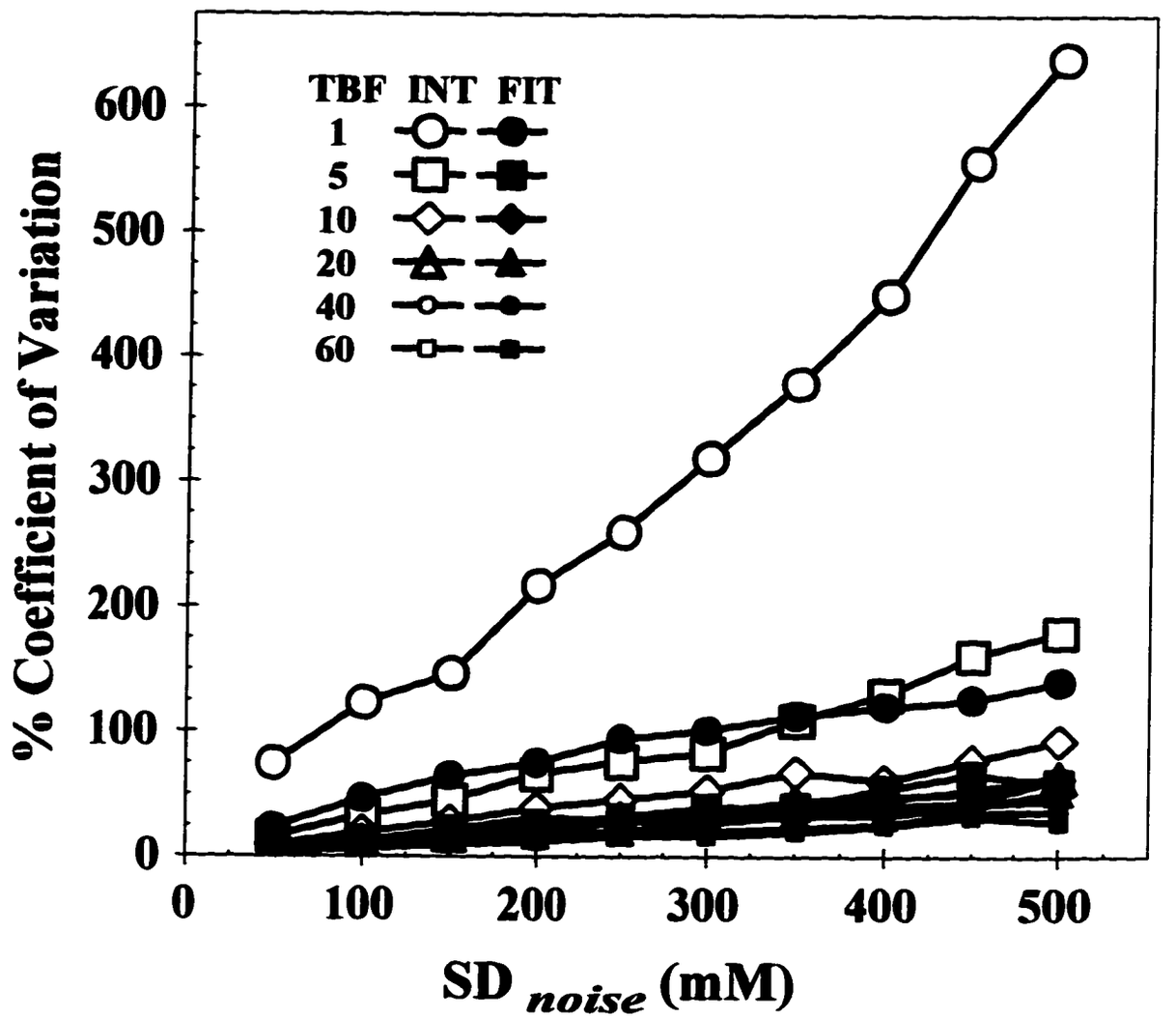

Figure 2.16 Computer simulated effect of random noise on the precision of derived perfusion using either the INT or FIT approaches over a range of perfusions {1, 5, 10, 20, 40 & 60 ml/(100 g·min)}. Random (uncorrelated) noise (50-500 mM) was added to simulated tracer concentration curves, and repeated 100 times to determine the coefficient of variation. The accuracy of the perfusion measurements was not affected by the addition of random noise.

data tend to be less noisy due to the generally larger volume from which one extracts signal. The accuracy of either analytic approach in deriving perfusion is unaffected by random noise, as determined from the average perfusion value of the 100 repeated measurements.

D. Discussion

1. Extraction of the AIF

Consistent and accurate measurements of perfusion through external detection of a tracer by application of the Kety model (such as when detecting deuterated water tracer with NMR) has previously required knowledge of each animal's individual AIF. Often, when tracer methods are employed in experiments, a constant volume of tracer is given to all animals within the experiment (regardless of body mass), and the behavior of this tracer is used to estimate the perfusion through the tissue of interest [*e.g.* 10,76,83,88]. However, though this constant volume technique is in general use, consideration of the strengths and weaknesses of this approach have not been rigorously studied, particularly concerning its impact on the AIF.

Though it is possible to measure an individual AIF in larger animals, the commonly used exsanguinous method for direct measurement of the AIF in rats results in the immediate death of the animal, and by its nature changes the cardiac output (and therefore the AIF) during the measurement. Through use of a carotid observation chamber and application of Iida's approach [92], this research indicates that indirect measurement of an apparent AIF can be executed in rats. The apparent AIFs extracted by this method [Fig. 2.5 & 2.12] have characteristics and shapes similar to AIFs directly measured from larger

animals and humans [73,88], with the tracer rapidly rising then falling, and, in the case of the non-decaying (isotopically stable) NMR tracer, eventually reaching a non-zero equilibrium value. Importantly, the extracted AIFs from the animals are similar in shape to those extracted from the *in vitro* setting [Fig. 2.4], suggesting that though assumptions and modeling are used in extracting the AIFs from the data, their application results in reasonable curves of the arterial concentration of the injected tracer.

Even though a reasonable measurement of an apparent AIF can be estimated using the carotid observation chamber approach, the procedure is difficult to perform in small laboratory animals such as rats. If tissue perfusions are desired from an animal, the combined surgeries necessary to extract the AIF and the perfusion are taxing on the animal. Moreover, to perform perfusion NMR studies as well as obtain the AIF during the same session complicates the experiment. If one desires to perform NMR perfusion studies, one would rather not have to measure the AIF of each animal. It is more desirable to use the carotid observation chamber approach in a few animals to derive a representative common AIF, then apply this common AIF when determining tissue perfusion values in future studies, thus eliminating the need to extract the AIF from each subsequent animal. Therefore, a common AIF was derived from the apparent AIFs of a group of animals to determine the effect that variations in individual AIFs may have on the general applicability of using a common AIF in subsequent perfusion measurements.

2. Influence of AIF alterations on perfusion

As is shown in Fig. 2.6, using a common AIF derived from animals receiving a constant tracer volume is not an appropriate method when estimating the true perfusion with either the INT or FIT analytic approaches. The substantial differences in shape

between the common and extreme AIFs [Fig. 2.5] is reflected in a large difference in the A values (the Molar·second area under the input curve). Furthermore, the equilibrium values of the extreme cases differ by up to 50% from the common AIF. As is shown in Figures 2.7 - 2.10, the features of the modeled AIF which can most likely affect the measurement of perfusion when using a common AIF are the A and B modeled parameters. Small changes in these can result in substantial perfusion estimation errors. Changes in the C and t_p parameters, however, have little effect on the perfusion estimation even when undergoing extremely large variation.

3. Constant dose

A Pearson test demonstrated a significant correlation between the animal mass and the equilibrium concentration (B) value ($n = 10$; $p = 0.00002$), which suggested that any variation in B between animals and a common AIF could be minimized by administering an injection volume corrected for the animal mass (the constant *dose* method). This correlation can be better understood by considering the tracer to have a certain volume of distribution within the animal. By adjusting the tracer volume by the animal's weight (effectively the volume of distribution in animals), a desired equilibrium concentration value can be approached. It should be noted that animals used in a study should have similar body fat compositions so that their effective volumes of distribution are comparable, since fat is not an effective repository for the tracer (effectively water) used here.

The delivery of a dose of tracer based on weight has an immediate advantage in that the variation of the equilibrium concentration is reduced considerably in the extracted AIFs {$< \pm$ 15% deviation from the common AIF for the two extreme cases; [Fig. 2.12]}

from that observed with the constant tracer volume technique {$< \pm$ 50% deviation from the common AIF for the two extreme cases [Fig. 2.5]}. Moreover, the A value has threefold less variation with the constant dose than found with the constant tracer volume technique. When the constant dose method is implemented to derive perfusion values from tissue, the % error in perfusion estimation is reduced to acceptable levels ($< \pm$ 10% for the extreme cases) for both the INT and FIT approaches up to perfusions of 60 ml/(100 g·min); [Fig. 2.14]. This suggests that in order to take advantage of using a common AIF when applying the Kety equation to analyze tracer uptake data, one should use a constant tracer dose both for deriving the common AIF, and for subsequent perfusion experiments. Once a common AIF has been determined for an animal model of study using the constant dose, the derived common AIF can be used in all subsequent perfusion estimations, eliminating the need for the difficult measurement of the AIF in every animal.

4. Optimum analytic approach

The implications of the computer simulations on the effect that random noise, heterogeneity and the AIF have on measuring tissue perfusion indicate that the proper choice of analytic approach (INT *vs.* FIT) may be critical to reduce errors when estimating perfusion by the tracer uptake approach. When obtaining large volume-average perfusion measurements with relatively low perfusions, as is done with NMR whole-volume spectroscopy of solid tumors or resting muscle, the INT approach may be superior, since this approach is not as sensitive to the flow heterogeneities which may commonly occur in large tissues/tumors (yet often absent in smaller volumes) [9-11,90], and it is not greatly affected by noise due to the relatively large S/N. This advantage appears to be reduced at

higher perfusions, but this is because the INT approach was windowed to be optimal at lower perfusions. For studying perfusions in tissues with higher values (such as is found in organs), the windowing should be changed. By so doing, the INT approach can maintain it's superiority over the FIT approach over other perfusion ranges.

Whatever the advantage which the INT approach has over the FIT approach in terms of sensitivity to perfusional heterogeneity when the FIT approach is applied to data sets acquired over a long time period with poor temporal resolution (such as those acquired with imaging experiments), it remains to be seen whether this sensitivity remains when applying the FIT approach to short time data sets with good temporal resolution.

When measuring perfusion in tissues with high perfusion rates (organs), the INT approach becomes more sensitive to differences between the true AIF and the applied common AIF [Fig. 2.7]. This sensitivity of the INT approach to the AIF suggests that the FIT may be superior for any perfusion estimations performed in tissues which are believed to have high perfusions (> 50 ml/(100g·min), even if whole-volume spectroscopy is performed. As tumors are generally considered to have perfusions below this value, the INT method is appropriate for whole-volume tumor perfusion studies.

When analyzing perfusion imaging data from many small volume elements (which are less likely to contain large perfusion heterogeneities, but have relatively low S/N), the FIT approach is always recommended. This is because the FIT approach is not as affected as the INT approach by the inherently low S/N found in small volume elements, and since the potential for heterogeneity (to which the FIT approach is sensitive) is markedly reduced when observing small volumes. It may well be that there is a trade-off when applying either of these approaches, but one may exploit S/N sensitivity for higher

resolution (or *visa versa*) if the case permits. This conclusion, that the method and details of analysis are dictated by the type of experiment performed, is valid not only for the deuterium NMR techniques described here and elsewhere, but for any technique which measures perfusion through the external detection of the tissue residue of freely-diffusible tracers (*i.e.* all techniques based on the Kety model).

5. Factors influencing the AIF

Computer simulations demonstrate that one can use a common AIF for perfusion analysis with less than a 10% error in perfusion measurement if one administers the indicator as a bolus dose. However, the AIFs used in this study were extracted from animals under the same experimental conditions. To better appreciate the limits of applying an AIF in perfusion estimations, there should be an understanding of how the AIF relates to the physiology of an animal. The AIF we use is described by certain modeled features (or parameters). These parameters, even though modeled, allow for changes in the AIF to be evaluated, or predicted with changes to the tracer input.

Two factors which can influence the AIF are the rate of tracer injection and the rate of flow of the carrier fluid through the vascular vessel in which the tracer is injected. How these factors can alter the AIF may be understood by considering the concentration of the tracer at the site of entry. If the flow rate through the vessel at the site of tracer injection is lower (*i.e.* if the cardiac output of the animal has decreased), the tracer concentration will peak later, at a higher concentration (since there is more tracer per unit volume blood at the site of injection than when the flow rate in this vessel is higher), and result in a higher A value in the AIF. Likewise, if the flow rate at the site of injection is higher, the peak time will be earlier, the peak concentration will be lower, and the effective

A value will be lower. As described earlier, the B value can be essentially fixed (through administration of a constant tracer dose), and even a great change to the C parameter has little consequence. These changes in the AIF shape and model parameter values have been observed qualitatively with *in vitro* studies extracting an apparent AIF from the bypass chamber after tracer injection into the efferent catheter perfused with carrier water at known flow rates, as described in section 2.B.1.b.

As Figure 2.7 shows, if the individual AIF A value increases (from either a decrease in the cardiac output, or an increase in the tracer delivery rate), but is analyzed with a somewhat lower-A-valued common AIF, the perfusion through a tissue will be overestimated. If the individual A value decreases, the perfusion may be underestimated. Since simulations illustrated in Figure 2.14 show that little error occurs if using a common AIF for perfusion measurements with animals under similar experimental conditions, one can deduce that the variation of AIFs within a group of animals experiencing the same conditions is small enough to be of little concern. But if there are larger differences between the group from which the common AIF was derived and the experimental group (which could occur if the two groups had substantially different cardiac outputs), the errors shown in Figure 2.7 can occur. The message here is that the experimental conditions should be held constant for all members of both the experimental group and the small group from which the AIF was derived. It is imperative that if experimental conditions change (*e.g.* physiological, experimental or anesthetic changes), a new common AIF should be derived under these new conditions to analyze the data obtained under these new conditions. In other words, there is no single common AIF which can be used under all experimental conditions. For example, if perfusion is to be measured at two

separate time-points under anesthesia, common AIFs for each time-point should be obtained and applied to the appropriate data. These separate common AIFs can be created by using the carotid observation chamber method as described here on a small group of animals for any experimental condition encountered.

6. Limitations

A limitation which should be mentioned is that it is not possible to measure the AIF, even using the indirect method described above, in mice. Without the derivation of a representative common AIF for a given experimental condition, the resultant perfusion measurements in mice will not be absolute (though they will be quantitative, as long as the conditions, and therefore the AIFs, do not change). However, *if* methods are ever developed to allow the determination of AIFs from mice, the above observations and limitations discussed above will apply (*e.g.* administration of a bolus tracer dose; use of an appropriate analytic method; and use of a common AIF appropriate for the experimental condition under which the perfusion is measured).

There are some important experimental procedures which need attention to ensure that the perfusion results obtained reflect reality. One of these is to maintain a constant tracer injection rate for all experiments performed, so as not to greatly alter the shape of the AIF; an important parameter in the model used here which would be affected is A. If the rate of injection increases, the concentration of the tracer at the injection site will be higher (similar to what happens when the carrier fluid flow at the site of injection is decreased). Constant injection rates can be accomplished by either careful and consistent injection (as was done in these experiments), or by mechanizing the injection (with the use of a rapid push pump or syringe driver). Changing the rate of tracer injection may alter

the true AIF shape enough to make accurate measurement of perfusion difficult with a common AIF. Lastly, one should strive to use animals with similar levels of body fat in experiments: fatter animals have equilibrium concentration values which do not necessarily represent their mass (in the AIF model used here, the B value will be higher than predicted due to the tracer insolubility of the fat: the volume of distribution is less than what would be predicted based on the animal mass). For rats, animals under 300 g are generally acceptable, since they do not have large stores of fat. Alternatively, one could give a test dose of the tracer some time beforehand, and measure the equilibrium concentration at an appropriate time after administration to obtain the true volume of distribution for that particular tracer in that specific animal. Then, accurate dosing could be done for each individual animal, resulting in an improvement in forcing the B term to a desired value, and perhaps tightening the AIFs from a group of animals [as in Fig. 2.12]. This would lead to even less error than what was observed before [Fig. 2.14] when applying the common AIF to analyze data.

CHAPTER III TUMOR PERFUSION DETERMINED BY NMR USING DEUTERATED WATER AS A TRACER: USE OF AN OPTIMIZED METHOD COMPARED WITH MICROSPHERES

A. Introduction

As discussed in Chapter I.C, perfusion (*i.e.* the blood flux through tissue, commonly expressed in ml/100 g·min, and alternatively termed blood flow) can have a significant impact on the response of tissues to many common and experimental modes of therapy (chemotherapy, radiation therapy, hyperthermia, bioreductive therapy). Since manipulating tumor vasculature and tumor perfusion has become a recent focus in anticancer research [32], accurate measurement of tumor perfusion, and observation of this perfusion throughout a course of therapy, are of interest. These measures may also be useful in interpreting how perfusion impacts the physiological environment.

A non-invasive, repeatable method with which to measure perfusion was discussed in Chapter I.F.4, along with the strengths and weaknesses of this NMR uptake approach. In brief, the weaknesses of the NMR uptake approach are that it requires knowledge of the AIF (which is difficult to measure), while data analysis to extract tumor perfusion measures is potentially complicated by tumor characteristics such as the potential for large flow heterogeneities [20-22,25], and generally low perfusion, which reduces the signal-to-noise ratio (S/N). To address this, Chapter II reported computer simulations showing optimum criteria for data analysis as well as the methods allowing extraction of an apparent AIF from rats. More importantly, simulations suggest that one

may apply a derived common AIF in calculating NMR perfusion measurements if a bolus injection of a constant tracer *dose* (rather than volume) is used. These computer simulations led to modifications of the NMR uptake approach of measuring perfusion. The significant modifications were to administer the tracer as a bolus dose (based on the animal mass); to analyze the data with the proper analytic approach; and importantly, to use a derived common AIF in studies. The next step was to test the validity of such a modified approach in accurately measuring perfusion. This was accomplished by first designing the apparatus which would allow comparative experiments, then developing techniques to allow the comparison of the modified and optimized NMR method with the commonly used microsphere method. Since quantitative perfusion values are necessary when deriving meaningful physiological relationships between therapy and response in tumors (as well as other tissues), we have tested the validity of this optimized NMR approach by comparing it to the commonly used microsphere measurement (which is presumed to be quantitative [23] if appropriate sized spheres are used) to measure whole-volume TBF in an *in vivo* rat tumor model (the 9L gliosarcoma).

B. Materials and Methods

1. Host and tumor line

The animals used in these studies were syngeneic adult male Fisher 344 rats obtained from Harlan Sprague-Dawley [Indianapolis, IN], weighing between 205 and 300 g. Animals were supplied with food and water *ad libitum*, and were housed and cared for in accordance with institutional guidelines. The tumor line used in these experiments was the 9L gliosarcoma obtained courtesy of Drs. K. T. Wheeler and C. A. Wallen (Bowman

Gray School of Medicine). The parent line was originally developed by investigators at Massachusetts General Hospital following induction of brain tumors in CD Fisher rats by N-nitrosomethylurea [93]. The cells were maintained *in vitro* in Eagle's medium [Gibco, Grand Island, NY] supplemented with 15% fetal calf serum [HyClone, Logan, UT], 1% L-glutamine, 1% amino acids, 1% vitamins [all Gibco BRL, Grand Island, NY], and antibiotics (penicillin and streptomycin [Sigma, St. Louis, MO], each at 80.5 units/ml), and passaged as described by Wheeler [94]. *In vitro* passage was limited to twelve weeks (one passage each week), with cells brought out of frozen stock after twelve passages to reestablish the line and limit potential genetic drift and ensure fidelity of the cell line. Cells for tumor initiation were always obtained from *in vitro* cultures and never from another animal. The tumors were initiated by implanting $3 \cdot 10^5$ cells (in 0.15 ml) *s.c.* approximately 1 cm above the left inguinal region of the rats. The resultant tumors, weighing between 0.9 - 2.2 g at the time of the studies, appeared within three weeks, and were used in all tumor perfusion determinations.

2. Anesthesia

Isoflurane [Aerrane: Ohmeda, Madison, WI] was given as an inhalant through a homebuilt mask at 2% V/V in O_2 to induce anesthesia, and maintained throughout the surgery and perfusion experiment at 1.8% V/V. Expired air and excess anesthetic was removed from the mask *via* an attached vacuum salvage line. The choice of this inhalant anesthetic is in part due to the fact that Isoflurane does not impair the cerebrovascular autoregulation or the mean arterial pressure as much as does an alternative inhalant anesthetic Halothane [95].

3. Restraining table

After anesthesia was induced (< 4 min at 2% V/V in O_2), animals were placed supine onto a homebuilt Plexiglas table [Fig. 3.1], with the animal's nose placed into an anesthesia mask. The entire experiment, including surgery, was done with the animal on this table. The table was heated by a coil of tubing through which warmed water circulated, and also held the RF coil, circuit board and anesthesia mask. Since the NMR experiment occurs well inside a small-bore magnet (the gradient insert has a 20.5 cm i.d. bore; the center of the magnet is 46 cm into the bore), the ability to perform distant manipulations was necessary; therefore microvalves (dead volumes on the order of 10 μl) and pushrods connected to syringes attached to homebuilt catheters were included in the table design to facilitate administration of the microspheres, deuterated water and KCl from a distance. An illustration of an animal with the experimental catheter attachments is shown in Fig. 3.2.

4. Euthanasia

At the conclusion of the NMR data collection, the animal was euthanized while in the magnet (and still under anesthesia) by administration of 0.5 ml KCl [Sigma, St. Louis, MO] directly into the heart. The catheter used was the same catheter with which the microspheres were injected. Switching between the microspheres and the KCl was accomplished with a home-built microvalve.

5. NMR conditions

The nuclear magnetic resonance spectroscopic measurements were performed in a Bruker Biospec II spectrometer [Bruker Instruments, Billerica, MA]. Whole-volume perfusion was measured by placing the tumor within a 3 turn, 15 mm i.d. solenoid coil

double tuned to both proton (200 MHz) and deuterium (30.8 MHz). Magnetic field homogeneity was optimized by maximizing the free induction decay (FID) lifetime of the water proton signal from the tumor. By placing a copper radio-frequency shield (with the tumor protruding through a hole cut out of the shield) over the body, extraneous signal from the body was essentially eliminated. The deuterated water (HOD) concentration was calculated by the method of Thulborn and Ackerman [96]. Proton acquisition parameters were a 65° flip angle; 1024 data points; 20 kHz spectral width; 1.75 s repetition time; and 32 averages. Deuterium acquisition parameters were a 65° flip angle; 512 data points; 2 kHz spectral width; 250 ms repetition time; and 8 averages (360 averages for background collection). The details of extracting perfusion from the NMR data are described in detail elsewhere [58]. Briefly, a proton spectrum is acquired, then a background deuterium spectrum. Immediately before remote bolus injection of the tracer, continuous deuterium spectra are acquired. An uptake-integral (with acquisition limits of 30 and 120 s after initial arrival of the tracer in the tissue) is generated by summing the 16th through 60th spectra, and subtracting the background spectrum (either representative of natural abundance HOD or residual HOD from previous experiments). The absolute molar·second (M·s) value of this integral is calculated from the ratio of the deuterium signal to the proton signal by reference to a calibration curve [Fig. 3.3]. The M·s value can then be related to a perfusion by comparison to a look-up table which was generated from the Kety equation.

6. Microspheres

An adaptation [50] of the reference sample method for determining regional blood perfusion with microspheres in rats [48] was used to calculate volume-average tissue

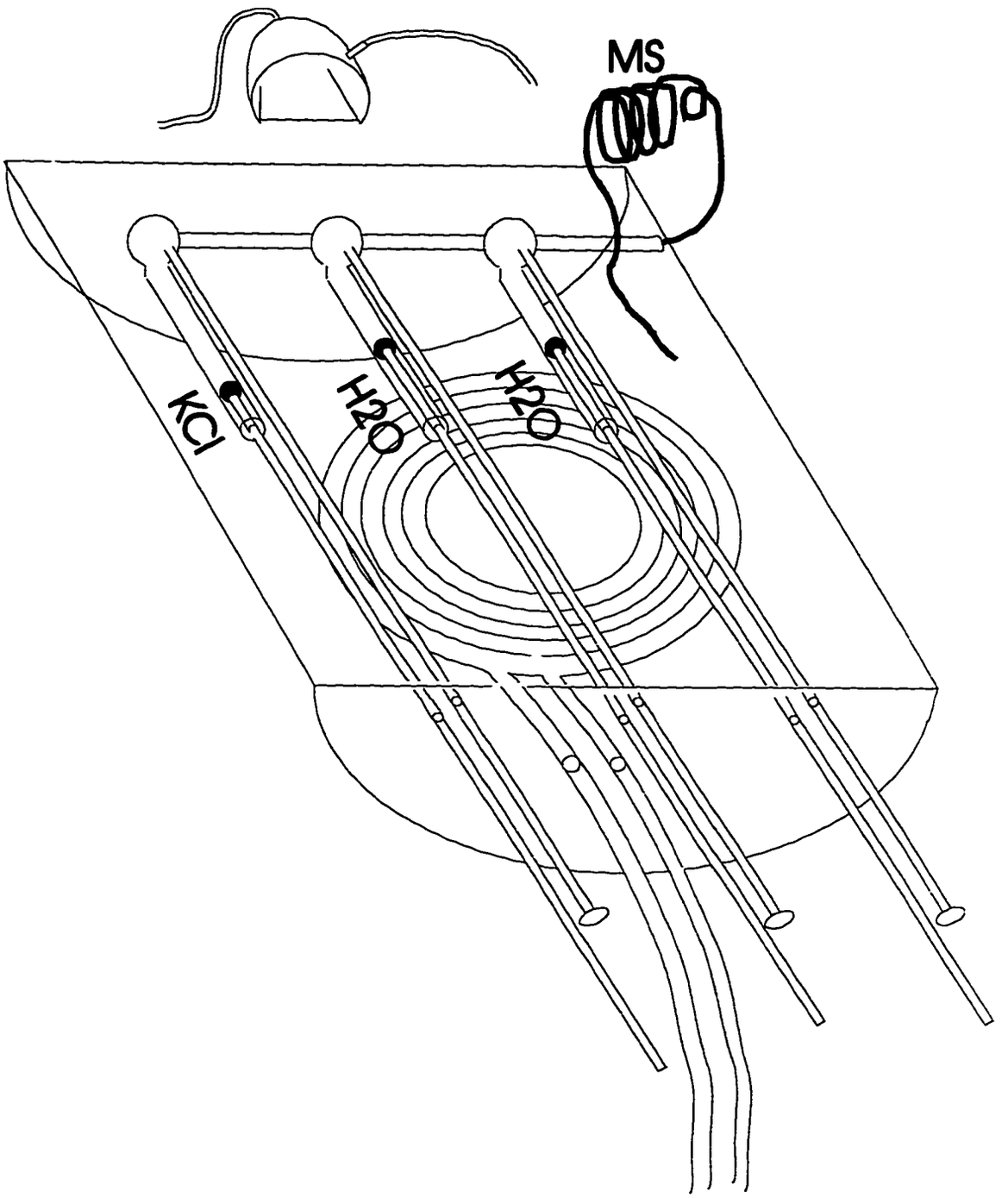

Fig. 3.1 Illustration of the experiment table. Shown are the three syringes attached to extended pushrods; three microvalves; waterpad; microsphere delivery coil; and the anesthetic nose-cone with vacuum line. The heating pad is shown beneath the pushrods to allow visualization of the pushrods: it actually lies just beneath the tabletop surface. Deuterium is injected through a separate catheter (not shown).

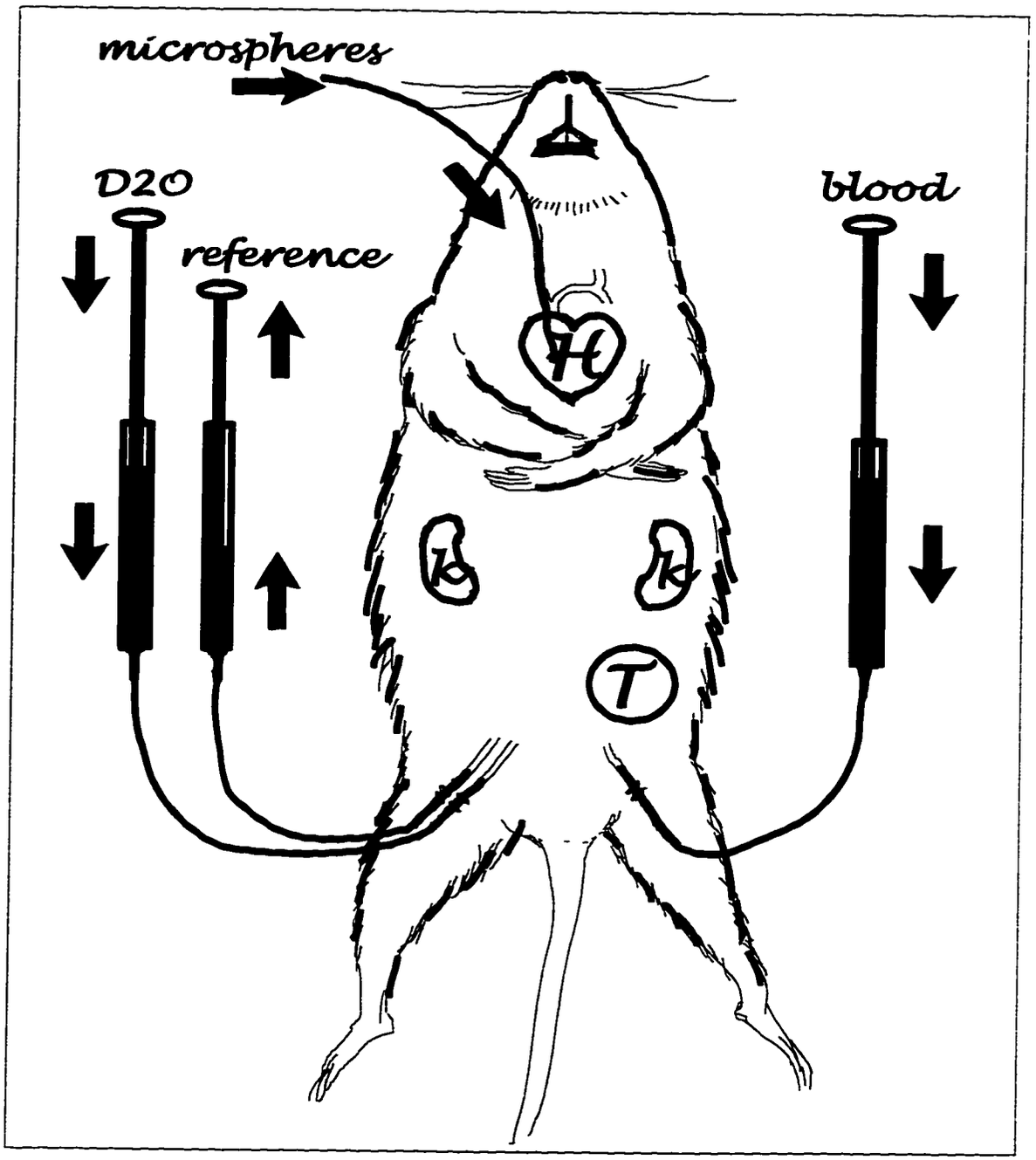

FIG. 3.2 Schematic of a rat with the implanted catheters used in the head-to-head perfusion comparison experiments. Inputs include microspheres (MS), the deuterated tracer (D_2O), and replacement blood. A reference organ withdrawal catheter is also represented. Tissues are designated as **H** - heart; **K** - kidney; **T** - tumor.

perfusion from microsphere deposition. Technical considerations are described elsewhere [50,48,51,96]. Rather than using the traditional radiolabeled microspheres, fluorescently labeled microspheres [45,46] were used. The main advantage of this method is that the expense, exposure, and storage problems associated with radioactive microspheres are eliminated. This fluorescent microsphere method uses polystyrene latex microspheres which contain a large amount of proprietary fluorescent dyes [FluoSpheres: Molecular Probes, Eugene, OR]. Three sizes were used in these studies; 10.3, 15.5, and 21.0 μm diameter microspheres, each loaded with dyes whose fluorescence wavelengths were well separated from each other. The coefficient of variation in diameter was less than 5% for each size used. A homebuilt carotid catheter was surgically implanted and pushed towards the heart until the open end was in the left ventricle (the blood pressure in this catheter falls to zero when the end enters the heart chamber). A standard concentration of FluoSpheres were placed into a volumetric coil made from PE50 tubing (~240 μl), which was placed in-line between the implanted catheter and a syringe. To deliver the microspheres into the left ventricle of the heart, the pushrod attached to the appropriate syringe was pushed. The catheter was then flushed with 0.8 ml saline [Abbott Labs, N. Chicago IL] to ensure delivery of all beads into the animal. A heparinized femoral artery catheter was used to withdraw the "reference organ" blood sample at 0.5 ml/min for 90 seconds (10 seconds before microsphere injection to 80 seconds post injection) by placing the attached syringe into a modified Harvard Apparatus Pump [Harvard Apparatus, Millus, MA]. A separate femoral vein catheter was attached to a syringe filled with replacement blood from a matched littermate. This syringe was also attached to the Harvard Pump to allow for simultaneous replacement of the blood and

avoid hemodynamic complications associated with substantial blood loss.

7. Collection of tissues

Once the animal was euthanized and removed from the magnet, the tumor, reference blood sample and both kidneys were removed, weighed, then placed in FluoSphere filtration devices [Molecular Probes, Eugene OR]. These filtration devices trap the microspheres, and allow for handling of the microspheres without transfer losses. Each sample was digested by alkaline hydrolysis, accomplished by immersing the tissue and filtration devices in a 4M KOH [Aldrich, Milwaukee, WI] bath for 24 hours. The samples were maintained at ~ 40° C by placing the bath on a hot plate. The heat assisted in the alkaline hydrolysis. The resultant hydrosylate was removed through centrifugation of the filtration devices (1000G x 15 min), which traps the FluoSpheres. The microspheres were rinsed by addition of deionized water into the filtration devices, recentrifuged, rinsed again with 5 ml isopropyl alcohol [J.T. Baker, Phillipsburg, NJ], recentrifuged, then allowed to air dry. The dyes within the dried microspheres remain stable for at least 7 months (Molecular Probes), but all samples were analyzed within three days.

8. Dye measurement

A known volume of *Cellosolve* acetate [Aldrich, Milwaukee WI] was added to the filtration devices to dissolve the trapped beads and release the fluorescent dye. Fluorescent activity of the dye was measured by placing a glass cuvette containing a 1.0 ml sample in a fluorescent spectrophotometer [Shimatzu ETC, Japan], and reading the resultant light intensity. By comparing the activity to a calibration curve [Fig. 3.4], the number of beads within the sample was calculated. The "reference organ" was used to

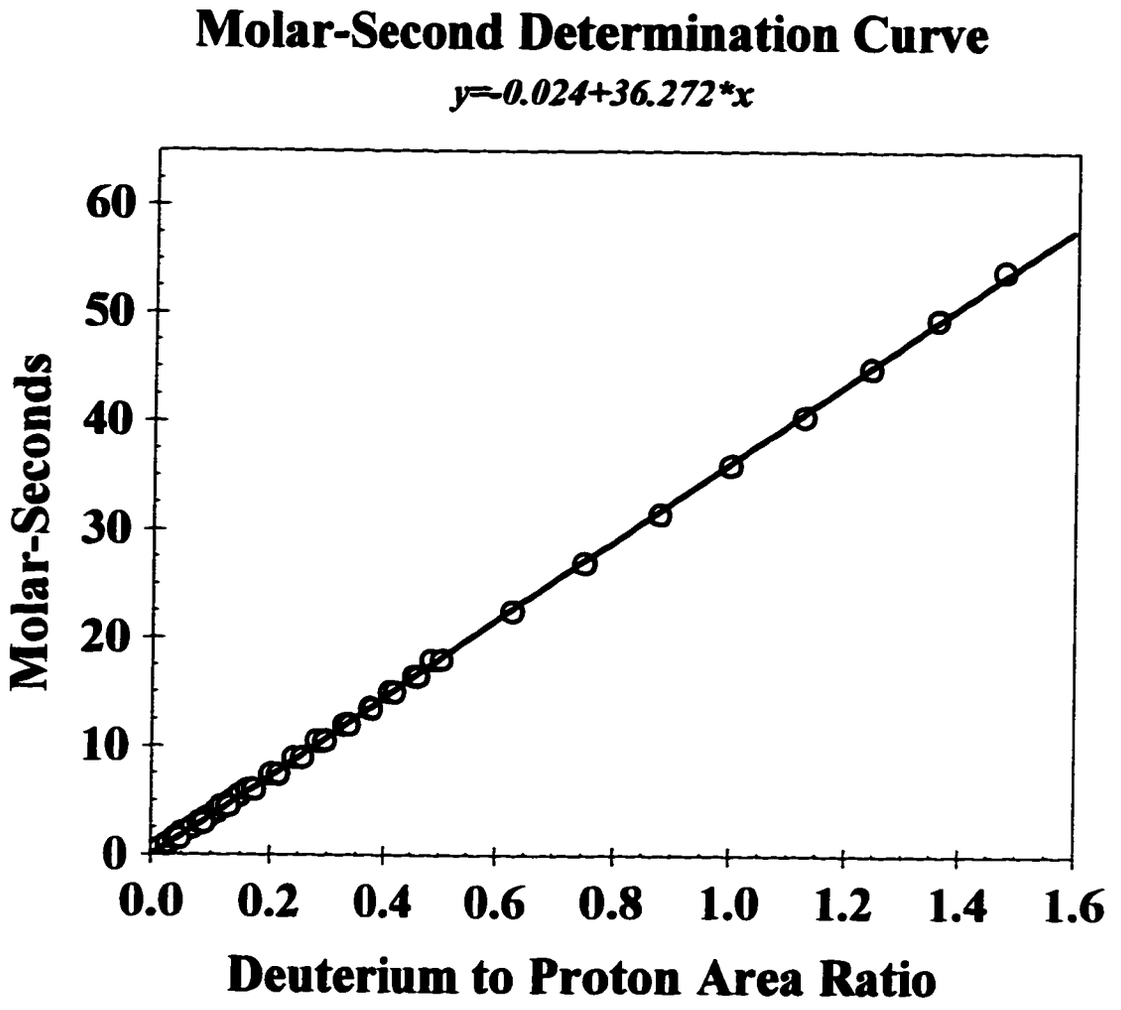

Fig. 3.3 Calibration curve using the double-tuned proton/deuterium circuit and coil. The absolute molar-seconds value of an observed volume can be determined by the ratio of the deuterium signal to the proton signal from that volume. Using the molar-second value, one can obtain the perfusion to the volume through use of a lookup table which relates perfusion to molar-second values.

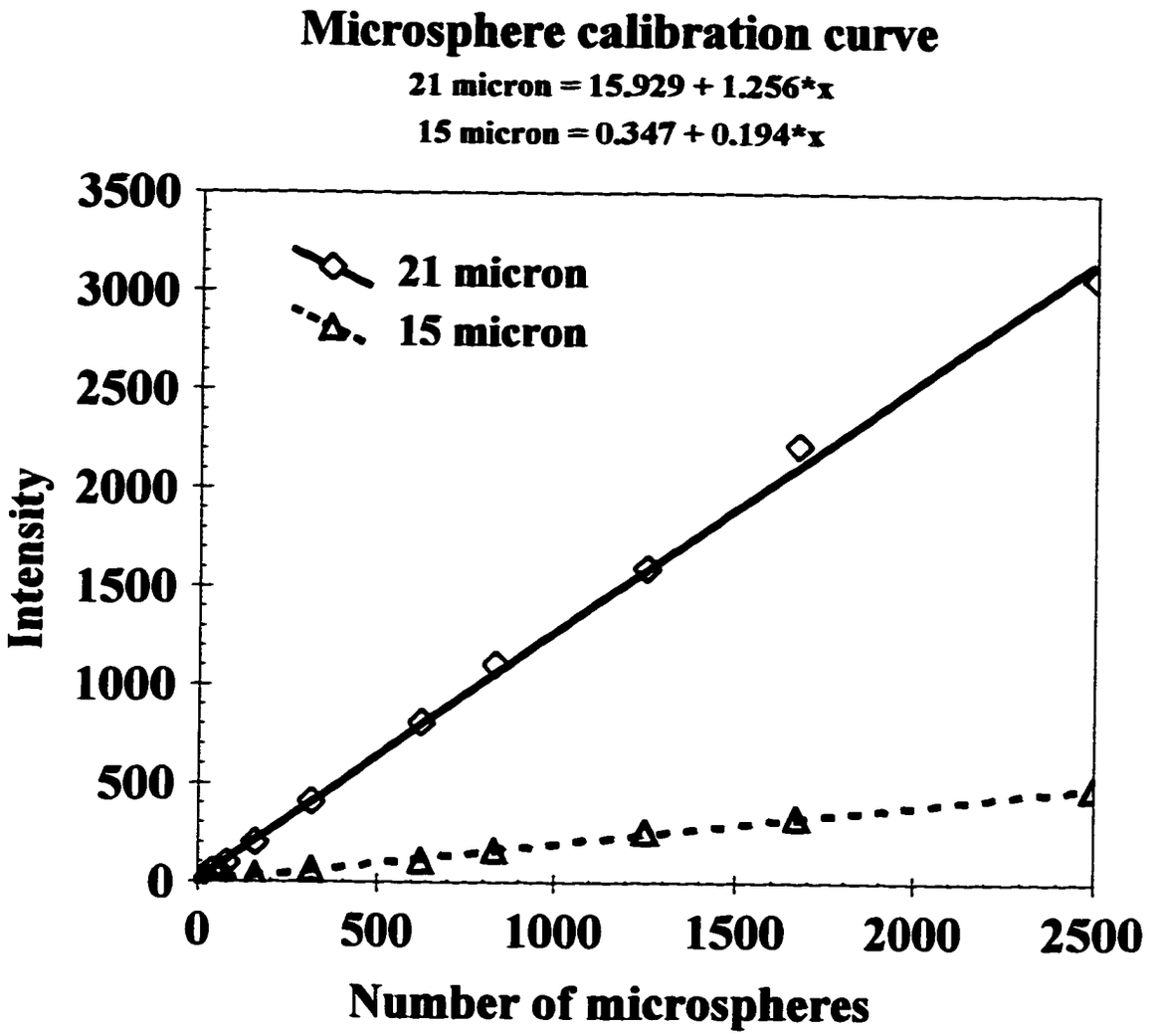

Fig. 3.4 Calibration curve for the 15- and 21-micron diameter microspheres. The curves begin to flatten out at microsphere numbers much greater than 4000 (data not shown) due to extinction of the fluorescence. If the intensity exceeds the linear portion of the curves, the sample is diluted and remeasured.

determine the number of beads that would be trapped in a volume at a given perfusion rate. Since the fluorescence intensity is directly proportional to the number of beads dissolved, and the number of beads trapped is linearly related to the perfusion through the tissue, the fluorescence can directly be used to calculate the average perfusion through the tissue sample. Absolute perfusion in terms of ml/100 g-min can be calculated by considering the mass of the sample. Kidney perfusions were also calculated and compared as a control to ensure proper mixing and delivery of spheres. Spectrophotometer excitation and emission slit widths were set to 5 nm for each dye. Optimum excitation/emission frequencies for the three microsphere sizes used are as follows: 10.3 μm, 578/595 nm; 15.5 μm, 536/551 nm; 21.0 μm, 492/505 nm.

9. Microsphere size verification

An appropriate microsphere size for normal tissues is one which experiences minimal shunting, has non-distorted distribution, and yields reproducible measurements [98], provided that a sufficient number of microspheres are trapped to maintain precision [53]. Determination of a suitable microsphere size for measurement of an unexplored tissue is based on which size traps most efficiently in the tissue [99-102]. Previously, microspheres on the order of 20-30 μm in diameter were found to be most appropriate for measuring tumor perfusion [23,103] rather than the 10-15 μm diameter microspheres used for normal tissues because small-tumor vasculature and capillaries are somewhat larger than those found in normal tissues [24]. To verify that the larger microspheres are appropriate for measuring perfusion in the 9L tumor model, three different sizes of microspheres were simultaneously delivered 10 seconds prior to NMR deuterium uptake collection (n = 7). The approximate number of microspheres (as well as their diameters)

delivered per animal were as follows: 200,000 10.3-μm, 150,000 15.5-μm, 125,000 21-μm. The criterion for choosing the appropriate size for the tissue under study was to determine which yielded the highest perfusion value.

Microspheres larger than 21-μm were not tested in these experiments. Normal tissues have flow measured optimally with microspheres on the order of 10-15 μm in diameter, depending on the site of interest being measured. Tumors are routinely measured with microspheres around 25-μm in diameter. Spheres much larger than this are known to encounter a problem whereby the microspheres preferentially stream in the center of a high speed arterial supply, and do not distribute randomly at branching points in the arterial system [55,56], a physical process termed axial streaming. This leads to perfusion mismeasurement in certain tissues, with those tissues having relatively low perfusion (such as tumor tissue) being underestimated.

10. Method comparison

To compare the NMR *vs.* the microsphere measurement in determining *in vivo* whole-volume TBF in the 9L tumor, approximately 600,000 21-μm microspheres were delivered midway through the NMR uptake collection (n = 13). Tissue perfusions were calculated, and a Pearson Product Moment correlation was performed to test for a correlation between the tissue perfusions extracted by the NMR and microsphere methods.

11. Anesthetic effect on AIF

It was important to determine the effect of time under anesthesia on the AIF of animals, and the subsequent effect on accurately measuring tissue perfusion using a common AIF. Therefore, individual AIFs were extracted from a group of rats (n = 9) at two time-points: 60 and 120 minutes post-anesthesia. This was accomplished by NMR

observation of the tracer through an implanted carotid chamber, then considering the observed signal to be the AIF convolved with a dispersion function, and extracting the AIF by a method described previously in Chapter II B.1. Of the nine animals tested, all nine had AIFs at 120-minutes post-anesthesia extracted, whereas only five AIFs could be extracted from the animals at the 60-minute time point. Four animals were not tested at the 60-minute time point due to problems encountered that took the experiment past this time point. Common AIFs were derived from each set of animals (60- and 120-minute groups) by taking the mean of each parameter that describes the modeled AIF. NMR uptake tumor perfusions for each animal in the comparison experimental set (n = 13) were calculated using the Kety equation and each common AIF, with these perfusions compared to the microsphere-derived perfusion.

C. RESULTS

Figure 3.5 shows the results of the trial to verify the most appropriate size of microsphere to measure whole volume perfusion in a 9L rat gliosarcoma (n = 7). As stated previously, the criterion for "appropriateness" was highest perfusion value (best trapping in the capillary or arteriole bed). For ease of viewing, only the 15- and 21-μm microsphere data are included on the graph. The 21-μm diameter microspheres give somewhat higher perfusion values than do the 15-μm microspheres in this tumor model. The 10-μm spheres were widely variable, unpredictable, with three of the measurements giving a zero perfusion value.

A Pearson Product Moment Test of all data was done to test for correlations between the NMR and microsphere derived tumor perfusions. The highest correlation

between the NMR and microsphere methods was with the 21-μm spheres ($R = 0.758$, $p < 0.05$). Neither the 15-μm nor the 10-μm microspheres correlated ($R = 0.525$, $p = 0.23$; and $R = -0.11$, $p = 0.81$, respectively).

As a control for proper delivery and cardiac mixing of the microspheres, bilateral kidney perfusions were estimated for each animal [Fig. 3.6]. There was a correlation between the left and right kidney perfusions as measured with either the 10- and 15-μm microspheres (Pearson Product Moment Test: $p < 0.00005$; $p < 0.01$, respectively), while the kidney perfusions did not correlate when measured by the 21-μm spheres ($p > 0.25$). Furthermore, the average perfusion to the kidneys was highest when measured with 10-μm spheres (494 ml/100 g·min), and lowest when measured with 21-μm spheres (413 ml/100 g·min).

Figure 3.7 shows the results of the simultaneous NMR *vs.* microsphere perfusion measurements performed on the 13 rats, using the most appropriately sized microsphere (21-μm diameter), and a common AIF derived under similar experimental conditions. A Pearson Product Moment test indicates a highly significant correlation between the two measurements ($R = 0.857$, $p < 0.002$). Perhaps most importantly, the data points are scattered about the line of unity. If both sets of experimental *in vivo* data using the 21-μm microspheres are combined [Fig. 3.8] ($n = 20$), the Pearson correlation is highly significant ($R = 0.833$; $p < 0.000003$).

The potential consequence of estimating perfusion with the NMR approach while applying an AIF obtained under conditions differing from those of the experiment was studied. The derived common AIFs extracted from rats under 60- and 120-minutes of Isoflurane anesthesia are shown in Fig. 3.9. Since the comparison studies between the

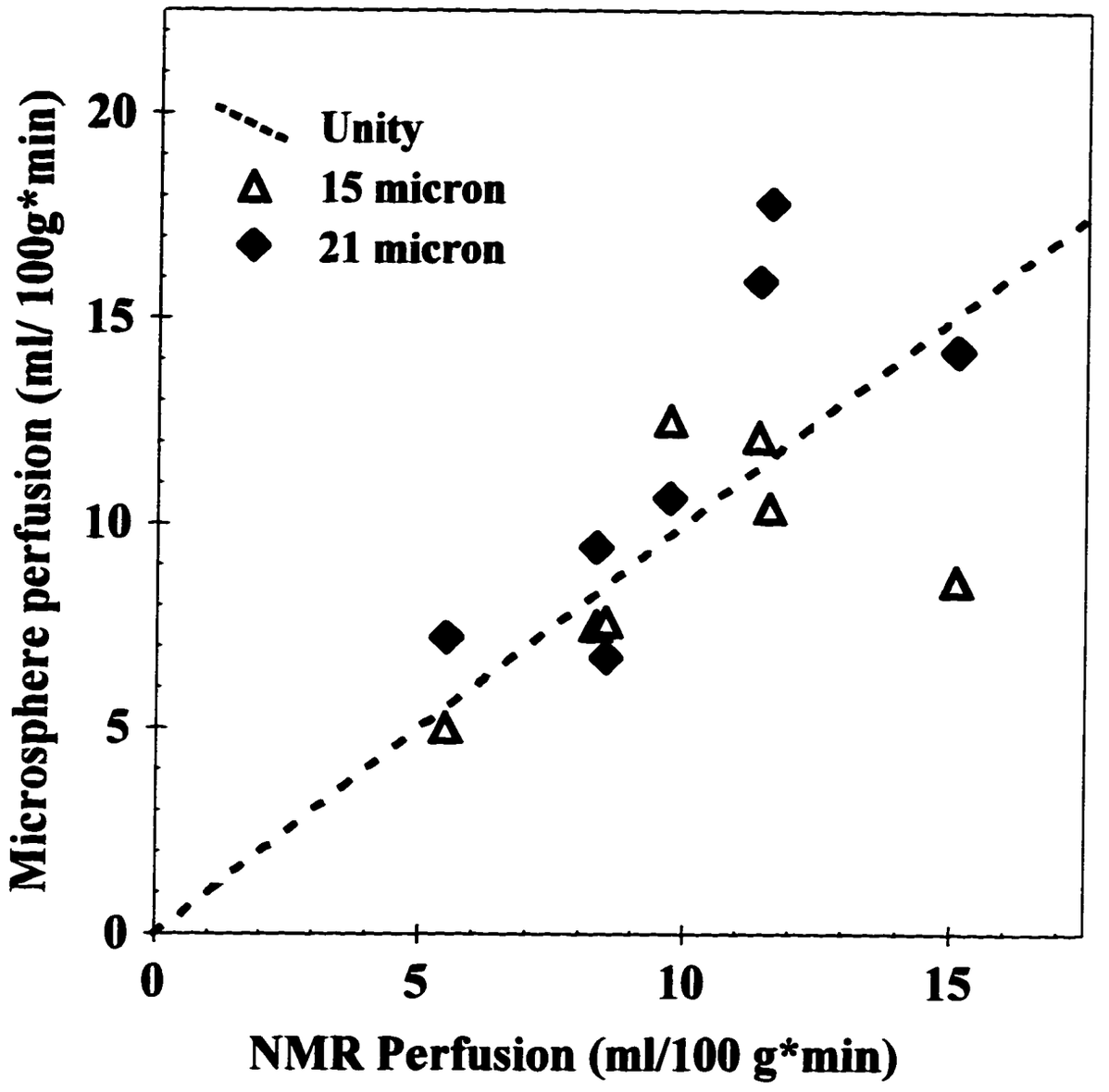

FIG. 3.5 Results of the *in vivo* study to determine an optimum microsphere size appropriate for whole-volume perfusion measurement of a 9L gliosarcoma tumor model in rats (n = 7). Simultaneous injection of three sizes of microspheres (diameters of 10-, 15- & 21-μm) was performed immediately after the NMR derived perfusion data was obtained. The highest perfusion values, and the only significant correlation between the methods, occurred with the 21-μm microspheres ($R = 0.758$; $p < 0.05$). The 10-μm spheres are not included on the graph for ease of viewing. The dashed line indicates the line of unity. Rats were under anesthesia for approximately 120 minutes before this study was performed and the NMR data was analyzed using a common AIF derived under similar experimental conditions.

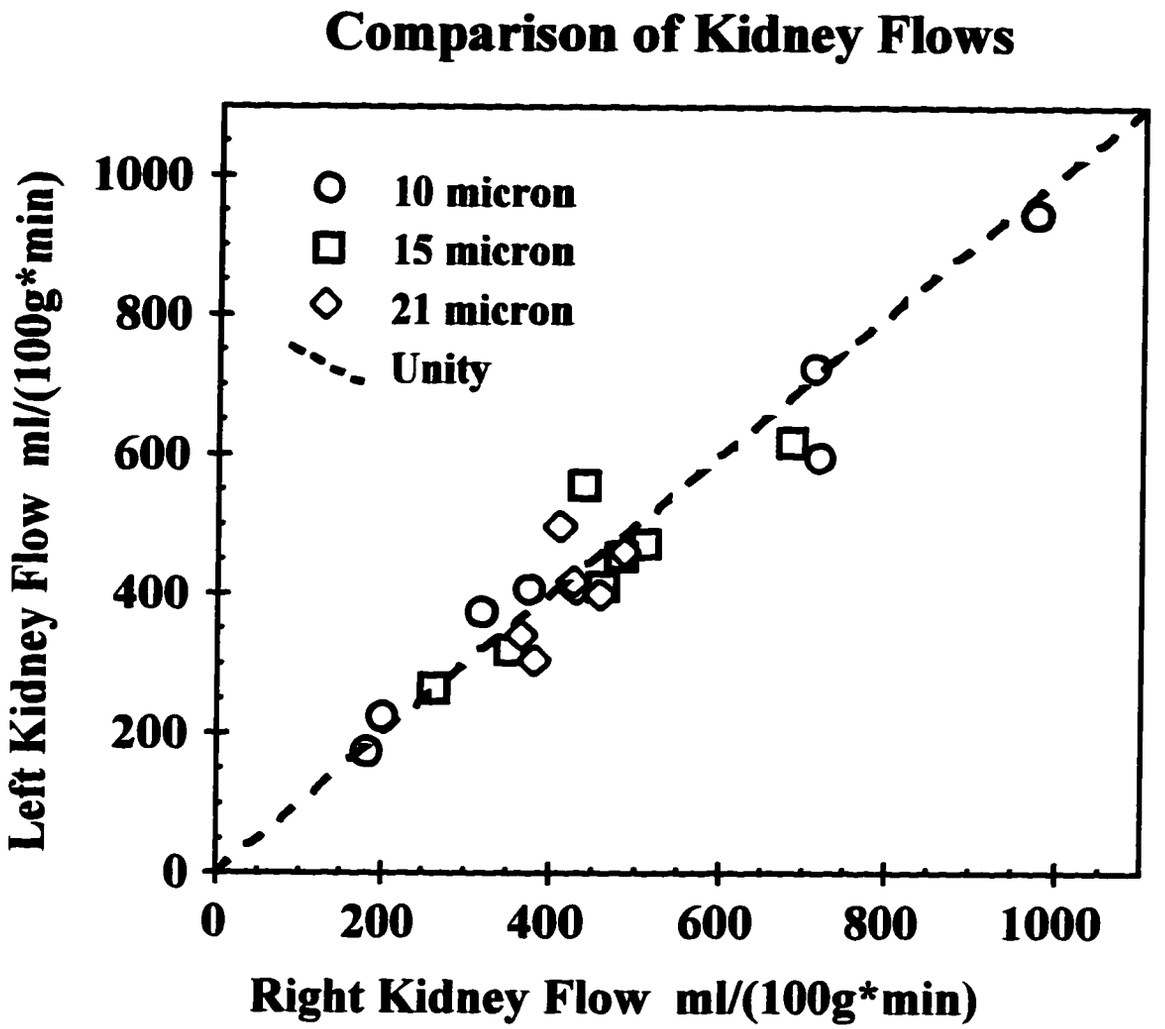

Fig. 3.6 Comparisons between the left and right kidney perfusions estimated with microspheres following simultaneous delivery of three different diameter microspheres (10-, 15-, and 21-micron). The bilateral kidney perfusions determined with the 10- and 15-micron microspheres correlated with each other, but not with the 21-micron spheres {$p < 0.00005$; $p < 0.01$, $p > 0.25$, respectively}.

microspheres and the modified NMR uptake method were performed after approximately 120 minutes of anesthesia, the AIF extracted 120 minutes post-anesthesia is the appropriate common AIF to use in NMR calculations with the comparison data. The 120-minute common AIF has a larger area-under-the-curve, and peaks at a slightly higher value and at a later time than does the common AIF derived from animals under 60 minutes of anesthesia. These differences can be explained in terms of the anesthetic effect on the cardiac output of the animals from which the AIFs were extracted. The result of applying these common AIFs to the NMR uptake data from the perfusion comparison experiment is shown in Fig. 3.10. As shown in Fig. 3.7, using the correct common AIF results in data distributed about the line of unity. However, although using either common AIF retains the correlation between the two perfusion methods (R = 0.857), using the inappropriate common AIF results in a shift of the NMR data points to higher perfusions, with this shift perfusion-dependent (*i.e.* the shift is greater at larger perfusions). Consequently, when the NMR data are analyzed with the inappropriate common AIF, the comparison perfusion data are no longer distributed about the line of unity.

D. DISCUSSION

It is often desirable to be able to obtain quantitative measurements of tissue perfusion in laboratory animal models. This is particularly true in the area of cancer research, since tumor perfusion measurements may be vital in monitoring and designing therapeutic approaches to eradicate the disease, as well as in aiding the comprehension of relationships between perfusion and response. In tissue perfusion measurement, microspheres have been an extensively used "gold-standard". This perfusion method measures the entrapment of microspheres in the small arterial vasculature; mainly in the

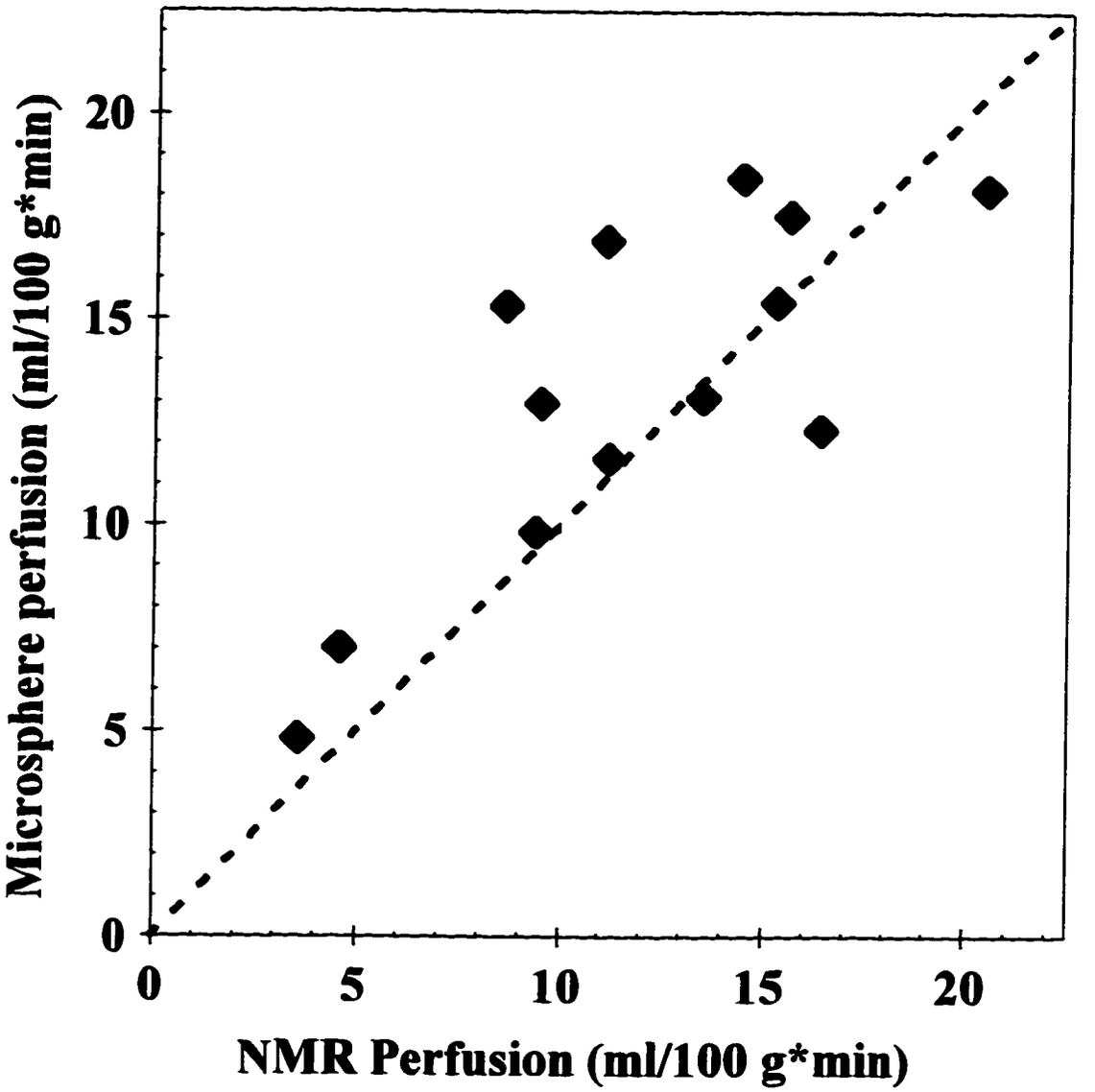

FIG. 3.7 Results of the simultaneous NMR *vs.* microsphere *in vivo* perfusion measurements using the "appropriately" sized (21-μm) microsphere (n = 13). Microspheres were administered during acquisition of the NMR data. There is a highly significant correlation between the two measurements ($R = 0.857$; $p < 0.002$). The dashed line indicates the line of unity. The rats were under anesthesia approximately 120 minutes before this study was performed, and the NMR data was analyzed using a common AIF derived under similar experimental conditions.

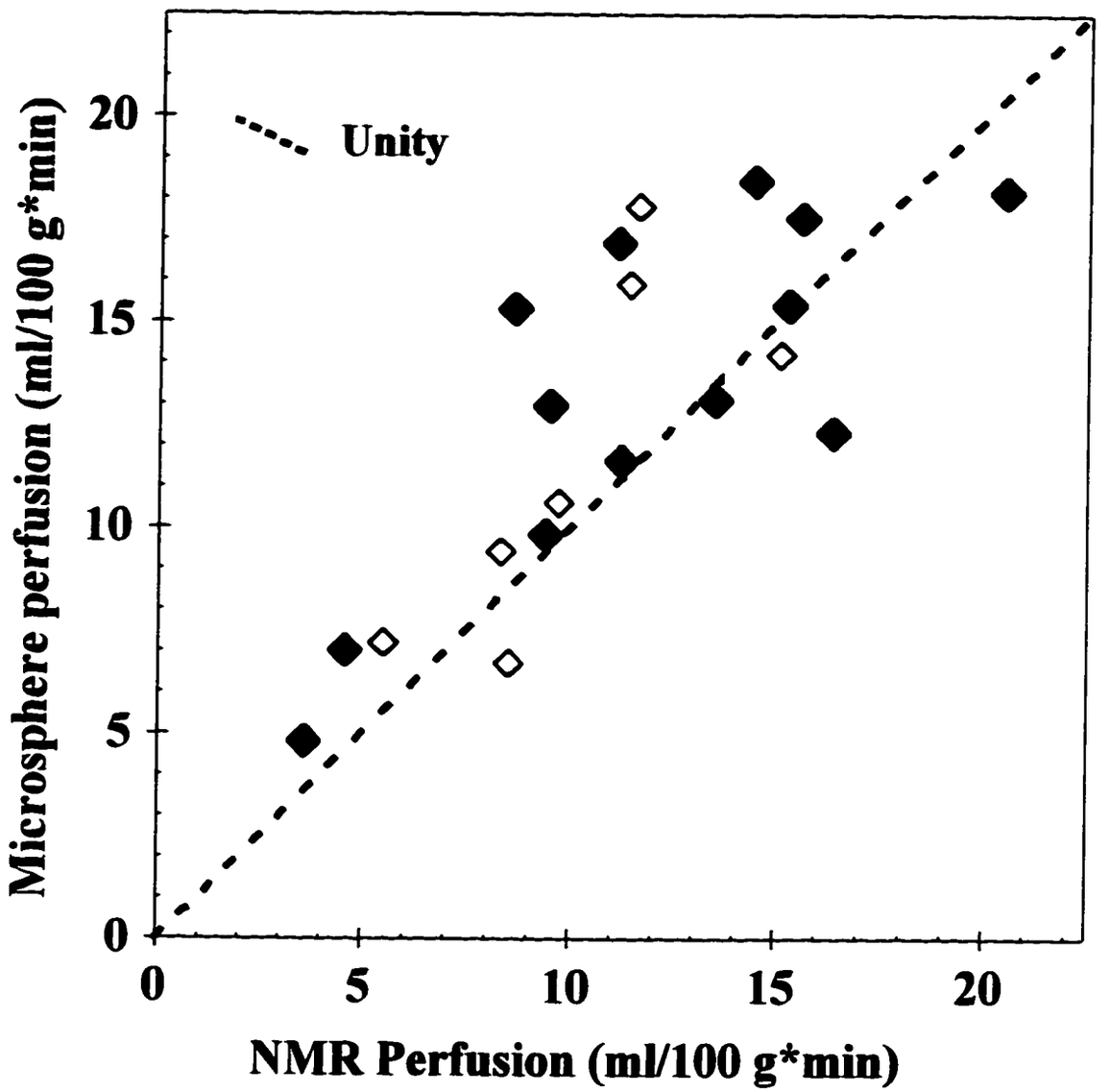

FIG. 3.8 Results of the NMR *vs.* microsphere *in vivo* perfusion measurements combining all data from animals receiving the 21-μm microspheres (n = 20). Animals from the different experiments are shown with separate symbols, with the open symbols representing the data from the size validation study. There is a highly significant correlation between the two measurements (R = 0.833; p < 0.000003). The dashed line indicates the line of unity. The rats were under anesthesia approximately 120 minutes before the study was performed, and the NMR data was analyzed using a common AIF derived under similar experimental conditions.

arterioles right before the capillary bed [48]. However, the high potential for vascular shunting [20], aborted blind ends [22], and the non-uniformity of vascular vessel diameters [22,23,103] in tumor tissues challenges microsphere methods. By determining optimum microsphere sizes for the tissue under study, including tumors, microsphere methods can obtain what are considered quantitative perfusion measures [23,103]. Microspheres have been extensively used in cancer research, and have provided valuable insight. New perfusion methods are often compared to this microsphere method. Therefore, in order to determine whether the modified NMR method can yield comparable tumor perfusion measures without determination of an individual AIF, a simultaneous comparison was performed between the NMR method and microspheres.

Among the many difficulties when performing perfusion measurements with microspheres is deciding upon an optimum size for use in a tissue. Because quantitative perfusion measurement requires maximum embolization within the capillary bed (for any given tissue under study), there exists some optimum microsphere size. This is because normal tissue has a characteristic blood supply, with capillaries of a certain average size [24]. In normal rodent tissues, the arterioles have a mean diameter of approximately 7.0 μm, with capillaries of 3.7 μm [24], and microspheres of 10-15 μm quantitatively measure average perfusion through these tissues very well (though optimization of size should be performed with any tissue under experimentation). Tumors are a different matter. Generally, the microvasculature of tumors contains a substantial number of capillary-like vessels with diameters greater than 12 μm [23]. This physiological anomaly requires use of microspheres with a larger diameter than what is commonly used with normal tissues to obtain quantitative results of nutritive perfusion, though the optimum sphere size may

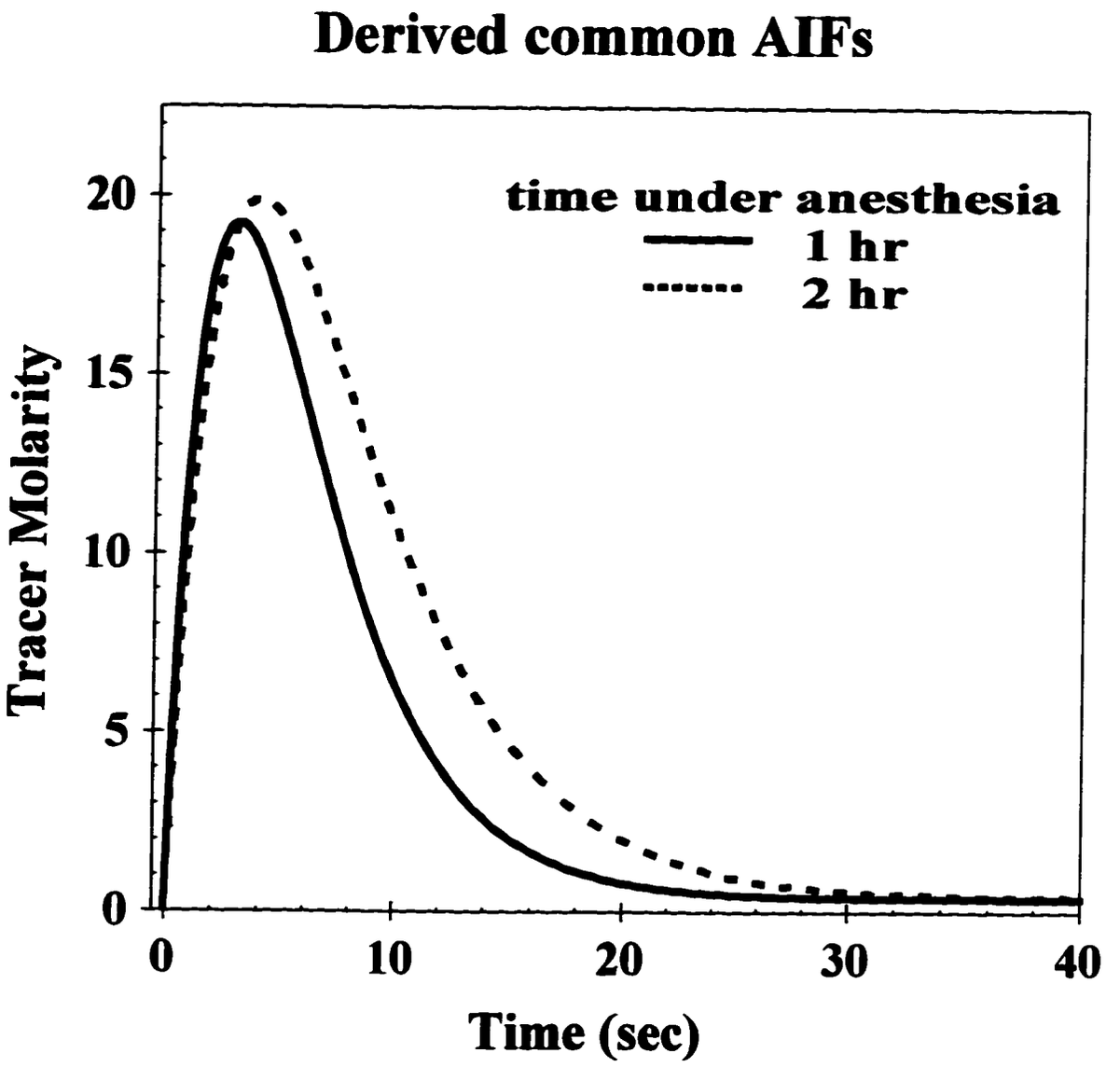

FIG. 3.9 Depiction of the common AIFs derived from rats (n = 9) under different experimental conditions. One derived from rats after 60 minutes of anesthesia (AIF_{60}), the other from the same rats after 120 minutes of anesthesia (AIF_{120}). The curves differ from each other, in that AIF_{120} peaks higher, at a later time point, and has a greater area under the curve than does AIF_{60}.

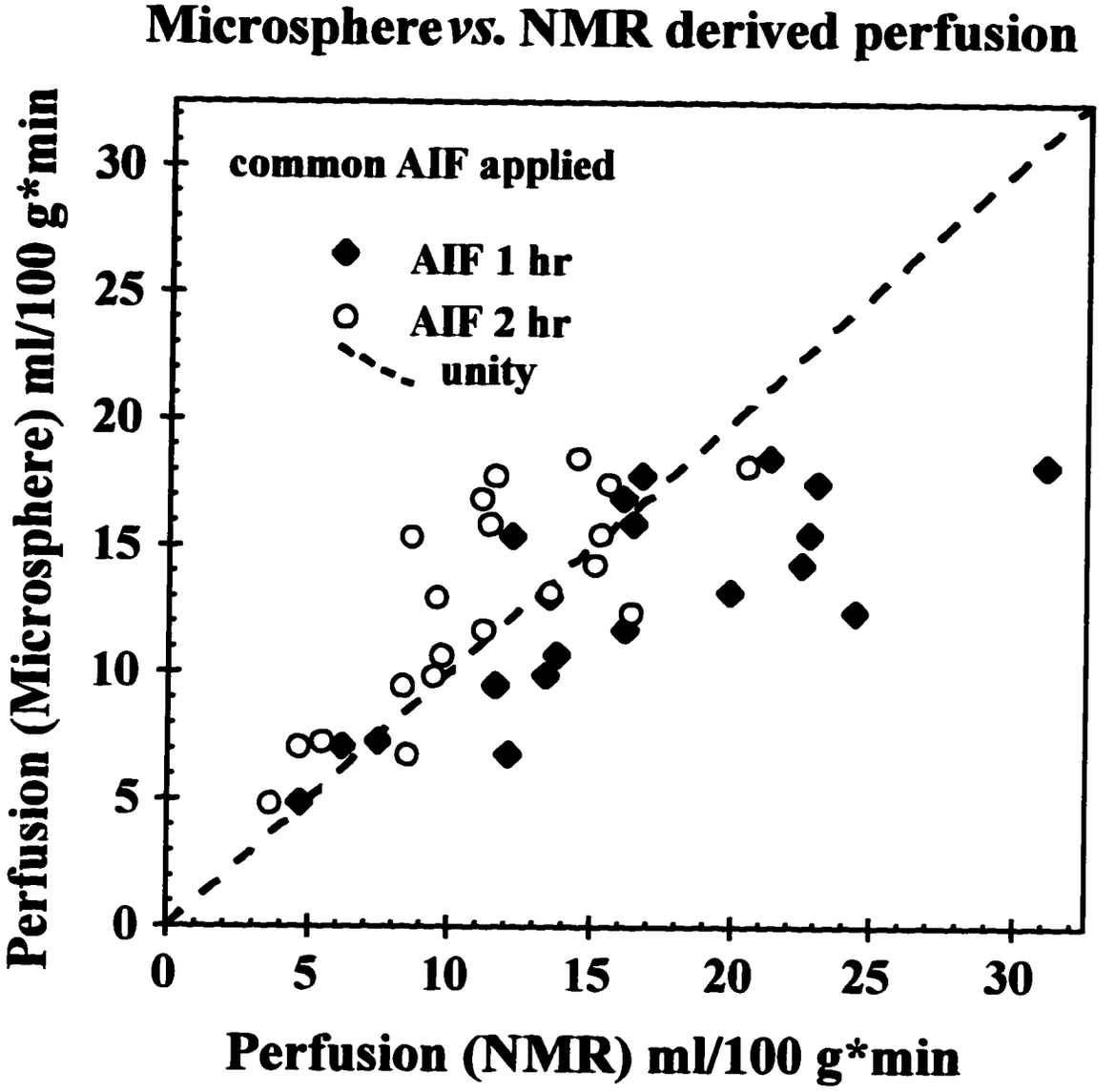

FIG. 3.10 Results of the simultaneous NMR *vs.* microsphere *in vivo* perfusion measurements using the "appropriately" sized (21-μm) microsphere (n = 13), but applying an improper common AIF (derived under 60 minutes of anesthesia) for the NMR perfusion analysis. Animals undergoing the perfusion comparison tests were under anesthesia approximately 120 minutes, while the applied common AIF was derived from rats under 60 minutes of anesthesia. The dashed line represents the line of unity, and the results shown in Figure 3.4 (common AIF derived under 120 minutes of anesthesia) are repeated here for comparison. There is a highly significant correlation between the two measurements ($R = 0.833$; $p < 0.002$, for either common AIF applied); however, the data analyzed with the improper common AIF do not fall about the line of unity.

vary between tumor lines, or between animals with the same tumor line.

That the optimum microsphere size for the 9L tumor line was 21-μm corroborates previous work [103] indicating that larger sized spheres on the order of 21-25 μm are necessary when measuring perfusion in tumor tissue. Likewise, the normal kidney tissue was best measured with the smaller 10-μm spheres (and not well at all with the 21-μm spheres), as has been previously demonstrated [104,105]. Further, correlation between the left and right kidneys with the small spheres means that all spheres were well mixed in the heart, and equally distributed in the branches from the descending aorta, a confirmation of proper delivery technique [97]. Lack of correlation with the large microspheres in the normal kidney tissue does not mean that these 21-μm microspheres were not also well mixed (since the spheres were all injected simultaneously, this is unlikely). Rather, the renal arteries branch from the descending abdominal aorta at nearly right angles, and the descending aorta contains blood moving at a high velocity. These conditions may lead to axial streaming, as discussed in Chapter I E.2.e. It is possible that non-representative delivery to one kidney may occur as a result of the streaming effect which occurs with large microspheres.

The range of perfusions found in the experiments {ranging from 5 to 20 ml/(100 g·min)} is not atypical for solid tumors, which generally have lower average perfusions than normal tissues. The 9L tumor line has been generally determined to have perfusions averaging closer to 30 ml/(100 g·min). The animals in this study experienced longer anesthesia duration prior to perfusion determination studies (2 hours), and the discrepancy between the results in this study with those of other workers is likely due to the anesthetic effect on the C.O. There was no correlation between tumor volume and perfusion.

E. Conclusions

Using an appropriately sized (21 μm) microsphere for tumor perfusion measurement results in a strong correlation between the two methods [Fig. 3.8 & 3.7]. Moreover, there is a scatter of the compared datapoints around the line of unity when the proper common AIF is used in the NMR analysis. This suggests that the modified NMR method can yield perfusion information similar to that obtained with the microsphere approach. Thus, this NMR approach provides an alternative method to measure tissue perfusion, with some key advantages over the microsphere or iodo-antipyrine methods. One is that the NMR method is non-destructive to the tissue under study. A second is that either whole-volume or regional perfusion information can be obtained by either performing the NMR method spectroscopically or in an imaging mode. Perhaps the greatest benefit of the NMR approach is that because it is both non-destructive and repeatable, the method has the ability to correlate perfusion with response in individual animals.

The lack of an exact one-to-one correspondence between the two methods for each tumor studied is not surprising. First of all, there is no reason for the tumor vasculature to be constructed similarly through all the tumors tested [22] (especially concerning the distribution of capillary diameters). Changes in this distribution will affect the accuracy of the microsphere perfusion measurement, meaning that the appropriate microsphere size may differ somewhat from tumor to tumor. Without *a priori* knowledge of the ideal microsphere size for any one given tumor, use of the 21 μm microspheres may cause an underestimation of the true perfusion. This is not generally the case when using microspheres to measure perfusion through normal tissue, since the normal tissue

vasculature is quite constant from animal to animal, both in average capillary diameter and distribution of capillary diameters.

A second reason for the perfusion measures differing from the microsphere measures could be attributable to the fact that the true AIF of each animal is not known, but a common AIF derived from a set of animals is implemented in subsequent perfusion calculations. In addition, our method of extracting an individual AIF may not yield the animal's absolute AIF, but is rather a derived estimate calculated from models. However, when considering the difficulty of obtaining each individual animal's AIF, and given that computer simulations have demonstrated that the variability between AIFs derived from animals under similar experimental conditions is small enough to allow use of a common AIF with slight error in perfusion estimation (< 10% error), a common AIF may be used.

To further minimize changes in the derived common AIF which could affect perfusion measurement by tracer-uptake methods, the following improvements could be implemented: 1) since the tracer injection should be constant and rapid so that the rate of injection does not vary between the animals in which the common AIF was derived and the animals in the perfusion experiment, the injection could be mechanized; 2) because the individual AIF may be affected by the experimental conditions, the common AIF used in the perfusion calculations must be obtained under conditions similar to those experienced by the animals in the perfusion measurement. Moreover, if the experimental conditions change, or there are alternate timepoints, an appropriately derived common AIF should be applied for proper data analysis; 3) by determining the true volume-of-distribution of the tracer in the animal, an accurate dose can be administered, resulting in reduced errors when applying a common AIF.

An explanation for why substantial changes in the experimental conditions can affect the NMR perfusion measurement may be understood in terms of the cardiac output (C.O.) effect on the AIF. It is known that anesthetics can alter many facets of the hemodynamics in rodents [106-109]. Anesthetics can alter heart rate, blood pressure, cardiac output, stroke volume, as well as alter the perfusion to organs. However, these effects are dependent on the anesthetic and the time under anesthesia. Certain anesthetics increase blood pressure [106], while others decrease blood pressure [107,108]. Likewise, anesthetics can increase heart rate [107] or reduce heart rate [108]. Surgical manipulations and drugs may also affect the cardiac output of the animal under study by changing the peripheral resistance. A consequence of these conditions imposed on an animal is that, generally, as the C.O. changes so too does the AIF. The gross changes to the shape of the AIF as a function of anesthesia (which we believe is reflective of a downward C.O. change associated with increased exposure to the anesthetic Isoflurane) can be seen in Fig. 3.9. In brief, the differences between these two common AIFs are as follows. The AIF derived from rats under 120 minutes of anesthesia peaks later, at a higher value, and has a greater area under the curve than does the common AIF derived from rats under 60 minutes of anesthesia. The later peaking of the common AIF_{120} makes intrinsic sense, since a decreased C.O. would result in the bolus reaching a maximum at a later time. The other changes may not be intuitive, unless one considers what occurs at the site of tracer injection. However, these changes are in agreement with computer simulations presented in Chapter II C.1, and have been observed with *in vitro* simulations [Fig. 2.4].

The reason the peak of common AIF_{60} is lower than that of common AIF_{120} is as follows. Blood in animals with a higher C.O. (*i.e.* less time under anesthesia, in this example) is generally flowing through main vasculature at a greater rate than in animals with a lower C.O. For a given tracer injection rate, the tracer concentration at the site of injection in an animal with a higher C.O. will consequently be lower than that from an equivalent injection in an animal with a lower C.O. (*i.e.* more time under anesthesia). Also, the mean time the tracer spends in the artery is decreased in a higher C.O. animal, resulting in a narrower AIF curve (*i.e.* a lower area under the curve) than what is observed in lower C.O. animals (a broader AIF, with larger area).

There could be similar problems at the site of tracer injection if the tracer is not administered at the same rate in all animals (both in the AIF-determining groups, and the experimental groups). For a given flow rate in the blood stream, a rate of tracer injection will yield some given maximum tracer concentration in the blood stream. If a faster bolus injection rate is given, the tracer concentration in the bloodstream will be higher, similar to what occurs when the C.O. is reduced, and the effects would be the similar (higher peak) over that same time frame. Because these will result in changes in the AIF, this will create miscalculation of true perfusion when using a common AIF. Therefore all animals should be injected at the same rate.

The problem one could encounter using a common AIF obtained under different experimental conditions from that of the experimental animals is illustrated in Fig. 3.10. In this example, the NMR perfusion measurement data are well correlated with the microsphere measures when either common AIF is applied. However, the NMR perfusions are much higher than the microsphere data when using an AIF extracted from

rats under only 60 minutes of anesthesia. This difference can be explained as a direct result of a higher cardiac output in the group of animals experiencing less anesthesia (rats from which a common AIF was extracted). Similarly, if the converse occurred, and the experimental animals had higher cardiac outputs than the animals from which the common AIF was extracted, the perfusions would then be consistently underestimated. These results suggest that if a quantitative measure of perfusion is desired, the applied common AIF must be obtained under conditions matching that of the experimental group. If conditions change during an experiment which may significantly alter the AIF (*e.g.* differing lengths of time under anesthesia, different anesthetic used, a drug being administered to the animal, new surgical procedure being implemented), an appropriate common AIF should be derived for each condition for proper analysis. As is shown in Figs. 3.7 & 3.8, when the proper common AIF is applied, the two methods yield similar information regarding tumor perfusion.

Most importantly, these studies indicate that deuterium uptake NMR measurement of tumor perfusion yields values comparable to those found using the well accepted microsphere method of perfusion determination. This concordance was found despite the intrinsic physiological variabilities between animals and tumors, hand-injecting the tracer, the use of a derived common AIF, and the fact that the perfusion methods are based on different principles. The results underscore the important conclusion that a common AIF must be determined under any specific experimental conditions that are present in the study in order for this NMR method to be quantitative. This research indicates that the deuterium NMR approach can be used for repeatable, non-invasive, and quantitative measurements of whole-volume tissue perfusion, even in tissue with unusual vasculature

such as solid tumor. Furthermore, the sensitivity of the tracer-uptake method should allow for quantitative perfusion measures of tissue heterogeneity (when using NMR in an imaging mode), at a resolution far superior to that possible through microspheres.

CHAPTER IV SUMMARY & CONCLUSIONS

A. Summary

1. Chapter I

The initial chapter discussed the importance of monitoring perfusion in tissues, particularly concerning the impact perfusion has on the efficacy of many therapies, with an emphasis placed on therapy against solid tumors. The concept of an ideal perfusion measuring method was also introduced, with the ideal method being a repeatable, non-invasive (to the tissue under study) measure of absolute perfusion. Common classes of methods with which to measure tissue perfusion were discussed (the particulate and indicator approaches), with an emphasis on the microsphere particulate technique, and the NMR indicator methods. The NMR uptake approach our laboratory developed was also introduced, along with preliminary studies which suggested the utility of such an approach in obtaining important information regarding solid tumor perfusion. Because the limitations of both the uptake approach and the analysis of the acquired data had not previously been determined, these were outlined, and led directly to the research contained in the remainder of this volume.

2. Chapter II

Chapter II was two-fold in its emphasis. It both presented a method with which to measure the individual AIF in a rat, and presented results from computer simulations that allowed a better understanding of the limitations of the uptake method, as well as insight into how better to design and perform *in vivo* experimentation using the uptake-integral approach. Measurement of the AIF of an individual rat was accomplished using NMR detection of the indicator flowing through a carotid observation chamber. The

advantages of this method over the presently used method (carotid puncture blood collection) are substantial. The most important advantage is that the NMR method does not result in the great loss of the animal's blood (though some is lost during the surgical procedure, this amounts to much less than a quarter of a ml). Use of this blood-preserving NMR method to derive the AIF ensures that the C.O. is not changing rapidly throughout the AIF measurement. Since the C.O. affects the AIF, the commonly used puncture method measures an AIF which is necessarily changing during the measurement. Moreover, the animal will not immediately die due to the implantation of the observation chamber and determination of the apparent AIF (as is the case with the commonly used carotid puncture method). This means that the animal can be used for other studies, or for repeated perfusion studies. In fact, it is possible that the animal could be kept alive for long-term studies. Although permanent catheterization techniques were not used in these studies, they do exist, and could be implemented and optimized if the experiment dictates it. In fact, there are studies at Henry Ford Hospital (Detroit, MI) being performed using two coils (one for determining an apparent AIF, the other used to observe the tissue of interest); so the technology exists for the potential to monitor the AIF and other tissue simultaneously.

However, computer simulations suggested that the individual AIF was not required for accurate perfusion measures. Rather, these simulations demonstrate that a common AIF derived from a small set of animals can be applied to the perfusion data obtained from subsequent animals and theoretically result in less than a ten percent error (if the indicator is given as a bolus dose: delivery of a constant indicator volume does not allow for accurate measures, and should not be implemented in any study). These results

have the impact of greatly simplifying the perfusion experiment by eliminating the need to measure the individual AIF of each animal within a study. Application of a common AIF eliminates the difficult complication that performing a carotid chamber implant has on an experiment and on an animal. However, computer simulations also suggested that large changes in the AIF may affect the perfusion measure. This suggests that the experimental conditions of all animals should be controlled, so as not to cause any large and significant changes in the AIF that may lead to errors in perfusion estimation when applying the NMR-uptake approach.

Other computer simulations contributed information regarding the optimum analytic approach to take when determining tissue perfusion estimations from uptake data. These experiments suggest that the FIT method is more sensitive to heterogeneity, but less sensitive to poor S/N. Conversely, the INT method, which is less affected by heterogeneity, is more sensitive to noise, particularly at low perfusions. Moreover, the INT method is more sensitive to changes in the AIF, particularly at perfusions exceeding 60 ml/(100 g·min). These simulation results suggest that when deriving perfusions from small volumes, such as in an imaging experiment, where the S/N is relatively poor but there is relatively homogeneous perfusion, the FIT approach is superior. And when deriving perfusions from large volumes, as in a whole-volume measurement, where the S/N is good but the perfusion is heterogeneous, the INT approach is recommended. However, due to the sensitivity of the INT approach to changes in the AIF at high perfusions, it may be that the FIT approach should be used for any measurement of tissue whose perfusion is believed to be greater than 60 ml/(100 g·min). Since tumors have perfusions generally lower than this, whole-volume measures of tumor perfusion may be

best estimated by analyzing the data by the INT method. It is worth repeating that the conclusions drawn in these studies are valid not only for this NMR uptake approach, but should be applicable with other uptake methods which use an indicator, regardless of the detector used to obtain the data.

3. Chapter III

This chapter applied the lessons learned in the studies and simulations performed in Chapter II, which suggested that one could theoretically improve the accuracy and precision of the NMR uptake method by including the following modifications: use of a common AIF; delivery of a bolus tracer dose; application of optimized data analysis. To determine how these modifications allow for accurate tissue perfusion estimation *in vivo*, the modified NMR uptake approach was simultaneously compared *vs.* a well used perfusion measurement standard which does not require knowledge of the AIF when deriving perfusions (the microsphere approach). An optimum microsphere size for tumor perfusion measurements was determined to be in the range of 21 microns in diameter, corroborating other workers' results using microspheres for perfusion measurements in tumors. When using these larger microspheres, simultaneous perfusion estimations by the modified NMR uptake approach and the microsphere approach yielded highly correlated estimates. More importantly, the perfusion estimates are distributed about the line of unity, suggesting that the measures are extracting similar information regarding the tumor perfusion. However, the NMR uptake approach has the advantage over the microsphere method in measurement of tissue perfusion because it does not require that the tissue be removed (as is the case in microsphere studies), and the NMR method can obtain both whole-volume and regional perfusion measures, at a resolution much greater than that

obtained by microspheres. The take-home lesson here is that the modified NMR uptake approach closely resembles the ideal perfusion measuring method. It is a repeatable, non-invasive (to the tissue under study) and absolute measure of perfusion which may play an important role in a range of future studies regarding the perfusion of tissues.

Much new insight into the sensitivity of the perfusion measures to altered AIFs (here studied as an altered C.O. due to anesthesia) was gleaned from the time-under-anesthesia study. This study confirms the computer simulations which predicted errors in measurement if an inappropriate AIF was applied to the analysis of an acquired data set. Moreover, the changes seen in AIFs extracted under different conditions behave in a manner which can be understood in terms of the altered C.O. This early appreciation of the qualitative changes that occur to an AIF as conditions change has led to a better understanding of how to better measure the delivery of both endogenous and exogenous substances to a tissue. A summary of the factors which influence the AIF is listed in Table IV.1 along with solutions to reduce changes in these factors in experiments.

B. Conclusions

As a tool in the research arsenal, this NMR uptake approach may allow for significant contributions to the understanding of relationships between tissue perfusions and response to therapy, physiology, treatment planning, or yet undetermined studies of interest. Its importance in animal model experimentation should not be overlooked. The principles are applicable in any animal model in which the AIF can be easily extracted. These animal models include such diverse species as rat, guinea pig, rabbit, cat, dog and simian models.

Table IV.1

Factors affecting the Arterial Input Function

Factor	*Change*	*Consequence*	*Solution*
rate of tracer injection	↑	peak concentration higher	mechanize injection
	↓	peak concentration lower	
tracer concentration	↑	peak and initial AUC higher	maintain concentration
	↓	peak and initial AUC lower	
blood flow at injection site	↑	peak and AUC lower; t_p shorter	inject at same rate and/or maintain C.O.
	↓	peak and AUC higher; t_p longer	

As stated earlier, the utility of this approach in murine models is limited, because the AIF has not yet been demonstrated to be accurately extractable from these animals. If one needs absolute measures of perfusion for correlation with physiological changes (*e.g.* the delivery of endogenous factors such as oxygen, glucose, or hormones), the mouse model is not appropriate, since absolute measures of perfusion are critical to the understanding of the complex relationships between these. However, murine models may be acceptable for understanding measures of exogenous substances delivered to a tissue (*e.g.* chemotherapeutic agents), since the perfusion measurement will tell you quantitatively (though not absolutely) what is being delivered to the tissue (as long as the conditions remain constant). If AIF extraction in mice is one day attained, the problems associated with application of a common AIF, and the solutions discussed earlier will

apply.

One possible means by which one could extract an apparent AIF from a mouse (and other animals as well) is to perform NMR spin-tagging imaging of the blood coming out of the heart. By measuring the rate at which blood is extracted from the heart (through observation of the tracer through a cross-section of the aorta, for example), and by knowledge of the cross-sectional area of the vessel, one can obtain a cardiac output estimation if the heart rate is known. Even on animals as small as mice the heart rate can be determined with small pressure-transducer cuffs. It may be possible to extract the individual AIF information non-invasively through these means, resulting in an even more accurate method with which to determine absolute tissue perfusions.

There may be justifiable concern regarding the extraction of the AIF from the carotid, when the tissue having the perfusion measured in these studies is located near the inguinal region. The concern is that the AIF at the site of perfusion measurement is not identical to that in the carotid. In fact, there is undoubtedly some internal dispersion occurring as the tracer goes about the circulatory system. However, because using the common AIF derived from the carotid works when measuring perfusion in the rat suggests that the internal dispersion is not great enough to pose a significant problem. This is probably due to the small size of the animal, and the small distance for dispersions to occur within the vasculature. However, the dispersion may well be a problem in animals of greater size than rats, making the extraction of the AIF from the carotid not as useful in these animals. A solution to this problem is to add dispersion time to the derived AIF. This dispersed AIF would be more realistic of the AIF at the tissue site, and should result in a more useful AIF for perfusion measurements of tissues far removed from the carotid

in larger animals.

It should be stressed that the NMR technique using deuterium as a tracer for determining tissue perfusion has limited applicability outside the sphere of animal model research. For this approach (using the deuterated water as a tracer) to be used clinically in humans, the clinical machines presently used would have to have much stronger magnetic fields. This is due to the relative insensitivity of deuterium to detection by NMR. At the present magnetic field strengths used in the clinic (1.5 - 2 Tesla), achievement of a deuterium concentration in man comparable to that obtained in the rat, would require a bolus of approximately 200 mls. As this is too large a volume to administer as a rapid bolus, the clinical utility of the technique directly observing a deuterated water tracer is small. However, as the hardware technology improves, higher field magnets are becoming available. If the day comes when magnets with a field strength of 20 Tesla are available, the tracer would need be administered as a 20 ml bolus. Though this approaches an acceptable volume for delivery in human subjects, the spatial resolution obtained with presently available larger coils is inferior to that observed in these studies, precluding any imaging studies. It remains to be seen whether better hardware, new techniques such as indirect observation of the tracer through another nuclei, or alternative tracers will allow the determination of absolute perfusion in man using the principles set forth here.

Apart from demonstrating this method's utility in animal studies, and perhaps equally important, this research addresses questions concerning how best to approach the problem of measuring perfusion with tracers. It also has recently opened up new doors of research which will add to our understanding of the complex relationships between the measurement of perfusion and the factors which complicate this measurement. The

computer simulations presented here are a first step to address questions which are applicable not only to this deuterium method, but to a multitude of studies presently used in humans receiving contrast agents (agents delivered into the blood stream of subjects which enhances the contrast between tissues in an MR experiment). Contrast agents are becoming increasingly used in experimental clinical studies to determine if these agents can yield information on diagnostics, staging and therapeutic response. Few researchers are attempting to unravel the complexities of how these agents are delivered to a tissue under observation. By better understanding the AIF and how it is influenced by physiological changes, a better understanding of how agents are delivered to tissues, and the importance of this in terms of what is observed experimentally can be attained.

It has been said that new ideas must progress through three stages. The first stage is that the ideas are summarily rejected by others as false. The second stage is that the ideas are interesting, but contrary to dogma, and should not be seriously pursued. The last stage occurs when evidence is finally shown which demonstrates that the ideas are sound. Then, the concept is embraced as being true. However, those people who were previously skeptics will insist that of course it's true, but this has been known for a long time.

Similarly, the ideas introduced here are not entirely new, but based on the seminal work of Kety, work which has well over fifty years in the literature. However, acceptance of the NMR uptake method has been slow, despite the fact that many invasive methods based on the Kety approach have been validated, accepted and used. Hopefully, the results presented in this dissertation will lead researchers to use this modified NMR method in earnest, and address important questions concerning tissue perfusion. Perhaps it will also spur further research towards understanding the factors which influence these

types of perfusion measurements- an understanding that can only serve to strengthen the advancement of methods such as the NMR approach studied here.

REFERENCES

1. A. Ljunqvist and C. Lagergren, The arterial vasculature of renal adenocarcinomas. *Acta Pathol. Microbiol. Scand.* **67**, 55-66 (1966).

2. H.-I. Peterson, L. Appelgren, G. Lundborg and B. Rosengren, Capillary permeability of two transplantable rat tumours as compared with various normal organs of the rat. *Bibl. Anat.* **12**, 511-518 (1973).

3. P. M. Gullino and F. H. Grantham, Studies on the exchange of fluids between host and tumor, II. The blood flow of hepatomas and other tumors in rats and mice. *J.N.C.I.* **27**, 1465-1491 (1961).

4. P. M. Gullino and F. H. Grantham, The vascular space of growing tumors. *Cancer Res.* **24**, 1727-1732 (1964).

5. C. W. Song, J. H. Sung, J. J. Clement and S. H. Levitt, Vascular changes in neuroblastoma of mice following X-irradiation. *Cancer Res.* **34**, 2344-2350 (1974).

6. W. H. Lewis, The vascular pattern of tumors. *Johns Hopkins Hosp. Bull.* **41**, 156-162 (1927).

7. I. Kjartansson, L. Appelgren and H.-I. Peterson, Intratumor flow distribution studied by ^{86}Rb and ^{125}I. 1. Methodological aspects with a comparison of two different tracers. *Acta Chir. Scand. Suppl.* **471**, 1-74 (1976).

8. G. M. Tozer, S. Lewis, A. Michaelowski and V. Aber, The relationship between regional variations in blood flow and histology in transplanted rat fibrosarcoma. *Brit. J. Cancer* **61**, 250-257 (1990).

9. J. B. Larcombe-McDouall, J. Mattiello, C. L. McCoy, N. E. Simpson, M. Sayedsadr and J. L. Evelhoch, Size dependence of regional tumor blood flow in murine tumors using deuterium magnetic resonance imaging. *Int. J. Radiat. Biol.* **60**, 109-113 (1991).

10. B. Endrich, H. S. Reinhold, J. F. Gross and M. Intaglietta, Tissue perfusion inhomogeneity during early tumor growth in rats. *J.N.C.I.* **62**, 387-395 (1979).

11. S. Schultz-Hector, J. Kummermehr and H. D. Suit, Vascular architecture of experimental tumors - influence of tumor volume and transplantation site. *Int. J. Radiat. Biol.* **60**, 101-107 (1991).

12. C. W. Song, J. C. Lyons and Y. Luo, Intra- and extracellular pH in solid tumors:

influence on therapeutic response. *In*: Drug Resistance in Oncology. B. A. Teicher, *ed.* NY: *Marcel Dekker*, 25-51 (1993).

13. H. Holthusen, Beiträge zur Biologie der Strahlenwirkung. Untersuchungen an Askarideneiern. *Pfluger Archiv. Physiol.* **187**, 1-24 (1921).

14. G. L. Chu and W. C. Dewey, The role of low intracellular or extracellular pH in sensitization to hyperthermia. *Radiat. Res.* **114**, 154-167 (1988).

15. M. R. Horsman, K. L. Christensen and J. Overgaard, Hydralazine-induced enhancement of hyperthermic damage in a C_3H mammary carcinoma *in vivo*. *Int. J. Hyperth.* **5**, 123-126 (1989).

16. E. M. Zeman, J. M. Brown, M. J. Lemmon, V. K. Hirst and W. W. Lee, A new bioreductive agent with high selective toxicity for hypoxic mammalian cells. *Int. J. Radiat. Onc. Biol. Phys.* **12**, 1239-1242 (1986).

17. J. M. Brown, Exploitation of bioreductive agents with vasoactive drugs. *Proc. 8th Int. Cong. Radiat. Res.* E. M. Fielden, *ed.* London: *Taylor & Francis*. **v.2**, 719-724 (1987).

18. D. J. Chaplin, Hypoxia-targeted chemotherapy: a role for vasoactive drugs. *Proc. 8th Int. Cong. Radiat. Res.* E. M. Fielden, *ed.* London: *Taylor & Francis*. **v.2**, 731-736 (1987).

19. D. J. Chaplin and M. J. Trotter, Chemical modifiers of tumor blood flow. *Funktionanalyse Biologischer*. **20**, 65-85 (1991).

20. J. R. Less, T. C. Skalak, E. M. Sevick and R. K. Jain, Microvascular architecture in a mammary carcinoma: branching patterns and vessel dimensions. *Cancer Res.* **51**, 265-273 (1991).

21. J. Mattsson, L. Appelgren, B. Hamberger and H.-I. Peterson, Tumor vessel innervation and influence of vasoactive drugs on tumor blood flow. *In*: Tumor blood circulation. H.-I. Peterson, *ed.* Boca Raton: *CRC Press*, 129-135 (1979).

22. M. A. Konerding, F. Steinbach and V. Budach, The vascular system of xenotransplanted tumors - scanning electron and light microscopic studies. *SEM.* **3**, 327-336 (1989).

23. R. L. Jirtle, Blood flow to lymphatic metastases in conscious rats. *Europ. J. Cancer*. **17**, 53-60 (1981).

24. M. P. Wiedeman, Dimensions of blood vessels from distributing artery to collecting vein. *Circul. Res.* **12**, 375-378 (1963).

25. R. K. Jain, Determinants of tumor blood flow: a review. *Cancer Res.* **48**, 2641-2658 (1988).

26. H. F. Dvorak, J. A. Hagy, J. T. Dvorak and A. M. Dvorak, Identification and characterization of the blood vessels of solid tumors that are leaky to circulating macromolecules. *Amer. J. Pathol.* **133**, 95-109 (1988).

27. B. A. Warren, The ultrastructure of the microcirculation of the advancing edge of Walker 256 carcinoma. *Microvasc. Res.* **2**, 443-453 (1970).

28. N. Taginawa, T. Kanazawa, K. Satomura, Y. Hikasa, M. Hashida, S. Muranishi and H. Sezaki, Experimental study on lymphatic vascular changes in the development of cancer. *Lymphology.* **14**, 149-154 (1981).

29. J. Delarue, J. Mignot and T. Caulet, Modifications vasculaires de la poche jugale du hamster dore au dours du developpement de greffes d'une tumeur melanique. *Comptes Rendus Seances Soc. Biol. Paris.* **157**, 69-71 (1963).

30. B. Endrich, M. Intaglietta, H. S. Reinhold and J. F. Gross, Hemodynamic characteristics in microcirculatory blood channels during early tumor growth. *Cancer Res.* **39**, 17-23 (1979).

31. Y. Boucher, J. M. Kirkwood, D. Opacic, M. Desantis and R. K. Jain, Interstitial hypertension in superficial metastatic melanomas in humans. *Cancer Res.* **51**, 6691-6694 (1991).

32. J. Denekamp, The current status of targeting tumor vasculature as a means of cancer therapy: an overview. *Int. J. Radiat. Biol.* **60**, 401-408 (1991).

33. R. Wootton, Theory of blood flow measurement with tracers. R. T. Mathie, *ed. In*: Blood flow measurement in man. Kent, GB: *Castle House Publications* 3-13 (1982).

34. V. E. Steinach, Studien Über den Blutkreislauf der Niere. *Sitzungsber. Math. Naturwiss. Kl. Akad. Wiss.* **90**(III), 171-189 (1884).

35. A. G. Pohlman, The course of the blood through the heart of the fetal mammal, with a note on the reptilian and amphibian circulation. *Anat. Rec.* **3**, 75-110 (1909).

36. M. Prinzmetal, B. Simkin, H. C. Bergman and H. E. Kruger, Studies on the coronary circulation II. The collateral circulation of the normal human heart by coronary perfusion with radioactive erythrocytes and glass spheres. *Amer. Heart. J.* **33**, 420-442 (1947).

37. E. Grim and E. O. Lindseth, Distribution of blood flow to the tissues of the small intestine of the dog. *Med. Bull. Univ. Minn.* **30**, 138-145 (1958).

38. E. Grim and E. O. Lindseth, Measurement of regional blood flow in dog intestine. *Circulation.* **18**, 728 (1958).

39. L. D. MacLean, Y. S. Kim and P. H. Hedenstrom, Distribution of blood flow in canine and human hearts. *Surgical Forum* **12**, 221-223 (1961).

40. L. D. MacLean, P. H. Hedenstrom and Y. S. Kim, Distribution of blood flow to the canine heart. *Proc. Soc. Exp. Biol. Med.* **107**, 786-789 (1961).

41. M. Rudolph and M. A. Heymann, The circulation of the fetus *in utero*. Methods for studying distribution of blood flow, cardiac output and organ blood flow. *Circul. Res.* **21**, 163-185 (1967).

42. S. L. Hale, K. J. Alker and R. A. Kloner, Evaluation of nonradioactive, colored microspheres for the measurement of regional myocardial blood flow in dogs. *Circulation* **78**, 428-434 (1988).

43. G. E. Austin, D. Martino-Salzman, A. G. Justicz, *et al.*, Determination of regional myocardial blood flow using fluorescent microspheres. *Am. J. Cardiovasc. Pathol.* **4**, 352-357 (1993).

44. P. Kowallik, R. Schulz, B. D. Guth, A. Schade, W. Paffhausen, R. Gross and G. Heusch, Measurement of regional myocardial blood flow with multiple colored microspheres. *Circulation* **83**, 974-982 (1991).

45. R. W. Glenny, S. Bernard and M. Brinkley, Validation of fluorescent-labeled microspheres for measurement of regional organ perfusion. *J. Appl. Physiol.* **74**, 2585-2597 (1993).

46. F. L. Abel, R. H. Cooper and R. R. Beck, Use of fluorescent latex microspheres to measure coronary blood flow distribution. *Circul. Shock* **41**, 156-161 (1993).

47. E. L. Makowski, G. Meschia, W. Droegemueller and F. C. Battaglia, Measurement of umbilical arterial blood flow to the sheep placenta and fetus *in utero*: distribution to cotyledons and the cotyledonary chorion. *Circul. Res.* **23**, 623-631 (1968).

48. A. B. Malik, J. E. Kaplan and T. M. Saba, Reference sample method for cardiac output and regional blood flow determination in the rat. *J. Appl. Physiol.* **40:3**, 472-475 (1976).

49. S. Ishise, B. L. Pegram, J. Yamamoto, Y. Kitamura and E. D. Frolich, Reference

sample microsphere method: cardiac output and blood flows in conscious rat. *Am. J. Physiol.* **239**, H443-H449 (1980).

50. R. F. Tuma, U. S. Vasthare, G. L. Irion and M. P. Weideman, Considerations in use of microspheres for flow measurements in anesthetized rats. *Am. J. Physiol.* **250**, H137-H143 (1986).

51. B. A. Levine, K. R. Sirinek and H. V. Gaskill III, The radiolabeled microsphere technique in gut blood flow measurement - Current practice. *J. Surg. Res.* **37**, 241-255 (1984).

52. F. W. Prinzen and R. W. Glenny, Developments in non-radioactive microsphere techniques for blood flow measurement. *Cardiovasc. Res.* **28**, 1467-1475 (1994).

53. G. D. Buckberg, J. C. Luck, D. B. Payne, J. I. E. Hoffman, J. P. Archie and D. E. Fixler, Some sources of error in measuring regional blood flow with radioactive microspheres. *J. Appl. Physiol.* **31**, 598-604 (1971).

54. P. Dole, D. L. Jackson, J. I. Rosenblatt and W. L. Thompson, Relative error and variability in blood flow measurements with radiolabelled microspheres. *Am. J. Physiol.* **243**, H371-H378 (1982).

55. R. H. Phibbs and L. Dong, Nonuniform distribution of microspheres in blood flowing through a medium-size artery. *Canadian J. Physiol. & Pharmacol.* **48**, 415-421 (1970).

56. Y.-C. Fung, Stochastic flow in capillary blood vessels. *Microvasc. Res.* **5**, 34-48 (1973).

57. A. Fick, Ueber die Messung des Blutquantums in den Herzventrikeln. *Verhandl. Phys. Med. Ges. Würzburg* **2**, 16-17 (1870).

58. J. Mattiello and J. L. Evelhoch, Relative volume-average murine tumor blood flow measurement *via* deuterium nuclear magnetic resonance spectroscopy. *Magn. Reson. Med.* **8**, 320-334 (1991).

59. G. N. Stewart, Researches on the circulation time and on the influences which affect it. IV: The output of the heart. *J. Physiol.* **22**,159-183 (1897).

60. V. Henriques, Über die Verteilungdes Blutes vom linken Herzen zwischen dem Herzen und dem übrigen Organismus, *Biochem. Zeitschr.* **56**, 230-248 (1913).

61. W. F. Hamilton, J. W. Moore, J. M. Kinsman and R. G. Spurling, Simultaneous determination of the pulmonary and systemic circulation times in man and of a figure related to the cardiac output. *Am. J. Physiol.* **84**, 338-344 (1928).

62. J. W. Moore, J. M. Kinsman, W. F. Hamilton and R. G. Spurling, Studies on the circulation. II: Cardiac output determinations. Comparison of the injection method with the direct Fick procedure. *Am. J. Physiol.* **89**, 331-339 (1929).

63. S.S. Kety and C. S. Schmidt, The determination of cerebral blood flow in man by the use of nitrous oxide in low concentrations. *Am. J. Physiol.* **143**, 53-66 (1945).

64. S. S. Kety and C. S. Schmidt, The nitrous oxide method for the quantitative determination of cerebral blood flow in man: theory, procedure and normal values. *J. Clin. Invest.* **27**, 484-492 (1948).

65. S. S. Kety, Measurement of regional circulation by the local clearance of radioactive sodium. *Am. Heart J.* **38**, 321-328 (1949).

66. M. M. Ter-Pogossian, J. O. Eichling, D. O. Davis, M. J. Welch and J. M. Metzger, The determination of regional cerebral blood flow by means of water labelled with radioactive oxygen 15. *Radiology* **93**, 31-40 (1969).

67. J. A. Johnson, H. M. Calvert and N. Lifson, Kinetics concerned with distribution of isotopic perfused dog heart and skeletal muscle. *Am. J. Physiol.* **171**, 687-693 (1952).

68. M. E. Phelps, E. J. Hoffman, N. A. Mullani and M. M. Ter-Pogossian, Application of annihilation coincidence detection to transaxial reconstruction tomography. *J. Nucl. Med.* **16**, 210-223 (1975).

69. T. Jones, D. A. Chesler and M. M. Ter-Pogossian, The continuous inhalation of oxygen-15 for assessing regional oxygen extraction in the brain of man. *Br. J. Radiol.* **49**, 339-343 (1976).

70. R. S. J. Frackowiak, G.-L. Lenzi, T. Jones and J. D. Heather, Quantitative measurement of regional cerebral blood flow and oxygen metabolism in man using ^{15}O and positron emission tomography: theory, procedure and normal values. *J. Comput. Assist. Tomogr.* **4**, 727-736 (1980).

71. M. E. Raichle, J. Markham and K. Larson, Measurement of local cerebral blood flow in man with positron emission tomography. *J. Cereb. Blood Flow Metabol.* **1**, 519-520 (1981).

72. S.-C. Huang, R. E. Carson and M. E. Phelps, Measurement of local cerebral blood flow and distribution volume with short-lived isotopes: A general input technique. *J. Cereb. Blood Flow Metabol.* **2**, 99-108 (1982).

73. P. Herscovitch, J. Markham and M. E. Raichle, Brain blood flow measured with

intravenous $H_2{}^{15}O$: I. Theory and analysis. *J. Nucl. Med.* **24**, 782-789 (1983).

74. M. E. Raichle, W. R. W. Martin, P. Herscovitch, M. A. Mintun and J. Markham, Brain blood flow measured with intravenous $H_2{}^{15}O$: II. Implementation and validation. *J. Nucl. Med.* **24**, 790-798 (1983).

75. P. T. Fox and M. E. Raichle, Stimulus rate dependence of regional cerebral blood flow in human striate cortex, demonstrated by positron emission tomography. *J. Neurophysiol.* **51**, 1109-1120 (1984).

76. J. J. H. Ackerman, C. S. Ewy, N. N. Becker and R. A. Shalwitz, Deuterium nuclear magnetic resonance measurements of blood flow employing D_2O as a freely diffusible tracer. *Proc. Natl. Acad. Sci.* **84**, 4099-4112 (1987).

77. J. J. H. Ackerman, C. S. Ewy, S.-G. Kim and R. A. Shalwitz, Deuterium magnetic resonance *in vivo*: The measurement of blood flow and tissue perfusion. *In*: Physiological NMR spectroscopy: from isolated cells to man. S. M. Cohen *ed.* N.Y.: *Ann. N. Y. Acad. Sci.* **508**, 89-98 (1987).

78. S.-G. Kim and J. J. H. Ackerman, Multicompartment analysis of blood flow and tissue perfusion employing D_2O as a freely diffusible tracer: A novel deuterium technique demonstrated *via* application with murine RIF-1 tumors. *Magn. Reson. Med.* **8**, 410-426 (1988).

79. S.-G. Kim, Y. C. Hwang and J. J. H. Ackerman, Measurement of tumor blood flow by deuterium nuclear magnetic resonance spectroscopy: Application to murine RIF-1 tumor. *In*: Magnetic resonance in experimental and clinical oncology. J. L. Evelhoch, W. Negendank, F. A. Valeriote and L. H. Baker *eds.* Boston, *Kluwer Academic Publishers*, 59-90 (1990).

80. J. J. Neil, S.-K. Song and J. J. H. Ackerman, Concurrent quantification of tissue metabolism and blood flow *via* $^{2}H/^{31}P$ NMR *in vivo*. II. Validation of the deuterium NMR washout method for measuring organ perfusion. *Magn. Reson. Med.* **25**, 56-66 (1992).

81. S-.G. Kim and J. J. H. Ackerman, Quantitative determination of tumor blood flow and perfusion *via* deuterium nuclear magnetic resonance spectroscopy in mice. *Cancer Res.* **48**, 3449-3453 (1988).

82. NMR Frequency Table, *In*: Bruker Almanac 1988, Tables and other useful information. Bruker Instruments, Billerica, MA. p. 76 (1988).

83. J. B. Larcombe McDouall and J. L. Evelhoch, Deuterium nuclear magnetic resonance imaging of tracer distribution in D_2O clearance measurements of tumor blood flow in mice. *Cancer Res.* **50**, 363-369 (1990).

84. H. Wiig, E. Tveit, R. Hultborn, R. K. Reed and L. Weiss, Interstitial fluid pressures in DMBA-induced rat mammary tumours. *Scand. J. Clin. Lab. Invest.* **42**, 159-164 (1982).

85. J. Mattiello, J. L. Evelhoch, E. Brown, A. P. Schaap and F. W. Hetzel, Effect of photodynamic therapy on RIF-1 tumor metabolism and blood flow examined by ^{31}P and ^{2}H NMR spectroscopy. *NMR Biomed.* **3**, 64-70 (1990).

86. S. S. Kety, Theory and application of the exchange of inert gas at the lungs and tissues. *Pharmacol. Rev.* **3**, 1-41 (1951).

87. K. Hoedt-Rasmussen, E. Sveinsdottir and N. A. Lassen, Regional cerebral blood flow in man determined by intra-arterial injection of radioactive inert gas. *Circ. Res.* **19**, 237-247 (1966).

88. M. E. Raichle, W. R. W. Martin, P. Herscovitch, M. A. Mintun and J. Markham, Brain blood flow measured with intravenous $H_2{}^{15}O$: 2. Implementation and validation. *J. Nucl. Med.* **24**, 790-798 (1983).

89. A. D. Edwards, J. S. Wyatt, C. Richardson, D. T. Delpy, M. Cope and E. O. R. Reynolds, Cotside measurement of cerebral blood flow in ill newborn infants by near infrared spectroscopy. *Lancet* **2**, 770-771 (1988).

90. J. L. Evelhoch, J. B. Larcombe McDouall, J. Mattiello and N. E. Simpson, Measurement of relative regional tumor blood flow in mice by deuterium NMR imaging. *Magn. Reson. Med.* **24**, 42-52 (1992).

91. J. J. H. Ackerman, D. G. Gadian, G. K. Radda and G. G. Wong, Observation of ^{1}H NMR signals with receiver coils tuned for other nuclides. *J. Magn. Reson.* **42**, 498-500 (1981).

92. H. Iida, I. Kanno, S. Miura, M. Murakami, K. Takahashi and K. Uemura, Error analysis of a quantitative cerebral blood flow measurement using $H_2{}^{15}O$ autoradiography and positron emission tomography, with respect to the dispersion of the input function. *J. Cereb. Blood Flow and Metabol.* **6**, 536-545 (1986).

93. H. H. Schmidek, S. L. Nielsen, A. L. Schiller and J. Messer, Morphological studies of rat brain tumors induced by N-nitrosomethylurea. *J. Neurosurg.* **34**, 335-340 (1971).

94. K. T. Wheeler, M. Barker, C. A. Wallen, B. F. Kimler and S. D. Henderson, Evaluation of 9L as a brain tumor model. In: Methods in tumor biology: tissue culture & animal tumor models. (1988).

95. W. A. C. Mutch, P. M. Patel and T. S. Ruta, A comparison of the cerebral

pressure-flow relationship for halothane and isoflurane at haemodynamically equivalent end-tidal concentrations in the rabbit. *Can. J. Anaesth.* **37**, 223-230 (1990).

96. K. R. Thulborn and J. J. H. Ackerman, Absolute molar concentrations by NMR in inhomogeneous B_1: a scheme for analysis of *in vivo* metabolites. *J. Magn. Reson.* **55**, 357-371 (1983).

97. M. A. Heymann, B. D. Payne, J. I. E. Hoffman and A. M. Rudolph, Blood flow measurements with radionuclide-labeled particles. *Prog. in Cardiovasc. Diseases* **20**, 55-79 (1977).

98. M. L. Marcus, D. D. Heistad, J. C. Ehrhardt and F. M. Abboud, Total and regional cerebral blood flow measurement with 7-10-, 15-, 25- and 50- μm microspheres. *J. Appl. Physiol.* **40**, 501-507 (1976).

99. S. Haukaas, K. Svanes and A. Skarstein, Distribution of microspheres with different diameters in the small bowel wall of the cat. *Eur. Surg. Res.* **10**, 240-245 (1978).

100. W. H. Dickhoner, B. R. Bradley and G. S. Harell, Diameter of arterial microvessels trapping 8-10 μm, 15 μm and 25 μm microspheres as determined by vital microscopy of the hamster cheek pouch. *Invest. Radiol.* **13:4**, 313-317 (1978).

101. R. Y. Z. Chen, F.-C. Fan, G. B. Schuessler, S. Usami and S. Chien, Effects of sphere size and injection site on regional cerebral blood flow measurements. *Stroke* **14:5**, 769-776 (1983).

102. R. P. Hof, R. Salzmann and F. Wyler, Trapping and intramyocardial distribution of microspheres with different diameters in cat and rabbit hearts in vitro. *Basic Res. Cardiol.* **76**, 630-638 (1981).

103. R. Jirtle, K. H. Clifton and J. H. G. Rankin, Measurement of mammary tumor blood flow in unanesthetized rats. *J. N. C. I.* **60**, 881-886 (1978).

104. J. Sabto, L. Bankir and J. P. Grunfeld, The measurement of glomerular blood flow in the rat kidney: influence of microsphere size. *Clin. and Exp. Pharmacol. & Physiol.* **5**, 559-565 (1978).

105. A. Mimran and D. Casellas, Microsphere size and determination of intrarenal blood flow distribution in the rat. *Eur. J. Physiol.* **382**, 233-240 (1979).

106. K. A. Stanek, M. H. Davis and T. G. Coleman, Residual effects of ether anesthesia on whole-body hemodynamics and organ blood flows in the rat. *J. Pharmacolog.*

Meth. **20**, 95-102 (1988).

107. K. C. Skolleborg, J. E. Gronbech, K. Grong, F. E. Abyholm and J. Lekven, Distribution of cardiac output during pentobarbital *versus* midazolem/fenanyl/ fluanisone anaesthesia in the rat. *Lab. Animals* **24**, 221-227 (1990).

108. R. W. Barbee, B. D. Perry, R. N. Re and J. P. Murgo, Microsphere and dilution techniques for the determination of blood flows and volumes in conscious mice. *Am. J. Physiol.* **263**, R728-R733 (1992).

109. E. D. Miller, J. R. Kistner and R. M. Epstein, Whole-body distribution of radioactively labelled microspheres in the rat during anesthesia with halothane, enflurane, or ketamine. *Anesth.* **52**, 296-302 (1990).

ABSTRACT

ABSOLUTE TUMOR PERFUSION DETERMINED BY NUCLEAR MAGNETIC RESONANCE SPECTROSCOPY: OPTIMIZATION AND COMPARISON OF A DEUTERIUM UPTAKE METHOD

BY

NICHOLAS EDWARD SIMPSON

December 1997

Advisor: Dr. Jeffrey L. Evelhoch

Major: Cancer Biology

Degree: Doctor of Philosophy

The ultimate goal of this dissertation is to describe the optimization and implementation of an NMR indicator uptake technique which can non-invasively and repeatedly measure tissue perfusion. Chapter II concerns itself with the method optimization of the NMR approaches to measuring tissue perfusion. Since the primary goal of this dissertation research is to obtain absolute perfusion measures, and the AIF is required for this, Chapter II discusses the development of the apparatus and NMR method with which one can extract an apparent AIF from individual rats - a method which will not necessarily result in the animal's immediate death. As a further extension of this goal, research was performed to determine the feasibility of eliminating the need for individual AIF measurement by constructing a common AIF from a small set of animals, and then of using this derived common AIF for all subsequent animals within a study. Chapter II also describes results of computer simulations performed to assess the impact which tissue perfusional heterogeneity, indicator S/N within the tissue sample, and variations in the AIF have on determining absolute perfusion with the two methods of data analysis used with

the NMR uptake approach.

In Chapter III, a modified uptake approach is introduced (developed as a consequence of the results of the research performed in Chapter II) which uses a common AIF and a bolus indicator dose, as well as optimized data analysis. This modified uptake approach is tested against a commonly used method (which does not require knowledge of an AIF) in measuring absolute tissue perfusion. The comparison was done by designing apparatus and developing techniques which allowed the simultaneous performance of whole-volume average perfusion measurements of a rat tumor model with both the modified NMR uptake method and the commonly used microsphere approach. Finally, Chapter IV summarizes the dissertation experiments performed, and briefly comments on the significance of this research.

AUTOBIOGRAPHICAL STATEMENT

Nicholas E. Simpson, Ph.D.
291 Riverside Drive
Detroit, MI 48215
(313) 822-9696

Education

Ph. D. Cancer Biology — Wayne State University, Detroit, MI
December 1997
G. P. A. 3.92/4.00

Dissertation Title: "Absolute Tumor Perfusion Determined by Nuclear Magnetic Resonance Spectroscopy: Optimization and Comparison of a Deuterium Uptake Method

B. S. Cell and Molecular Biology — University of Michigan, Ann Arbor, MI
May 1986
G. P. A. 3.0/4.0

Experience

Wayne State University, Detroit MI — 9/91 - 5/97
Position: Graduate Research Assistant

Wayne State University — 5/87 - 9/91
Position: 4.7 T Operator/ Laboratory Assistant

Wayne State University — 8/86 - 5/87
Position: Research Assistant

Offices & Committees

1995 Student Representative of the Cancer Biology Program
1995 Cancer Biology Curriculum Committee
1995 Operating Committee of the Michigan Cancer Foundation
1995 Karmanos Cancer Center Program Leadership Committee

Awards

1994 National Research Service Award: CA-09531-08 NCI
1995 Radiation Research Student Travel Award
1995 American Cancer Society Research Award: 441694
1997 International Society of Magnetic Resonance in Medicine Travel Award